International Journal of Innovation Engineering and Science Research

Editorial Board

International Journal of Innovation Engineering and Science Research

Volume 6 ISSUE 2 March-April 2022

Sonification approach using human body movements and window functions 01-06

Daniela Hagiescu || Lidia Dobrescu

A Critical Review of Technology Adoption Theories and Models for E-Learning Systems, Kenya 07-15

Kelvin Kabeti Omieno

An Application of LADM-Padé Approximation for the Analytical Solution of the SIR Infectious Disease Model 16-30

L. Ebiwareme || R. E. Akpodee || R. I. Ndu

Study of Chemical ion Transport through the Soil using combined Variational Iteration and Homotopy Perturbation Methods. 31-42

Liberty Ebiwareme || Iyai Davies || Fun-Akpo Pere Kormane

Quad-Element MIMO Antenna with Enhanced Isolation for UWB Applications 43-57

Giday Gebrehiwot Bsrat || S.Aruna || K. Srinivasa Naik

Qualitative characteristics of small ruminant skins from Niger: comparative study of Maradi goats (Red and Black) vs Sahel goat and sheep (Oudah and Balami) 58-72

Adam Kadé Malam Gadjimi || Mamman Manim || Akourki Adamou || Charles-Dayo Guiguigbaza-Kossigan || Balkissa Maman Dabo || Marichatou Hamani

Common Prompters and Deterrents to Adoption of Insurance Policies as a Measure of Construction Risk Mitigation in South East Nigeria 73-81

WOKOCHA CHUKWULEKWURU CHRISTOPHER || NKELEME IFEANYICHUKWU EMMANUEL || EZEH CHRISTIAN CHINEDU || ACHIGBU ONYEMA IKENNA || OZOH CHUKWUDI STANLEY

International Journal of Innovation Engineering and Science Research
(ISSN: 2581-4591)

www.ijiesr.com

Sonification approach using human body movements and window functions

[1]Daniela Hagiescu
Advanced Slisys, Bucharest, Romania

[2]Lidia Dobrescu
Faculty of Electronics, Telecommunication and Information Technology, University POLITEHNICA of Bucharest, Bucharest, Romania

ABSTRACT

In this paper, a new sonification methods is proposed to generate piano music from webcam images and computed human joint coordinates. The music is generated using various window functions implying the pitch and velocity of the generated chords. The influence of the window function and their parameter is investigated.

Keywords—*Sonification, window function, convolutional pose machines.*

I. INTRODUCTION

There are numerous sonification techniques that uses data information from various sources (e.g. earthquake data, financial data, etc). The mapping of this data in sounds is usually arbitrary [1]. There are many methods to generate sounds from body movements that uses data from sensors or video recordings [1]-[5]. The approach with sensors attached to the body is sometime unpleasant and restraint the body movements. Using webcams or other image recording devices lead to a cheaper sonification solution and certainly less obtrusive. Examples of such solutions are EyesWeb [6], Motion Composer [7] or Point Motion Control [8] devices.

In [2] the "motiongrams" are used for sonification from video recordings. An image frame is considered as the spectrogram with frequency information on the Y axis and time on the X axis as the basis for synthesizing a sound file [5]. A sonification method based on optical flow computation was proposed in [15]. A musical note is played depending on the optical flow magnitude [5]. The pitch corresponds to the location and flow direction of the peak and the velocity (or intensity) of the note corresponds to the magnitude [2]. This method is very complex due to optical flow computation. In [5] a simpler method that uses the body joint coordinates obtained by the convolutional pose machines (CPM) approach [9] was proposed. The piano sounds were generated using a layout of pitches from low-level harmonic notions [2]. In this paper a novel approach based on applying different window functions to the computed pitch and velocities values is investigated. This is an original approach since they are not applied on the piano sounds themselves. Therefore, differently aesthetically pleasing piano sounds are generated from the same body movements.

The structure of the paper is the following: Section II concisely describes the approach using CPM, Section III the proposed approaches for sonification are presented and the conclusions close the article.

II. THE CPM BASED SONIFICATION METHOD

As shown in [5] the Convolutional Pose Machines (CPM) method is used to find the skeleton joints coordinates from webcam images. The convolutional pose machine is a human pose detector. The human pose detector algorithm finds 14 human skeleton joints for head, upper neck, shoulders, elbows, wrists, hips, knees, and ankles. An example of webcam image and skeleton joints is shown in Figure 1 [5].

a) Webcam image and CPM computed joints coordinates [5]

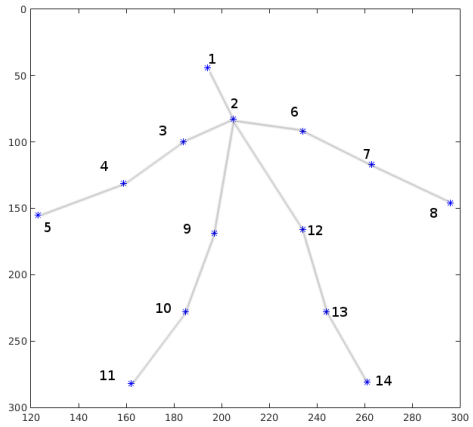

b) Skeleton joints [5]

Figure 1. Webcam image and skeleton joints

Two convolutional neural networks are trained for detecting a person in the image frame and to detect skeleton joints. Each stage produces belief maps being composed of a sequence of convolution and pooling layers. More details about the CPM method can be found in [9]. As shown in [5] there is a correlation between the obtained joint vectors due to the nature of the huma body and the possible movements. The CPM method is very good in handling non-standard poses in case of different relative camera views [9]. The few mismatches that might happen can be removed by using the Dynamic Time Warping (DTW) distance between consecutive normalized joint coordinates vectors [5]. The DTW algorithm [10] computes the optimal alignment between two time-series and proved a valuable tool in handwritten evaluation (e.g. [11]). A threshold of 0.05 was used to detect outliers [5].

2.1The computation of the pitch and velocity

The pitch mesh pairs method from [2] is used. The pitch mesh is obtained from vertically stacked pitch chains in parallel octaves [2]. The musical tone uses the dominance bit, the pitch, and the register values. The last two values are normalized between 0 and 128. The chromaticism of the generated music is altered by modifying the thresholds for the normalized coordinates. The method used in this paper for pitch and velocity computation is described in more details in [2] and [5].

If the music contains multiple notes on the same pitch, some values are filtered out and the filtered parameters are played using the Microsoft MIDI Mapper as the midi output device [5]. As shown in [5], the complexity of this approach is smaller in comparison with competing methods. There are numerous ways to obtain different piano sounds by varying the threshold, pitch range, register range and beat duration. However, for some human body movements consecutive identical notes are generated and there is a need to diversify them while still taking into account the movement for these consecutive image frames.

III. THE PROPOSED METHOD BASED ON WINDOW FUNCTIONS

The normalized joint coordinated are used to create a matrix. A pause for a fraction of a second on each column is considered. A note is triggered based on the normalized horizontal and vertical coordinates values and their location on the pitch mesh pair. The nearest pitch on the selected pitch mesh determines the pitch of the triggered note, and the value of the pixel determines its velocity [5]. The window functions are applied on the column of the matrix. In this paper two window functions are considered: the Hamming window and the Triangular window.

3.1 The Hamming window

The Hamming window it is a raised cosine window of length n having the filter coefficients w(i) = 0.54 - 0.46*cos(2*pi*i/(n-1)) [12]. Figure 2 shows the histograms of the pitch and velocities vectors after passing them through a Hamming window of length 7. It can be noticed that this simple approach modifies the pitch and velocities histogram values and, therefore, create different sounds.

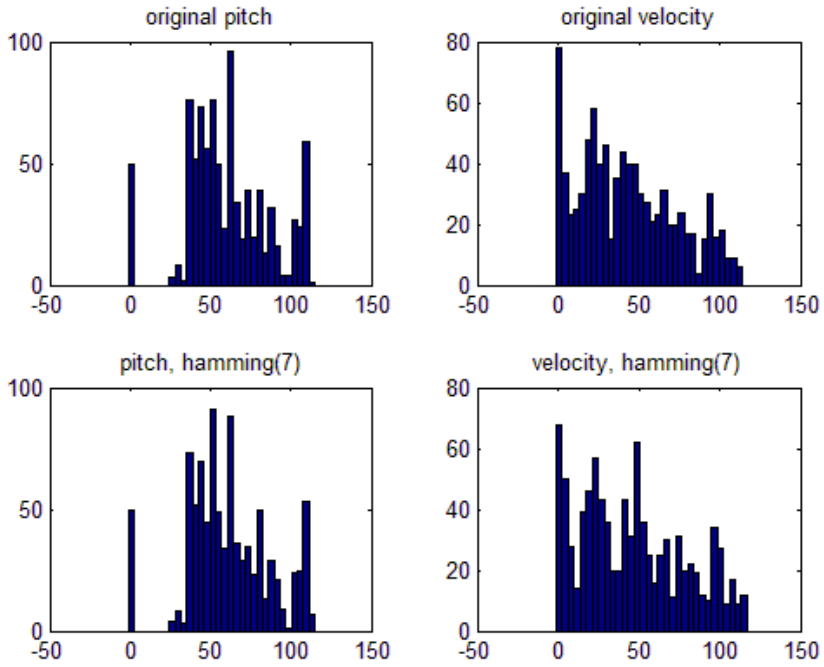

Figure 2. Left side: The histograms of the original pitch and the Hamming windowed pitch (n = 7). Right side: The histograms of the original velocity and the Hamming windowed velocity (n = 7).

Also, it can be noticed from Figure 3 that the Hamming window change the velocity values more than the pitch values. Figure 4 show a comparison of the effect of the window length on both pitch and velocities values. It can be noticed that there is a higher variance on the velocity's values than on the pitch values. Also, the window size influences the generated piano sounds. Therefore, multiple sounds can be generated by using variable length windows while still connecting them with the human body movements for several consecutive frames.

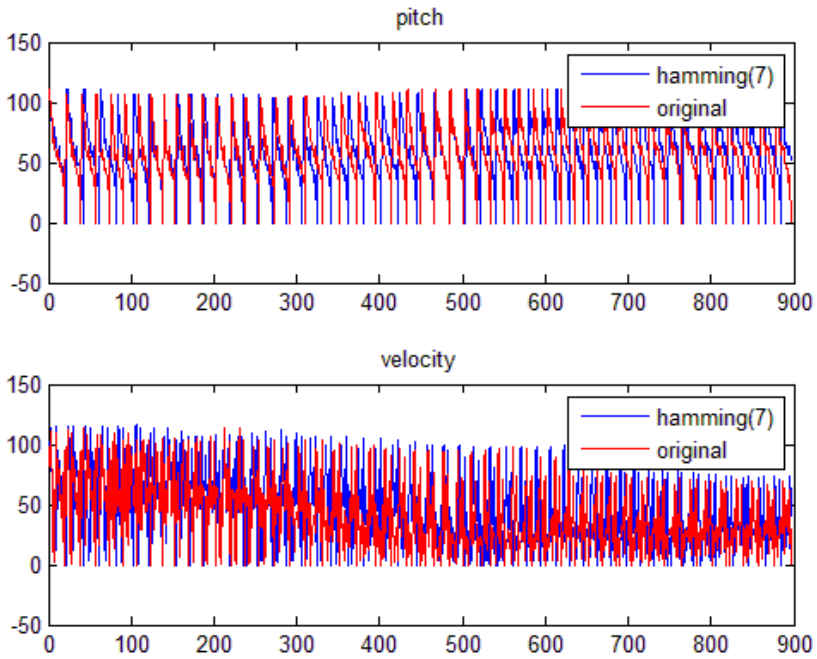

Figure 3. Top: The original pitch value and the Hamming windowed pitch values (n = 7). Bottom: The original velocity values and the Hamming windowed velocity values (n = 7).

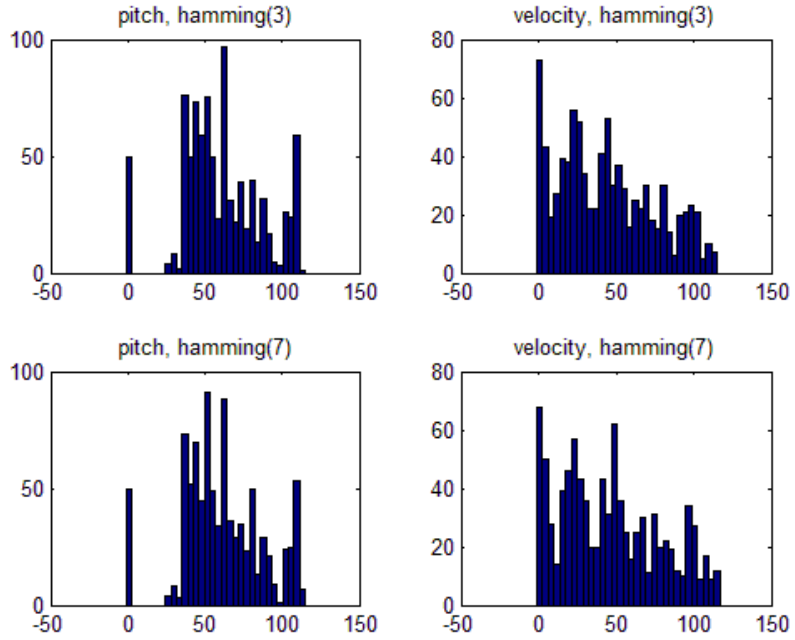

Figure 4 The histograms of the pitch and velocities. Top: Hamming windowed (n = 3). Bottom: Hamming windowed (n = 7).

3.2 The Triangular window

The triangular window can be considered as the convolution of two length (n-1)/2 rectangular windows, where n is an odd number and having the filter coefficients w(i) = 1-2*|i|/(n-1). Figure 5 shows the histograms of the pitch and velocities vectors after passing them through a triangular window of length 7.

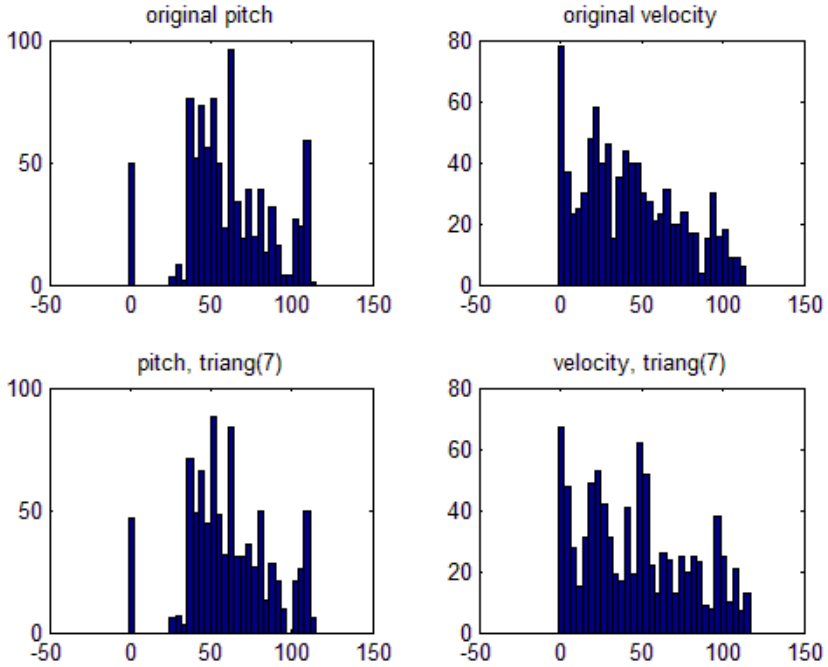

Figure 5 Left side: The histograms of the original pitch and the Triangular windowed pitch (n = 7). Right side: The histograms of the original velocity and the Triangular windowed velocity (n = 7).

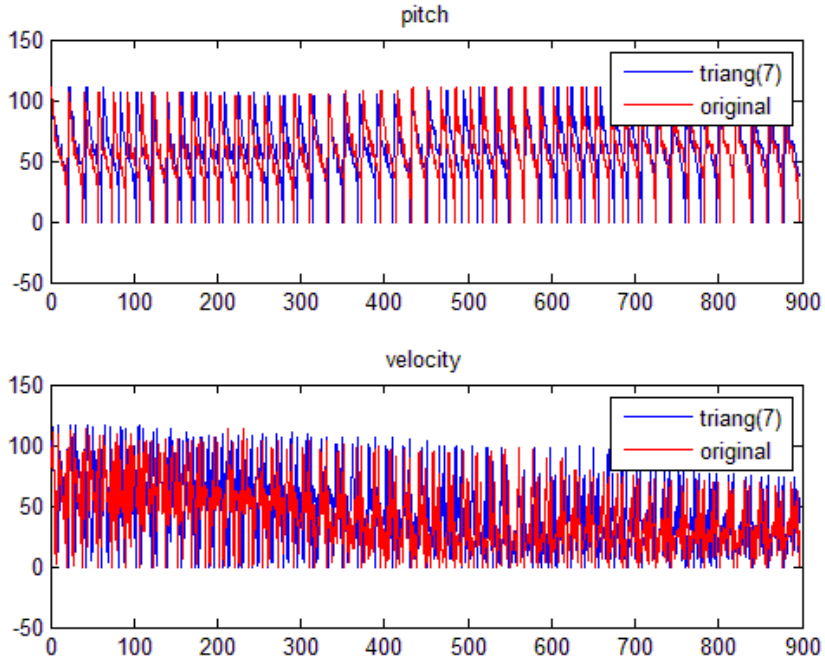

Figure 6 Top: The original pitch value and the Triangular windowed pitch values (n = 7). Bottom: The original velocity values and the Triangular windowed velocity values (n = 7).

Figure 6 shows the original pitch and velocity values and their corresponding triangular windowed values. It can be noticed that similar conclusions to those for the Hamming window can be drawn. There is also a higher variance on the velocity's values than that of the pitch values. By examining Figs. 2, 3, 5, and 6 it is clear that different sounds are generated in most cases by the Triangular window than those generated using the Hamming window. Therefore, the case of generating identical sounds for long periods of time for some repetitive human body movements can be avoided.
Future work will be focused on deriving new filtering methods for the sonification approach and combine various window functions. The use of other possible windows such as Hanning, Kaiser, Blackman [12] will be investigated too.

IV. CONCLUSIONS

An improved piano music generation approach based on human body movements and window functions. The generation of consecutive identical sounds is alleviated through a simple method using window functions operation on columns of joint coordinates matrix. The effectiveness of the method is proved and the influence of the parameters is investigated.

ACKNOWLEDGMENT

The results presented in this work concerns the research carried out for the "SENTIR" research project, co-financed through the European Regional Development Fund, POC–A.1–A1.2.1–D–2015 grant, research, development, and innovation supporting economic competitiveness and the development of businesses.

REFERENCES

[1] T. HERMANN, A. HUNT, J.G. NEUHOFF: The Sonification Handbook, *ISBN 978-3-8325-2819-5, Logos Verlag,* Berlin, 2011.

[2] A. M. TAYLOR, J. ALTOSAAR: Sonification of Fish Movement Using Pitch Mesh Pairs. In Proceedings of the International Conference on New Interfaces for Musical Expression, *Baton Rouge, USA*, June 2015, 28-29, doi: 10.5281/zenodo.1179138.

[3] A. R. JENSENIUS, R. I. GODOY: Sonifying the shape of human body motion using motiongrams. *Empirical Musicology Review*, 7(3), doi:10.18061/emr.v8i2 (2013).

[4] C. ERDEM, K.H. SCHIA, A. R. JENSENIUS: Vrengt: A Shared Body Machine Instrument for Music-Dance Performance. In Proceedings of the international conference on new interfaces for musical expression (nime).doi: 10.5281/zenodo.3672918 (2019)

[5] F. ALBU, M. NICOLAU, F. PIRVAN, D. HAGIESCU: Sonification Method using human body movements. In International Conference on Creative Content Technologies, *Barcelona, Spain*, February 2018, 18-22.

[6] A. CAMURRI, S. HASHIMOTO, M. RICHETTI, R. TROCA, K. SUZUKI, G. VOLPE: Eyesweb: Toward gesture and affect recognition in interactive dance and music systems. *Computer music Journal*, 24 (1), 57-69. Doi: 10.1162/014892600559182 (2000)

[7] MOTIONCOMPOSER software [Online]. http://motioncomposer.de 2021.11.27

[8] POINT MOTION CONTROL software [Online]. http://www.pointmotioncontrol.com/ 2021.11.27

[9] S. WEI, V. RAMAKRISHNA, T. KANADE, and Y. SHEIKH: Convolutional Pose Machines. In IEEE Conference on Computer Vision and Pattern Recognition, *Las Vegas, USA*, June 2016, doi: 10.1109/CVPR.2016.511.

[10] C. S. MYERS, L. R. RABINER: A Comparative Study of Several Dynamic Time-Warping Algorithms for Connected-Word Recognition. *Bell System Technical Journal*, 60 (7), 1389–1409, doi:10.1002/j.1538-7305.1981.tb00272 (1981)

[11] F. ALBU, D. HAGIESCU, M. A. PUICA, L. VLADUTU: Intelligent tutor for first grade children's handwriting application. In IATED 2015, *Madrid*, March 2015, 3708 – 3717.

[12] V. INGLE, J. PROAKIS: Digital signal processing using MATLAB. *ISBN-13: 978-1111427375*, *Brooks/Cole,* (2011)

International Journal of Innovation Engineering and Science Research
(ISSN: 2581-4591)

www.ijiesr.com

A Critical Review of Technology Adoption Theories and Models for E-Learning Systems, Kenya

Kelvin Kabeti Omieno

Senior Lecturer , Department of Information Technology
School of Computing and Information Technology
Kaimosi Friends University College, Kenya

ABSTRACT

E-learning has reshaped traditional education into more flexible and efficient learning in developed nations. However, e-learning remains underutilized and in the rudimentary stages of development in developing countries. Therefore, understanding the critical factors behind the adoption and acceptance of technology is a prime concern in developing countries like Kenya. Several models have been proposed in the literature to understand e-learning acceptance in which social environmental factors are not primarily addressed. This paper aims to improve understanding of what social forces influence employee's attitude and intention of e-learning adoption within an organizational context. This paper contributes to the existing literature by comprehensively reviewing the concepts, applications and development of technology adoption models and theories based on the literature review with the focus on potential application in E-Learning. These included, but were not restricted to, the Theory of Diffusion of Innovations (DIT) (Rogers, 1995), the Theory of Reasonable Action (TRA) (Fishbein and Ajzen, 1975), Theory of Planned Behavior (TPB) (Ajzen, 1985, 1991), Decomposed Theory of Planned Behavior, (Taylor and Todd, 1995), Theory of Human Behavior (Triandis, 1977) and Social Cognitive Theory (Bandura, 1977). These reviews provide a holistic picture for future researchers in selecting appropriate single/multiple theoretical models/constructs based on their strengths and weaknesses and in terms of predictive power and path significance will shed some light and potential applications for technology applications for e-learning. It is concluded that a well-established theory should consider the personal, social, cultural, technological, organizational and environmental factors.

Keywords—*e-learning; TAM; THB; TRA; TBP; DIT; TTF; technology adoption; SCT*

I. INTRODUCTION

In the era of the knowledge economy, knowledge workers need to enhance knowledge and skills continuously to advance their career development. "E-learning" has been expected to play an important role in providing continuing education for knowledge workers. E-learning Management System (EMS) have become one of the most important innovations for delivering education in many parts of the world, this has been facilitated by a rapid expansion of information technologies globally. However, successful implementation and management of these systems is primarily based on its adoption [1]. E-learning has continuously played a vital contribution to the progress of academic staff and students, and the improvement in the quality of teaching method and learning management system which have resulted in increased popularity of education in different educational institutions and organizations [2]. Further it has also enabled learners to access the system at any time and at any place as long as there is an Internet connection. Today, information technology (IT) is universally regarded as an essential tool in enhancing the competitiveness of the economy of a country.

Constant technological change simultaneously creates threats to established business models, while also offering opportunities for novel service offerings ([3], [4], [5], [6]). Leading firms often seek to shape the evolution of technological applications to their own advantage ([7], [4]). A significant number of Universities in Kenya are using E-learning management system as a platform to provide students

with online learning. This enables students to obtain their education in parallel with pursing their personal goals and maintaining their own careers, without a need to attend classes and be subjected to a rigid schedule [8]. These initiatives are however being affected by many barriers that are threatening to bring down this technological innovation. Therefore, this paper presents the literature review of the technology acceptance models and theories leading to the development of the novel technology single platform E-Learning theoretical framework.

This paper analyzed the technology adoption models and theories relevant to e-learning implementation. These included, but were not restricted to, the Theory of Diffusion of Innovations (DIT) [9] that started in 1960, the Theory of Task-technology fit (TTF) [10], the Theory of Reasonable Action (TRA) [11], Theory of Planned Behavior (TPB) [12], Decomposed Theory of Planned Behaviour [13], the Technology Acceptance Model (TAM) [14], Final version of Technology Acceptance Model (TAM) [15], Technology Acceptance Model 2 (TAM2) [15] Unified Theory of Acceptance and Use of Technology (UTAUT), Venkatesh, Morris, Davis and Davis [16] and Technology Acceptance Model 3 (TAM3) [17]. This review could shed some light and potential applications for technology applications for future researchers to conceptualize, distinguish and comprehend the underlying technology models and theories that might affect the previous, current and future application of technology adoption of e-learning systems.

II. RESEARCH METHODOLOGY

Methodology of literature survey was followed for this paper. Research papers with relevant keywords (such as technology adoption, technology adoption theory, technology adoption model etc) were downloaded from online databases like EBSCO, Google Scholar, Proquest, INFORMS etc. The papers were scrutinized to identify and classify them on the basis of themes on which they were focused.

III. TECHNOLOGY ADOPTION MODELS AND THEORIES

The author presents various theories and models for adoption and post adoption of e-lerning systems. Technology life cycle is presented first to appreciate life cycle of information systems in general:

A. Technology Life Cycle

The technology life cycle (TLC) describes the costs and profits of a product from technological development phase to market maturity to eventual decline. Research and development (R&D) costs must be offset by profits once a product comes to market. Varying product lifespans mean that businesses must understand and accurately project returns on their R&D investments based on potential product longevity in the market. Thus, TLC is focused primarily on the time and cost of development as it relates to the projected profits. TLC can be described as having four distinct stages discussed after Figure 1.

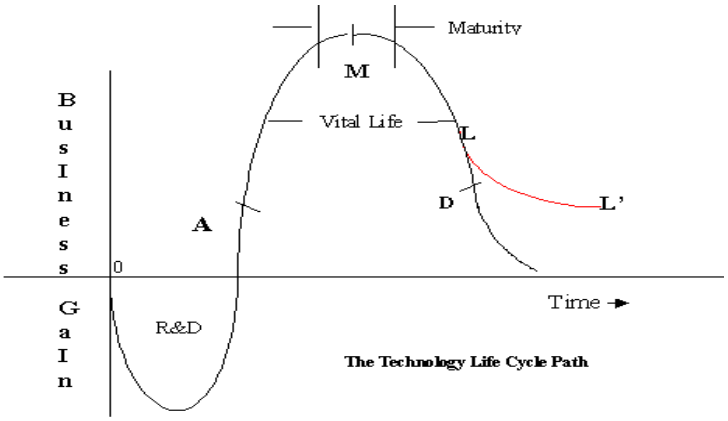

Fig. 1: Technology Life Cycle Chart

- Research and Development – During this stage, risks are taken to invest in technological innovations. By strategically directing R&D towards the most promising projects, companies and research institutions slowly work their way toward beta versions of new technologies.
- Ascent Phase – This phase covers the timeframe from product invention to the point at which out-of-pocket costs are fully recovered. At this junction the goal is to see to the rapid growth and distribution of the invention and leverage the competitive advantage of having the newest and most effective product.
- Maturity Stage – As the new innovation becomes accepted by the general population and competitors enter the market, supply begins to outstrip demand. During this stage, returns begin to slow as the concept becomes normalized.
- Decline (or Decay) Phase – The final phase is when the utility and potential value to be captured in producing and selling the product begins dipping. This decline eventually reaches the point of a zero-sum game, where margins are no longer procured.

B. Task-Technology Fit Theory

Task-technology Fit (TTF) emphasizes individual impact [10]. Individual impact refers to improved efficiency, effectiveness, and/or higher quality. Goodhue et al. [10] assumed that the good fit between task and technology is to increase the likelihood of utilization and also to increase the performance impact since the technology meets the task needs and wants of users more closely. As shown in Fig. 2. this model is suitable for investigating the actual usage of the technology especially testing of new e-learning technology to get feedback. This theory is good for measuring the technology applications already release in the marketplace such as Moodle.

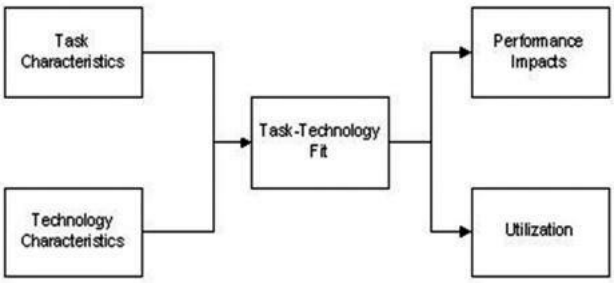

Fig. 2: Task-technology fit [10]

C. Diffusion of Innovation Theory

Rogers [9] proposed that the theory of 'diffusion of innovation' was to establish the foundation for conducting research on innovation acceptance and adoption. The diffusion of innovation theory explains that the innovation and adoption happened after going through several stages including understanding, persuasion, decision, implementation, and confirmation that led to the development of [9] S-shaped adoption curve of innovators, early adopters, early majority, late majority and laggards as shown in Fig. 3.

Diffusion of innovation is affected by readiness. Technology readiness (TR) refers to people's propensity to embrace and use of new technologies for accomplishing goals in home life and at work [19]. Based on individual's technology readiness score and the technology readiness, [9] further classified technology consumers into five technology readiness segments of explorers, pioneers, skeptics, paranoids, and laggards.

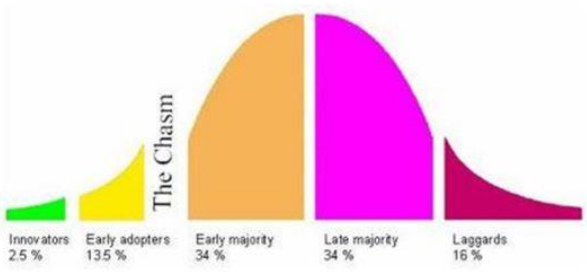

Fig. 3: Innovation Adoption Curve [9]

Rogers [9] S-shaped adoption curve consists of innovators, early adopters, early majority, late majority and laggards. This is actually what happens to various instituions adopting e-learning systems. The Diffusion of innovation or Technology readiness is vital for organization implementation success because it is market focus.

D. Theory of Reasonable Action

Fishbein and Ajzen [11] proposed the Theory of Reasonable Action. This is one of the most popular theories used and is about one factor that determines behavioral intention of the person's attitudes toward that behaviour as shown in Fig. 4. [11] defined "attitude" as the individual's evaluation of an object and defined "belief" as a link between an object and some attribute, and defined "behaviour" as a result or intention. Attitude has a great impact on the extent to which users will embrace e-learning solutions for their operations.

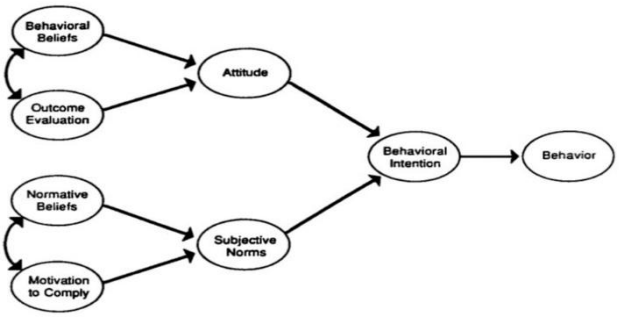

Fig. 4: The Theory of Reasonable Action [11]

E. Theory of Planned Behavior

This theory by Ajzen [1] is about perceived behavioral control as a factor that determines behavioural intention of the person's attitudes toward that behaviour as shown in Fig. 5. This factor is an addition to the first two factors as defined in Theory of Reasonable Action [11]. Perceived control behaviour is the control which users perceive that may limit their behaviour (e.g: Can I take online studies through Moodle learning management system and what are the requirements?). Fig.5. shows TPB.

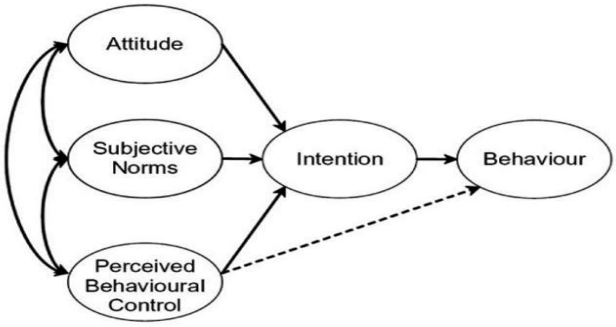

Fig. 5: The Theory of Planned Behavior [12]

However, there is an enhancement of the TPB. This is the Decomposed Theory of Planned Behaviour (Decomposed TPB) which was introduced by [13]. The Decomposed TPB consists of three main factors influencing behavior intention and actual behavior adoption which are attitude, subjective norms and perceived behavior control

F. Technology Acceptance Model

Technology Acceptance Model (TAM) was introduced by Davis in 1986 as shown in Fig. 6. An adaptation of Theory of Reasonable Action, TAM [19] is specifically tailored for modeling users' acceptance of information systems or technologies. TAM attempts to help researchers and practitioners to distinguish why a particular technology or system may be acceptable or unacceptable and take up suitable measures by explanation besides providing prediction

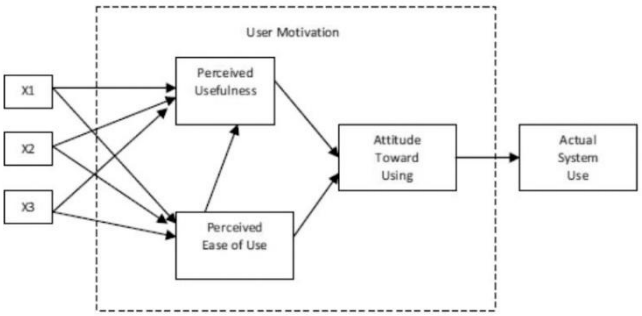

Fig. 6: Original Technology Acceptance Model [19]

In 1989 Davis used TAM to explain computer usage behaviour as shown in Fig. 7. The purpose for the modification of original TAM was to explain the general determinants of computer acceptance that lead to explaining users' behaviour across a broad range of end-user computing technologies and user populations. The basic TAM model included and tested two specific beliefs: Perceived Usefulness (PU) and Perceived Ease of Use (PEU). Perceived Usefulness is defined as the potential user's subjective likelihood that the use of a certain system (e.g: single platform E-Learning System) will improve his/her action and Perceived Ease of Use refers to the degree to which the potential user expects the target system to be effortless [20]. The belief of the person towards a system may be influenced by other factors referred to as external variables in TAM.

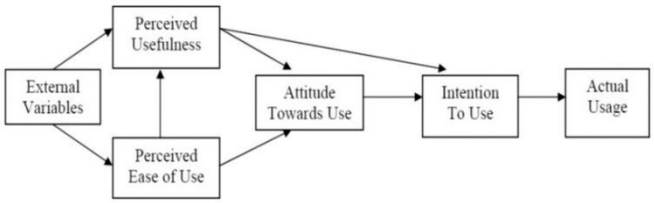

Fig. 7: First modified version of Technology Acceptance Model (TAM) [14]

The final version of Technology Acceptance Model was formed by [21] as shown in Fig. 8 after the main finding of both perceived usefulness and perceived ease of use were found to have a direct influence on behaviour intention, thus eliminating the need for the attitude construct.

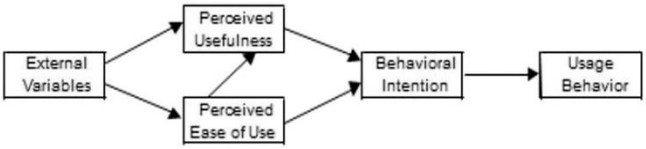

Fig. 8: Final version of Technology Acceptance Model (TAM) [21]

G. Theory of Human Behavior

This theory is drawn from social studies. The Model of PC Utilization [22]. The model is based on the Theory of Human Behaviour by [23] which differs in some ways from the Theory of Reasoned Action because it makes a distinction between cognitive and affective components of attitudes. Beliefs belong to the cognitive component of attitudes.

According to this theory "Behaviour is determined by what people would like to do (attitudes), what they think they should do (social norms), what they have usually done (habits), and by the expected consequences of their behavior". This theory primarily deals with extent of utilization of a computing device by a worker where the use is not mandated by the organization but is contingent on the option of the user. In such a setting, the theory posits that the use of computers is likely to be influenced by several factors such as his feelings (affect) toward using the devices, prevalent social norms regarding use of computing devices at the work place, general habits related to use of the computer, consequences expected through use of computing devices and extent of conditions that are present at the work place for facilitating use of technologies.

H. Social Cognitive Theory

Social Cognitive Theory (SCT) explains how people acquire and maintain certain behavioral patterns based on the learning from others [24]. SCT theorizes that portions of an individual's knowledge acquisition can be directly related to observing others within the context of social interactions, experiences, and outside media influences. The theory suggests that behavior is affected by both outcome expectations and self-efficacy, while outcome expectations and self-efficacy are in turn influenced by prior behavior. In the postadoption research self-efficacy also influences continued intention to use a technology ([25], [26]).

IV. E-LEARNING POST ADOPTION THEORIES

Since adoption research mainly focuses on the binary condition of people's initial adoption or non-adoption, these research studies have not captured the dynamics of the postadoption behavior of technology use. In this study, post-adoption behavior can be approached as a cognitive process where people consciously examine their technologies during the usage stage [31]. These theories also reflect on people's cognitive reasoning, in regards to their post-adoption decision making processes.

A. Expectation Confirmation Theory

This theory was originally developed by Oliver [28] and it theorizes that consumer's post-purchase satisfaction is jointly determined by prepurchase expectation, perceived performance (of technology), and expectancy confirmation. ECT is a cognitive theory which seeks to explain post-purchase or post-adoption satisfaction as a function of expectations, perceived performance, and disconfirmation of beliefs. The theory explains the cause of satisfaction by focusing on both the antecedents of satisfaction and the satisfaction formation process [29].

Fig. 11: Expectation Confirmation Theory [28]

There are several studies that used the ECT as a major theoretical framework in studying the post-adoption behavior of ICTs such as e-learning systems. Many of these studies found that confirmation has statistically significant relationships with various adoption and use constructs including perceived

usefulness ([30], [31], [32]), perceived ease of use ([30], [33]), perceived enjoyment [33], perceived behavioral control [34], and finally satisfaction [35], [36].

B. IS Continuance Model

Bhattacherjee [35] proposed a theoretical model of IS continuance that takes into account the distinctions between acceptance and continuance behaviors as illustrated in Fig. 12.

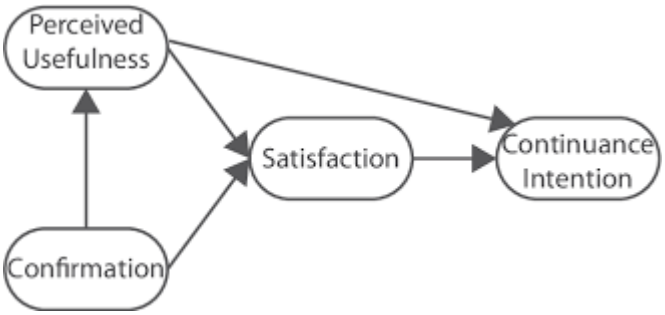

Fig. 12: IS Continuance Model [35]

This model is grounded on the resemblance between individuals' continuous IS usage decisions and consumers' repeated purchase decisions by using the ECT. In both ECT and IS Continuance model satisfaction is a key concept in post-adoption behavior. [37] also argued that satisfaction represents a construct that is partly cognitive and partly emotional. Various IS scholars found out that satisfaction is an important component of IS use and an indicator of system success [38, 39]. This has seen som scholars who have tried to integrate user satisfaction and technology acceptance [40]. It can be deduced that that users' continuance intention is determined by their satisfaction with IS use and perceived usefulness of continued IS use. User satisfaction, in turn, is influenced by their confirmation of expectation from prior IS use and perceived usefulness. Post- acceptance perceived usefulness is influenced user's confirmation level. This is a very important aspect when analyzing post-adoption trends of e-learning systems.

V. CONCLUSIONS

The main objective of this paper is to review theories and models that can be used in e-learning adoption research. Through this review, share the difference of technology adoption models and theories with different theoretical insights, research problems, variables, and measurements, we proposed some possible solutions for studying the post-adoption behavior of e-learning technology. The paper presents a theoretical framework by considering cognitive, affective, and habitual factors to study scientists continued use of e-learning technologies. These reviews will shed some light and potential applications for technology applications for future researchers to conceptualize, distinguish and comprehend the underlying technology models and theories that may affect the previous, current and future application of technology adoption in the area of learning. This research paper could be the first step in understanding the main adoption and continued-use factors for scientists on e-learning technologies in Kenya and beyond

REFERENCES

[1] Chiu, C., & Wang, E. T. G. (2008). Understanding web-based learning continuance intention: The role of subjective task value. Information & Management, 45(3), 194-201

[2] Basheer, A. A.-a., & Ibrahim, A. M. (2011). Measuring the acceptance and adoption of E-learning by academic staff. Knowledge Management & E-learning: An International Journal, 3 (2), 201 -221.

[3] Lai, P. C. (2006). The significant of E-business and knowledge-based Customer Relationship in the E-market Place Environment. INTI Journal, 2(1) 552-559.

[4] Lai, P. C. (2007). The Chip Technology Management Implication in the Era of Globalization: Malaysian Consumers' Perspective, Asia Pacific Business Review, 3(1), 91-96

[5] Lai, P. C. (2010). E-business and E-banking. Japan Society for Software Science and Technology, Itech research group.

[6] Lai, P. C. (2014) Factors influencing consumers' intention to use a single platform E-Learning System. UNITEN

[7] Lovelock, C. 2001. Services Marketing, People, Technology, Strategy, Prentice Hall, New Jersey.

[8] Borstorff, P. C., & Lowe, S. L. (2007). Students perceptions and opnions toward e-learning in the college environment. Academy of Educational Leadership Journal, 11 (2), 13 - 30.

[9] Rogers, E.M. (1995). Diffusion of Innovations. 4th ed., New York: The Free Press

[10] Goodhue, D. L., & Thompson, R. L. (1995). Task technology fit and individual performance. MIS Quarterly , 19, 213-236.

[11] Fishbein, M., & Ajzen, I. (1975). Belief, attitude, intention, and behavior: An introduction to theory and research. Reading, Mass; Don Mills, Ontario: Addison-Wesley Pub. Co.

[12] Ajzen, I. (1991). The Theory of Planned Behavior. Organization Behavior and Human Decision Processes, Academic Press, Inc. 179-211.

[13] Taylor, S. and Todd, P. A. (1995). Understanding Information Technology Usage: A Test of Competing Models. Information Systems Research , 6, 144-176.

[14] Davis, F. D., Bogozzi, R. P., & Warshaw, P. R. (1989). User acceptance of computer technology: A comparison of two theoretical models. Management Science, 35, 982-1003.

[15] Venkatesh, V., & Davis, F. D. (2000). A Theoretical Extension of the Technology Acceptance Model: Four Longitudinal Field Studies. Management Science , 46(2), 186-204.

[16] Venkatesh, V., Morris, M.G., Davis, F.D., & Davis, G.B. (2003). User Acceptance of Information Technology: Toward a Unified View. MIS Quarterly, 27, 425-478.

[17] Venkatesh, V. and Bala, H. (2008). Technology Acceptance Model 3 and a Research Agenda on Interventions. Decision Science, 39(2), 273-312.

[18] Chang, S. C., & Tung, F. C. (2008). An empirical investigation of students' behavioral intentions to use the online learning course websites. British Journal of Educational Technology, 39(1), 71-83

[19] Davis, F.D. (1986). A technology acceptance model for empirically testing new end-user information systems: Theory and results. Massachusetts, United States: Sloan School of Management, Massachusetts Institute of Technology.

[20] Davis, F. D. (1989). Perceived usefulness, perceived ease of use, and user acceptance of information technology. MIS Quarterly, 13(3), 319-340.

[21] Venkatesh, V., & Davis, F. D. (1996). A model of the antecedents of perceived ease of use: Development and test. Decision Sciences, 27(3), 451-481.

[22] Thompson, R. L., Higgins, C. A., & Howell, J. M. (1991). Personal computing: Toward a conceptual model of utilization. MIS Quarterly, 15(1), 124-143.

[23] Triandis, H. C. (1977). Interpersonal behavior. Monterey, CA: Brooke/Cole.

[24] Bandura, A. (1977). Social Learning Theory. Englewood Cliffs, NJ: Prentice-Hall.

[25] Parasuraman, A., & Colby, L. C. (2001). Techno-Ready Marketing, The Free Press.

[26] Keller, C., & Cernerud, L. (2002). Students' Perceptions of E-Learning in University Education. Journal of Educational Media, 27(1-2), 55-67.

[27] Chen, M. S., & Hsu, K. P. (2007). The Effects of Asynchronous E-learning Situation on Learning Perception and Usage Intention. Journal of Human Resource Management, 7(3), 25-44.

[28] Oliver, R. L. (1980). A Cognitive Model for the Antecedents and Consequences of Satisfaction. Journal of Marketing Research, 17, 460–469.

[29] Susarla, A., Barua, A., & Whinston, A. B. (2003). Understanding the Service Component of Application Service Provision: An Empirical Analysis of Satisfaction with ASP Services. MIS Quarterly, 27(1), 91-123.

[30] Hong, S., Thong, J. Y. L., & Tam, K. Y. (2006). Understanding continued information technology usage behavior: A comparison of three models in the context of mobile internet. Decision Support Systems, 42(3), 1819-1834.

[31] Lippert, S. K. (2007). Investigating Postadoption Utilization: An Examination Into the Role of Interorganizational and Technology Trust. IEEE Transaction on Engineering Management, 54(3), 468- 483.

[32] Roca, J. C., & Gagné, M. (2008). Understanding e-learning continuance intention in the workplace: A selfdetermination theory perspective. Computers in Human Behavior, 24(4), 1585-1604.

[33] Thong, J. Y. L., Hong, S.-J., & Tam, K. Y. (2006). The effects of post-adoption beliefs on the expectationconfirmation model for information technology continuance. International Journal of Human Computer Studies, 64(9), 799-810.

[34] Hsu, M.-H., & Chiu, C.-M. (2004). Predicting electronic service continuance with a decomposed theory of planned behaviour. Behaviour & Information Technology, 23(5), 359 - 373.

[35] Bhattacherjee, A. (2001a). An empirical analysis of the antecedents of electronic commerce service continuance. Decision Support Systems, 32(2), 201- 214.

[36] Bhattacherjee, A. (2001b). Understanding Information Systems Continuance: An Expectation-Confirmation Model. MIS Quarterly, 25(3), 351-370.

[37] Smith, A., & Bolton, R. (2002). The effect of customers' emotional responses to service failures on their recovery effort evaluations and satisfaction judgments. Journal of the Academy of Marketing Science, 30(1), 5- 23.

[38] DeLone, W. H., & McLean, E. R. (1992). Information Systems Success: The Quest for the Dependent Variable. Information Systems Research, 3(1), 60-95.

[39] Bailey, J., & Pearson, S. (1983). Development of a tool for measuring and analyzing computer user satisfaction. Management Science, 29(5), 530-545

[40] Wixom, B., & Todd, P. (2005). A theoretical integration of user satisfaction and technology acceptance. Information Systems Research, 16(1), 85-102

International Journal of Innovation Engineering and Science Research
(ISSN: 2581-4591)
www.ijiesr.com

An Application of LADM-Padé Approximation for the Analytical Solution of the SIR Infectious Disease Model

L. Ebiwareme, R. E. Akpodee, R. I. Ndu
Faculty of Science, Department of Mathematics, Rivers State University, Port Harcourt, Nigeria.

ABSTRACT

This article is aimed at finding analytical solution to the dynamics of the epidemic model. The autonomous nonlinear differential equation was reduced to algebraic equation via Laplace transform method subject to the initial condition. The LADM was then employed to obtain the approximate analytical solution for the pertinent parameters of interest. In view to match the obtained solution as far as possible, the Padé approximant is applied to the partial sum of the obtained analytical solution to improve its convergence. Maple is used in the computation and the results are presented graphically and in tables. The result obtained agrees with literature and shows the adopted method is accurate, flexible, and reliable.

Keywords: *Epidemic model, Adomian decomposition, LaplaceAdomian decomposition, Padé Approximation, Runge-Kutta, Decomposition series, Laplace Transformation*

I. INTRODUCTION

From prehistoric times until now, the world has been ravaged by diverse kinds of epidemics ranging from malaria, Ebola, Dengue, HIV-AIDS, COVID-19, and others. These diseases have caused mankind problems in their wake with severe fatalities especially in the third world countries who neither have the wherewithal nor the technology to nip them in the bud. For example, the world health organization in their latest bulletin stressed if the scourging effects of malaria is not mitigated by increased vaccination and qualified personnel, an estimated half a billion infant mortality wouldn't be averted in Africa and North America. Equally, the report painted a gory picture of paucity of funds from third world countries and donor organization to tackle frontally polio myelitis which have been prevalent and been the major cause of child mortality in sub-Saharan Africa.

Infectious diseases have adverse and tremendous effect on human population. Millions of human beings either suffer or die from diverse infectious disease every year [1]. Among these diseases, the childhood diseases are the most common form of killer infectious diseases. They include measles, mumps, chicken pox, polio myelitis etc... to which every child under age five is born susceptible to and contracts [2]. These diseases spread faster among children because they are always in close contact either at school or during play. Therefore, containing these childhood diseases to protect children from contracting them by way of early vaccination been the viable and effective strategy became a front burner among health authorities especially in the third world countries which are most prone [3]. Equally, aside early vaccination against these diseases, mathematical models have also been used extensively to study the dynamics and spread of these epidemics and diseases. The models can quantitatively predict how the disease spread and the factors responsible for their progression. The result obtained from these models are useful in the implementation of strategy to curb the spread and development of these diseases.Kermack and McKendrick developed the classical SIR model for

epidemic diseases in 1927. The framework for these model fits exactly how various diseases spread and affects humanity even after vaccination. In this model, the total population denoted N is subdivided into three class namely: Those susceptible to the disease denoted N, the infected number of people, I and the removed number or people immune to the disease after treatment, R. This model has been successfully used to describe several epidemiological diseases. [4-10].

The Adomian decomposition method introduced by G. Adomian [11-13] has shown great potential in solving a wide variety of problems ranging from linear as well as nonlinear differential and partial differential equations. This method requires writing the unknown function as a decomposition series, the nonlinear terms as an Adomian polynomial and matching both sides to obtain a recursive algorithm where the rapidly convergent series solution is then obtained which is equivalent to the closed form or exact solution of the problem if it exists. It has been successfully applied to solve problems in many scientific fields such as plasma physics, fluid mechanics, solid state physics, chemical kinetics, population dynamics and engineering. Equally, most recently most authors adore its appeal and has applied it to the following areas: A Comparison between Adomian decomposition method and Taylor series method in the series solutions, Analytical solution of a time-fractional Navier-Stokes equation by Adomian decomposition, delay differential equations, systems of nonlinear equations, nonlinear integro-differential equations, nonlinear analytical techniques, convergence of nonlinear equations and Falkner-Skan equation for a Wedge. [14-21]. This method is advantageous over other methods in that it does not require linearization, perturbation, and discretization.

The hybrid Laplace transform, and the domain decomposition method introduced by Khuri [22-23] has equally be given considerable attention. This method is powerful and preferable to Adomian decomposition because it accelerate the rapid convergence of the series solution. [24] employed the Laplace Adomian decomposition method to solve linear and nonlinear systems of PDEs. Coupled systems of PDEs have been examined using LADM by [25], [26] explored the Duffing equation numerically using the combined Laplace Adomian decomposition method. [27] used LADM to examine the HIV model. The Newell-Whitehead-Segel have been investigated using LADM by [28]. Combined Laplace transform and Adomian decomposition method have been used to analyze systems of systems of ordinary differential equation [29]. [30-38] have also employed LADM to investigate the following problems viz: linear and nonlinear Volterra integral equations with weak kernel, nonlinear Volterraintegro-differential equations, nth order integro-differential equations, integro-differential equations, two-dimensional viscous fluid with shrinking sheet, numerical solution of logistics differential equations, convection diffusion-dissipation equation, nonlinear fractional differential equation and numerical solution of the crime deterrence model in society.
In this article, we use the Laplace Adomian decomposition method to seek analytical solution of the SIR epidemic model. The nonlinear differential equations are solved for the governing parameters for the problem. The article is composed as follows. The introduction and fundamentals of the Adomian decomposition methods are in sections 1& 2. The combination of Laplace and Adomian decomposition method is contained in section 3. Sections 4& 5 presents the Padé approximation and application of LADM to the model. Section 6 presents the graphical representation of the analytical solution and its comparison in tables. Finally, the conclusion in section 7.

II. BASICS OF THE ADOMIAN DECOMPOSITION METHOD

Consider a functional inhomogeneous differential equation of the form

$$Fy = g(x) \tag{1}$$

Where F is a nonlinear differential operator and y, g are the unknown function and the source term. Dividing the operator as the sum of $L + R + N$ as follows. Eq. (1) now become

$$Ly + Ry + Ny = g(x) \tag{2}$$

Where L is the highest order derivative that's invertible, R is a linear differential operator, N is a nonlinear term and g is the source term.
Rewriting Eq. (2) in the form

$Ly = g(x) - Ry - Ny$

(3)Applying L^{-1}on both sides of the equation **(3)** to obtain

$L^{-1}(Ly) = L^{-1}\big(g(x)\big) - L^{-1}(Ry) - L^{-1}(Ny)$ (4)

$y(x) = L^{-1}\big(g(x)\big) - L^{-1}(Ry) - L^{-1}(Ny)$

Eq. (4**)** can be written alternatively as

$y(x) = \phi - L^{-1}(Ry) - L^{-1}(Ny)$ (5)

Where ϕ represents the term arising from integrating the source term, g. That is, $[L^{-1}(g)]$ and from the given conditions.

Using the standard Adomian decomposition method the zeroth component is written as,

$y_0 = \phi$

And the recursive relation is given by

$y_{n+1} = -L^{-1}(Ry_n) - L^{-1}(Ny_n), \quad n \geq 0$ (6)

For $n = 0$

$y_1 = -L^{-1}(Ry_0) - L^{-1}(Ny_0)$

For $n = 1$

$y_2 = -L^{-1}(Ry_1) - L^{-1}(Ny_1)$

For $n = 2$

$y_3 = -L^{-1}(Ry_2) - L^{-1}(Ny_2)$

Now, writing the unknown the solution of the problem as a decomposition series of the form

$y(x) = \sum_{n=0}^{\infty} y_n(x)$ (7)

Here, the nonlinear term can be determined by an infinite series of Adomian polynomials

$Ny = \sum_{n=0}^{\infty} A_n$ (8)

where $A_n^1 s$ are obtained from the relation

$A_n = \frac{1}{n!}\frac{d^n}{d\lambda^n}[N(\sum_{x=0}^{n} \lambda^i y_i)]_{t=0}, \qquad n = 0,1,2,3,\ldots$ (9)

III. FUNDAMENTALS OF THE LAPLACE ADOMIAN DECOMPOSITION METHOD

In this subsection, we discuss the use of the hybrid Laplace transformation and Adomian decomposition algorithm for the nonlinear autonomous first order differential equations governing the problem. For convenience, we consider a first order nonhomogeneous functional differential equation subject to initial condition of the form

$L[u(x)] + R[u(x)] + N[u(x)] = g(x)$ (10)

$u(0) = f(x)$ (11)

$L[u(x)] = g(x) - R[u(x)] - N[u(x)]$ (12)

Applying Laplace transform to both sides of Eq. (10), and using the differentiation property, we get

$s\mathcal{L}\{u(x)\} - f(x) = \mathcal{L}\{g(x)\} - \mathcal{L}\{Ru(x)\} - \mathcal{L}\{Nu(x)\}$

$s\mathcal{L}\{u(x)\} = f(x) + \mathcal{L}\{g(x)\} - \mathcal{L}\{Ru(x)\} - \mathcal{L}\{Nu(x)\}$

$\mathcal{L}\{u(x)\} = \frac{f(x)}{s} + \frac{1}{s}\mathcal{L}\{g(x)\} - \frac{1}{s}\mathcal{L}\{Ru(x)\} - \frac{1}{s}\mathcal{L}\{Nu(x)\}$ (13)

Applying the inverse Laplace transform to both sides of Eq. (13), we obtain

$u(x) = \phi(x) - \mathcal{L}^{-1}\left[\frac{1}{s}\mathcal{L}\{Ru(x)\} - \frac{1}{s}\mathcal{L}\{Nu(x)\}\right]$ (14)

Where $\phi(x)$ is the term arising from the first three terms on the right-hand side of Eq. (14).

Next, we assume the solution of the problem as a decomposing series in the form

$$u(x) = \sum_{n=0}^{\infty} u_n(x) \tag{15}$$

Similarly, the nonlinear terms are written in terms of the Adomian polynomials as

$$Nu(x) = \sum_{n=0}^{\infty} A_n \tag{16}$$

Where the $A_n^{'s}$ represents the Adomian polynomials defined in the form

$$A_n = \frac{1}{n!}\frac{d^n}{d\lambda^n}[N(\sum_{k=0}^{\infty}\lambda^i y_i)]_{i=0}, n = 0,1,2,3 \tag{17}$$

Plugging Eqs. (15) and (16) into Eq. (17), we obtain

$$\sum_{n=0}^{\infty} u_n(x) = \phi(x) - \mathcal{L}^{-1}\left[\frac{1}{s}\mathcal{L}\{R\sum_{n=0}^{\infty} u_n(x)\} - \frac{1}{s}\mathcal{L}\{N\sum_{n=0}^{\infty} A_n\}\right] \tag{18}$$

Matching both sides of Eq. (18), we obtain an iterative algorithm in the form

$$\begin{aligned} u_0(x) &= \phi(x) \\ u_1(x) &= -\mathcal{L}^{-1}\left[\frac{1}{s}\mathcal{L}\left\{R\sum_{n=0}^{\infty} u_0(x)\right\} - \frac{1}{s}\mathcal{L}\left\{N\sum_{n=0}^{\infty} A_0\right\}\right] \\ u_3(x) &= -\mathcal{L}^{-1}\left[\frac{1}{s}\mathcal{L}\{R\sum_{n=0}^{\infty} u_2(x)\} - \frac{1}{s}\mathcal{L}\{N\sum_{n=0}^{\infty} A_2\}\right] \end{aligned} \tag{19}$$

$$\vdots$$

$$u_{n+1}(x) = -\mathcal{L}^{-1}\left[\frac{1}{s}\mathcal{L}\left\{R\sum_{n=0}^{\infty} u_n(x)\right\} - \frac{1}{s}\mathcal{L}\left\{N\sum_{n=0}^{\infty} A_n\right\}\right]$$

Then the solution of the differential equation is obtained as the sum of decomposed series in the form

$$u(x) \approx u_0(x) + u_1(x) + u_2(x) + \cdots \tag{20}$$

IV. PADÉ APPROXIMATION

In mathematics and other applied sciences, rational functions are functions which the degree of the denominator is either equal or greater than the degree of the numerator all expressed as polynomials. In seeking to write these functions in Taylor series form, difficulties often arise in the form of divergent, singularities and radius of convergence which blow up occur. To curtail these inherent difficulties, there was need for a new way of expressing rational functions.

The Padé approximant is a particular and classical type of rational approximation originally credited to George Frobenius who introduced the idea and study the features of the rational power approximation. Henri Padé around 1890 was the one who made significant contributions by expressing it as the quotient of two polynomials with varying degrees. It is superior to the Taylor series expansion in that it provides better approximation of the function than truncating the Taylor series especially where the Taylor series does not converge and when it contains poles. The approximation has been extensively applied to calculate time delay and in computer science. [39-43].

Now, given two polynomials, $P_L(x)$ and $Q_M(x)$ with highest degrees of N and M. Then the Pade approximant of function, $f(x)$in each closed interval $[a, b]$ denoted $[L/M]$ is the ratio of the polynomials in the form.

$$[L/M] = \frac{P_L(x)}{Q_M(x)} \tag{21}$$

The power series of the given function is given as

$$f(x) = \sum_{n=0}^{\infty} a_k x^k \tag{22}$$

To determine the coefficients of the polynomials $P_L(x)$ and $Q_M(x)$, we use the equation

$$f(x) = \frac{P_L(x)}{Q_M(x)} + O(x^{L+M+1}) \tag{23}$$

Using the standard normalization condition

$$Q_M(0) = 1.0 \tag{24}$$

Expressing the coefficients of the two polynomials explicitly in the form

$$\begin{cases} P_L(x) = p_0 + p_2 x + \cdots + p_L x^L \\ Q_M(x) = 1 + q_1 x + \cdots + q_M x^M \end{cases} \tag{25}$$

In view of Eq. (25), multiplying both sides of Eq. (23) by $Q_M(x)$ yield the system of equations and linearized the coefficient equation in the form.

$$\left.\begin{array}{l} q_m a_{L-M+1} + q_{M-1} a_{L-M+2} + \cdots + q_0 a_{L+1} = 0 \\ q_m a_{L-M+2} + q_{M-1} a_{L-M+3} + \cdots + q_0 a_{L+2} = 0 \\ \cdots\cdots\cdots\cdots\cdots\cdots\cdots\cdots\cdots\cdots\cdots\cdots\cdots\cdots\cdots\cdots\cdots \\ q_M a_{L-M+2} + q_{M-1} a_{L-M+3} + \cdots + q_0 a_{L+2} = 0 \end{array}\right] \tag{26}$$

We set $q_0 = 1$, and if $j > 0$, then $a_i = 0$. The system in Eq. (26) reduced to the form

$$\begin{pmatrix} a_{L-M+1} & a_{L-M+2} \ldots . a_{L+1} \\ a_{L-M+2} & a_{L-M+3} \ldots\ldots a_{L+2} \\ \cdots\cdots\cdots\cdots\cdots\cdots\cdots\cdots \\ a_L & a_{L+1} \ldots\ldots\ldots\ldots\ldots\ldots\ldots a_{L+M} \end{pmatrix} \begin{pmatrix} q_m \\ q_{M-1} \\ \vdots \\ q_1 \end{pmatrix} = \begin{pmatrix} a_{L+1} \\ a_{L+2} \\ \vdots \\ a_{L+M} \end{pmatrix} \tag{27}$$

Solving the system in Eq. (27) produces the solution in the form

$$\left.\begin{array}{c} a_0 = p_0 \\ a_0 + a_0 q_1 + \cdots = p_1 \\ \cdots\cdots\cdots\cdots\cdots\cdots\cdots\cdots \\ a_L + a_{L-1} q_1 + \cdots + a_0 q_1 = p_L \end{array}\right] \tag{28}$$

The Padé approximant of different orders such as $[2/2], [3/3], [4/4], [5/5]$ and $[6/6]$ are obtained using Maple 20.

V. APPLICATION OF LADM TO THE EPIDEMIC MODEL

We consider the epidemiological disease model as follows

$$\left.\begin{array}{l} \frac{dS}{dt} = -\beta SI \\ \frac{dI}{dt} = \beta SI - \mu I \\ \frac{dR}{dt} = \mu I \end{array}\right] \tag{29}$$

Subject to the initial conditions

$$S(0) = 0.9,\ I(0) = 0.1, R(0) = 0 \tag{30}$$

Taking the Laplace transform of both sides of Eq. (29), we get

$$\begin{bmatrix} \mathcal{L}\left\{\frac{dS}{dt}\right\} = \mathcal{L}\{-\beta SI\} \\ \mathcal{L}\left\{\frac{dI}{dt}\right\} = \mathcal{L}\{\beta SI - \mu I\} \\ \mathcal{L}\left\{\frac{dR}{dt}\right\} = \mathcal{L}\{\mu I\} \end{bmatrix} \quad (31)$$

$$\begin{bmatrix} \mathcal{L}\left\{\frac{dS}{dt}\right\} = -\beta\mathcal{L}\{SI\} \\ \mathcal{L}\left\{\frac{dI}{dt}\right\} = \beta\mathcal{L}\{SI\} - \mu\mathcal{L}\{I\} \\ \mathcal{L}\left\{\frac{dR}{dt}\right\} = \mu\mathcal{L}\{I\} \end{bmatrix} \quad (32)$$

Applying the differentiation law of Laplace transforms, we obtain

$$w\mathcal{L}\{S\} - S(0) = -\beta\mathcal{L}\{SI\} \quad (33)$$

$$w\mathcal{L}\{I\} - I(0) = \beta\mathcal{L}\{SI\} - \mu\mathcal{L}\{I\} \quad (34)$$

$$w\mathcal{L}\{R\} - R(0) = \mu\mathcal{L}\{I\} \quad (35)$$

Using the initial condition to the above Eqs. (33) – (35), we get

$$\mathcal{L}\{S\} = \frac{0.9}{w} - \frac{\beta}{w}\mathcal{L}\{A\} \quad (36)$$

$$\mathcal{L}\{I\} = \frac{0.1}{w} + \frac{\beta}{w}\mathcal{L}\{A\} - \frac{\mu}{w}\mathcal{L}\{I\} \quad (37)$$

$$\mathcal{L}\{R\} = \frac{\mu}{w}\mathcal{L}\{I\} \quad (38)$$

Where $A = SI$

Next, we represent the pertinent parameters as an infinite series of the form

$$S = \sum_{n=0}^{\infty} S_n, \quad I = \sum_{n=0}^{\infty} I_n, \quad R = \sum_{n=0}^{\infty} R_n \quad (39)$$

Where the terms S_n, I_n and R_n are to be determined recursively.

Similarly, the nonlinear term is equally decomposed in the form

$$A = \sum_{n=0}^{\infty} A_n \quad (40)$$

Where A_n are called the Adomian polynomials. The first five polynomials are considered as follows

$$A = SI$$

$$A_0 = S_0 I_0$$

$$A_1 = S_0 I_1 + S_1 I_0$$

$$\begin{aligned} A_2 &= S_0 I_2 + S_1 I_1 + S_2 I_0 \\ A_3 &= S_0 I_3 + S_1 I_2 + S_2 I_1 + S_3 I_0 \end{aligned} \quad (41)$$

$$\begin{aligned} A_4 &= S_0 I_4 + S_1 I_3 + S_2 I_2 + S_3 I_1 + S_4 I_0 \\ A_5 &= S_0 I_5 + S_1 I_4 + S_2 I_3 + S_3 I_2 + S_4 I_1 + S_5 I_0 \\ A_6 &= S_0 I_6 + S_1 I_5 + S_2 I_4 + S_3 I_3 + S_4 I_2 + S_5 I_1 + S_6 I_0 \end{aligned}$$

Substituting Eqs (39) and (40) into Eqs (36) – (38) yield

$$\mathcal{L}\{\sum_{n=0}^{\infty} S_n\} = \frac{0.9}{w} - \frac{\beta}{w}\mathcal{L}\{\sum_{n=0}^{\infty} A_n\} \quad (42)$$

$$\mathcal{L}\{\sum_{n=0}^{\infty} I_n\} = \frac{0.1}{w} + \frac{\beta}{w}\mathcal{L}\{\sum_{n=0}^{\infty} A_n\} - \frac{\mu}{w}\mathcal{L}\{\sum_{n=0}^{\infty} I_n\} \quad (43)$$

$$\mathcal{L}\{\sum_{n=0}^{\infty} R_n\} = \frac{\mu}{w}\mathcal{L}\{\sum_{n=0}^{\infty} I_n\} \quad (44)$$

Matching the sides of Eqs. (42) – (44) yield the following iterative algorithm

$$\begin{aligned}
&\mathcal{L}\{S_0\} = \frac{0.9}{w} \\
&\mathcal{L}\{S_1\} = -\frac{\beta}{w}\mathcal{L}\{A_0\} \\
&\mathcal{L}\{S_2\} = -\frac{\beta}{w}\mathcal{L}\{A_1\} \\
&\mathcal{L}\{S_3\} = -\frac{\beta}{w}\mathcal{L}\{A_2\} \\
&\quad\vdots \\
&\mathcal{L}\{S_{n+1}\} = -\frac{\beta}{w}\mathcal{L}\{A_n\}
\end{aligned} \quad (45)$$

$$\begin{aligned}
&\mathcal{L}\{I_0\} = \frac{0.1}{w} \\
&\mathcal{L}\{S_1\} = \frac{\beta}{w}\mathcal{L}\{A_0\} - \frac{\mu}{w}\mathcal{L}\{I_0\} \\
&\mathcal{L}\{S_2\} = \frac{\beta}{w}\mathcal{L}\{A_1\} - \frac{\mu}{w}\mathcal{L}\{I_1\} \\
&\mathcal{L}\{S_3\} = \frac{\beta}{w}\mathcal{L}\{A_2\} - \frac{\mu}{w}\mathcal{L}\{I_2\} \\
&\quad\vdots \\
&\mathcal{L}\{I_{n+1}\} = \frac{\beta}{w}\mathcal{L}\{A_n\} - \frac{\mu}{w}\mathcal{L}\{I_n\}
\end{aligned} \quad (46)$$

$$\begin{aligned}
&\mathcal{L}\{R_0\} = 0 \\
&\mathcal{L}\{R_1\} = \frac{\mu}{w}\mathcal{L}\{I_0\} \\
&\mathcal{L}\{R_2\} = \frac{\mu}{w}\mathcal{L}\{I_1\} \\
&\mathcal{L}\{R_3\} = \frac{\mu}{w}\mathcal{L}\{I_2\} \\
&\quad\vdots \\
&\mathcal{L}\{R_{n+1}\} = \frac{\mu}{w}\mathcal{L}\{I_n\}
\end{aligned} \quad (47)$$

Applying the inverse Laplace transform to the first Eqs. (45) – (47), we get

$$\mathcal{L}\{S_0\} = \frac{0.9}{w}, \mathcal{L}\{I_0\} = \frac{0.1}{w}, \mathcal{L}\{R_0\} = 0 \quad (48)$$

Substitution of the above values of S_0, I_0 and R_0 into the second and third Eqs (45) – (47), we get

$$\mathcal{L}\{S_1\} = -\frac{0.18}{w^3}, \mathcal{L}\{I_1\} = \frac{0.18}{w^3} - \frac{0.05}{w^2}, \mathcal{L}\{R_1\} = \frac{0.05}{w^2} \quad (49)$$

$$\begin{aligned}
&\mathcal{L}\{S_2\} = \frac{0.1}{w^3} - \frac{0.144}{w^5} \\
&\mathcal{L}\{I_2\} = \frac{0.144}{w^5} - \frac{0.02}{w^3} - \frac{0.018}{w^4} + \frac{0.001}{w^3} \\
&\mathcal{L}\{R_2\} = \frac{0.018}{w^4} - \frac{0.001}{w^3}
\end{aligned} \quad (50)$$

Substituting the Laplace transform of the quantities on the right-hand side of Eqs (44) – (47) and applying the inverse Laplace transform, we obtain the values $S_2(t), I_2(t), R_2(t)$. Similarly, the other remaining terms $S_3(t), S_4(t) \dots S_n(t), I_3(t), I_4(t) \dots I_n(t)$ and $R_3(t), R_4(t) \dots R_n(t)$ can be recursively obtained.

VI. NUMERICAL APPLICATION

In this section, we apply the LADM to the epidemiological model. Taking $S(0) = 0.9, I(0) = 0.1$ and $R(0) = 0$ for the three parameters of interest. Setting $\beta = 2, \mu = 0.5$ and the first few calculations for $S(t), I(t)$ and $R(t)$ are calculated and presented below

$$\begin{aligned} S(t) &= \frac{0.9}{w} - \frac{0.16}{w^3} - \frac{0.144}{w^5} \\ I(t) &= \frac{0.1}{w} - \frac{0.01}{w^2} + \frac{0.161}{w^3} - \frac{0.018}{w^4} + \frac{0.144}{w^5} \\ R(t) &= \frac{0.1}{w^2} - \frac{0.001}{w^3} + \frac{0.018}{w^4} \end{aligned} \tag{51}$$

Applying the inverse Laplace transform on both sides of Eq. (51), we obtain the analytical solutions for the governing parameters.

$$\begin{aligned} S(t) &= 0.9 - 0.08t^2 - 0.006t^4 \\ I(t) &= 0.1 - 0.01t + 0.0805t^2 - 0.003t^3 + 0.0006t^4 \\ R(t) &= 0.1t - 0.0005t + 0.003t^2 \end{aligned} \tag{52}$$

Using symbolic computational software Maple 20, we calculate the $[5/5]$ Pade approximant of the infinite series of Eq. (52) which gives the following rational approximations to the solution.

$$S_{Pade}(t) = \frac{0.91234 - 1.45 \times 10^{-16} t - 0.080101t^2 - 3.69 \times 10^{-15} t^3 - 0.00112345t^4 + 5.7 \times 10^{-16} t^5}{1 - 1.6 \times 10^{-16} t - 1.2 \times 10^{-15} t^2 - 4.1 \times 10^{-15} t^3 - 7.3 \times 10^{-17} t^4 + 3.07 \times 10^{-16} t^5}$$

$$I_{Pade}(t) = \frac{0.1 - 0.00981t + 0.080t^2 - 0.0021782t^3 + 0.00059392226t^4 + 0.00000120892t^5}{1 + 0.020t - 2.32 \times 10^{-13} t^2 - 2.045 \times 10^{-14} t^3 + 8.42 \times 10^{-16} t^4 + 4.3 \times 10^{-17} t^5}$$

$$R_{Pade}(t) = \frac{0.1t - 0.0005t^2 + 0.00297t^3 + 3.014 \times 10^{-7} t^4 - 8.910731504 \times 10^{-7} t^5}{1 + 0.0059t - 0.0297t^2 - 5.174 \times 10^{-15} t^3 + 9.68 \times 10^{-17} t^4 + 1.559 \times 10^{-16} t^5}$$

Table 1: Numerical comparison for Susceptible using six iterates

t	LADM	LADM-Padé	4th Order R-K
0	0.900000	1.0000	1.0000
0.2	0.896790	0.896790	0.896800
0.4	0.88705	0.887046	0.887045
0.6	0.870422	0.870350	0.870421
0.8	0.846342	0.846344	0.8463450
1.0	0.814000	0.814000	0.814000
1.2	0.772358	0.772357	0.772350

Table 2: Numerical comparison for Infected using six iterates

t	LADM	LADM-Padé	4th Order R-K
0	0.10000	0.10000	0.10000
0.2	0.101197	0.1011641	0.101198
0.4	0.108703	0.108704	0.108705
0.6	0.122410	0.122410	0.122410
0.8	0.142230	0.142240	0.142235
1.0	0.16810	0.168100	0.168910
1.2	0.19998	0.19990	0.202882

Table 3: Numerical comparison for Removed using six iterates

t	LADM	LADM-Padé	4th Order R-K
0	0.0000	0.0000	0.0000
0.2	0.020004	0.0200023	0.0200040
0.4	0.040112	0.04112	0.040038
0.6	0.604680	0.603870	0.604680
0.8	0.081216	0.081215	0.0812160
1.0	0.102500	0.102501	0.102500
1.2	0.124464	0.1244640	0.1244604

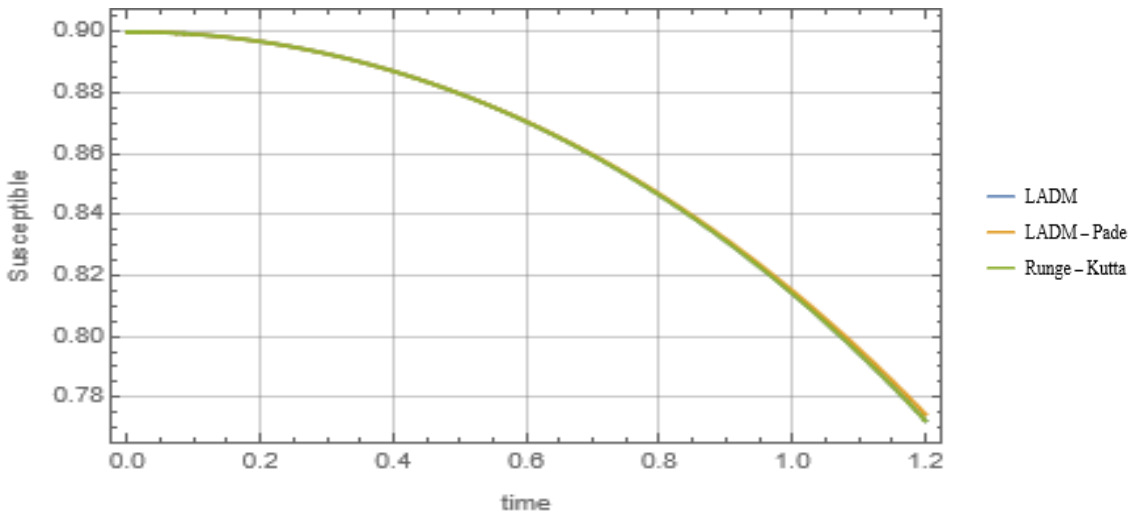

Figure 1. Comparison of LADM solution of Susceptible for six iterates

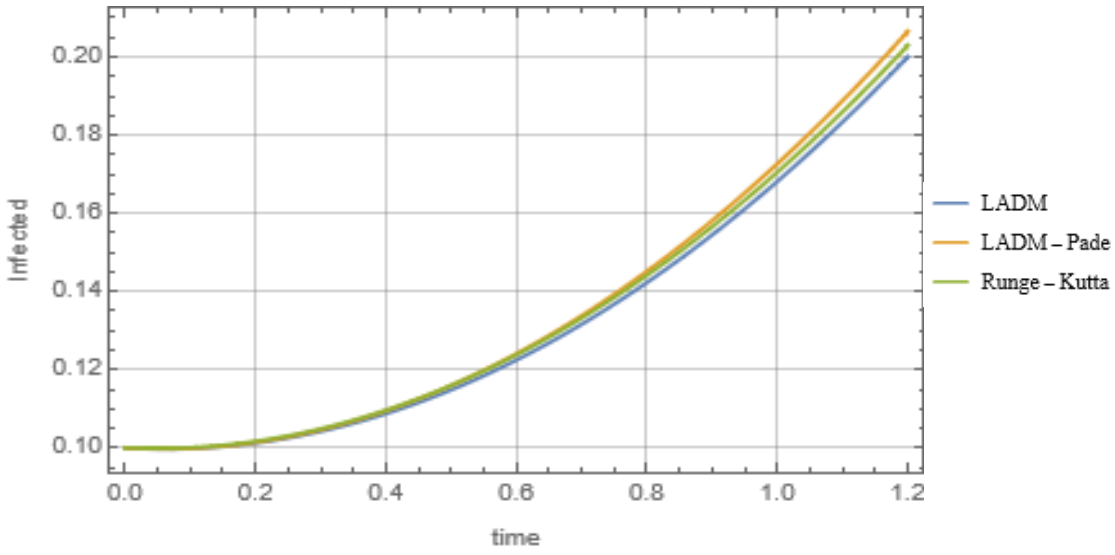

Figure 2. Comparison of LADM solution of Infected for six iterates

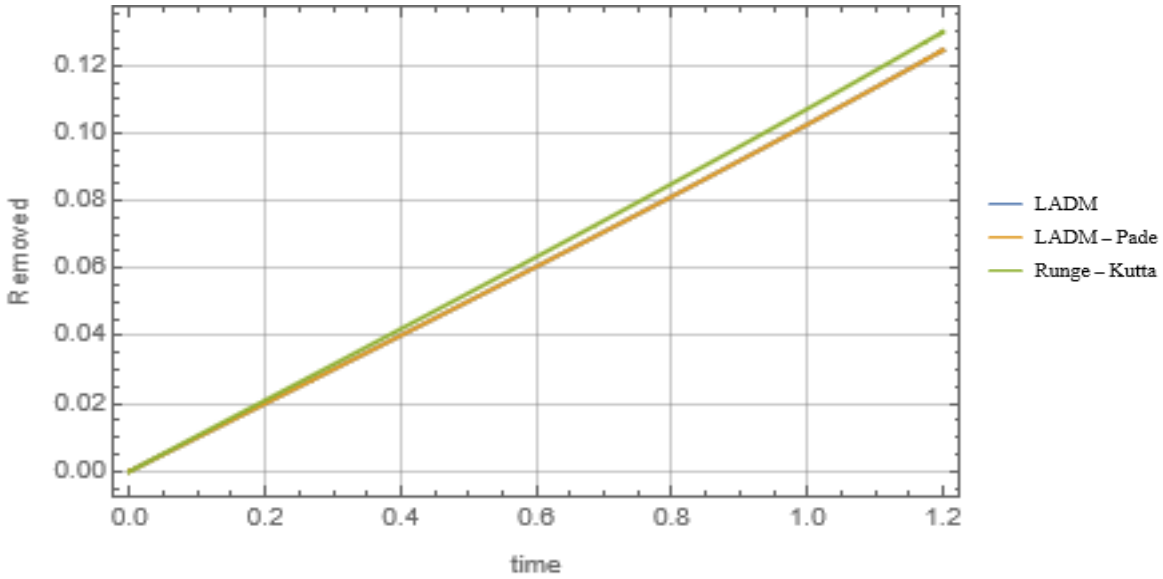

Figure 3. Comparison of LADM solution of Removed for six iterates

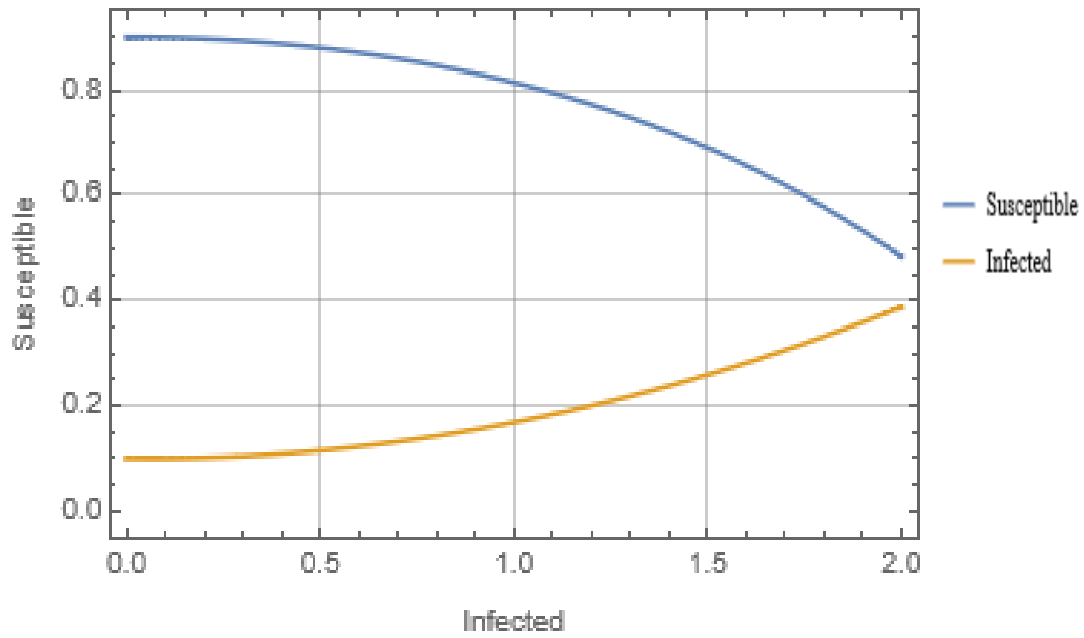

Figure 4. Comparison of Susceptible against Infected for six iterates

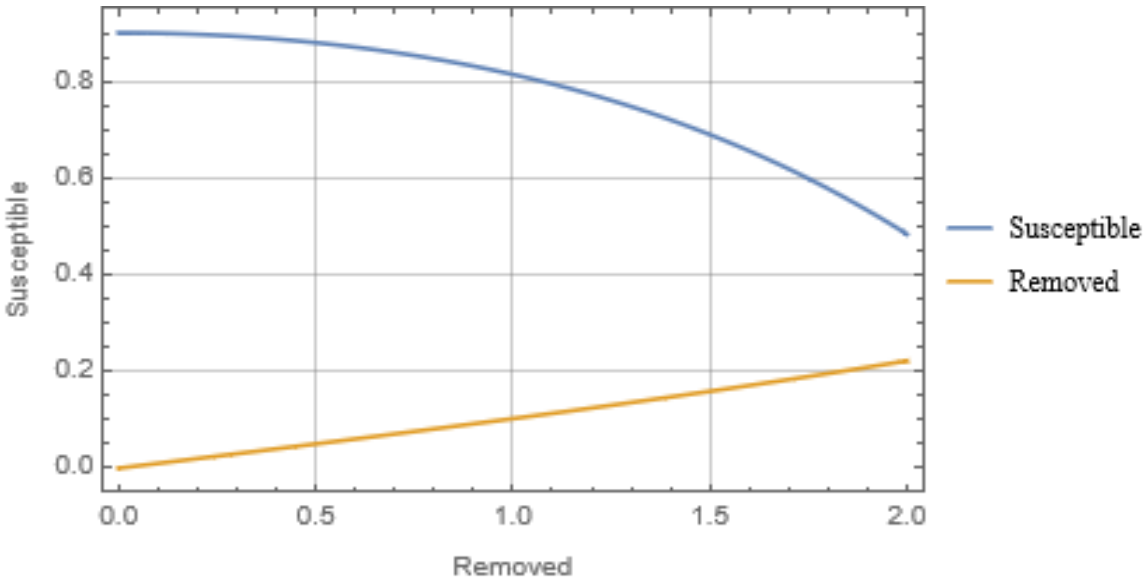

Figure 5. Comparison of Susceptible against Removed for six iterates

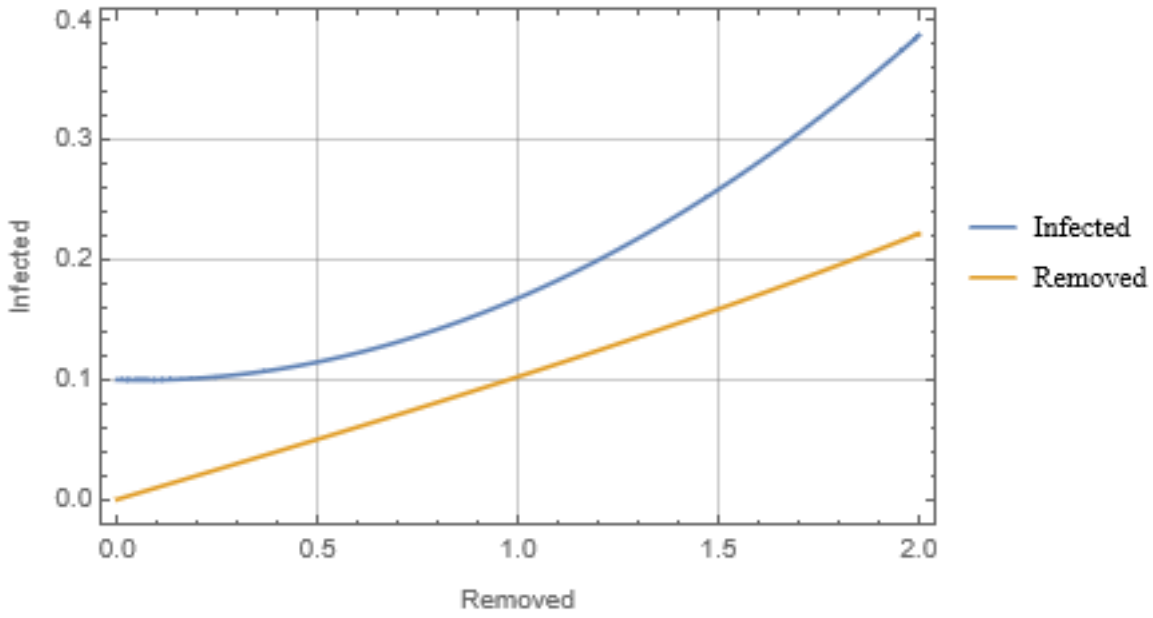

Figure 6. Comparison of Infected against Removed for six iterates

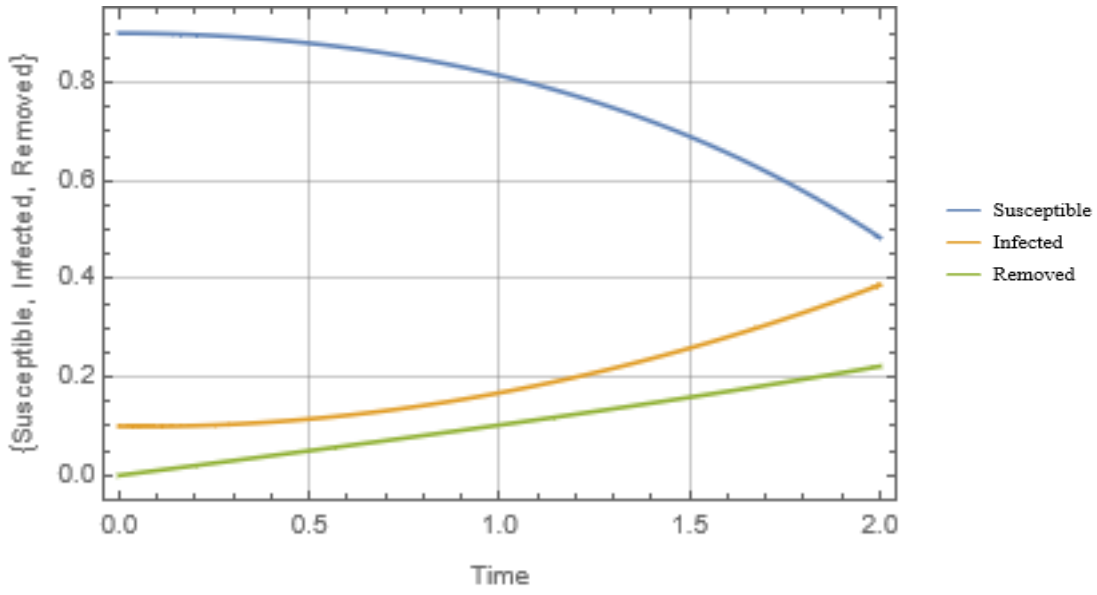

Figure 7. Comparison of Susceptible, Infected and Removed against Time

VII. CONCLUSION

In this research article, we proposed the Laplace Adomian decomposition method and the Padé approximant to find analytical solution to the SIR epidemic model. The governing nonlinear autonomous differential equations comprising the parameters of interest were solved using the LADM. The obtained results were approximated using the Padé approximant to validate the earlier result and improve upon it. Comparison is then made between the results with the fourth order Runge-Kutta method. The solution obtained agreed with literature, simple, efficient, and applicable for a large time interval.

REFERENCES

[1] M.S.A. George, D.J. Praveen. Qualitative Analysis of a Discrete Epidemic Model. International Journal of Computational Engineering Research (IJCER), 2015, Volume 05, Issue (e): 2250-3005.

[2] O.D. Makinde. Adomian decomposition approach to a SIR epidemic model with constant vaccination strategy. Applied Mathematics and computation, 2007, 184, 842-848.

[3] M. Xinzhu, C. Lansun. Global dynamical behaviours for an SIR epidemic model with time delay and pulse vaccination. Taiwanese Journal of Mathematics, 2008, Vol 12, No. 5, pp 1107-1122.

[4] R.M. Anderson, R.M. May. The invasion, persistence, and spread of infectious disease within animal and plant communities. Philos Trans R. Soc Lond B, 1986, 314, 533-570.

[5] Y. Kan-Hung, H. Ji-Yuan. A New SIR-based Model for Influenza Epidemic. World Academy of Science, Engineering and Technology, 2012, Vol 6, 07-020.

[6] W.O. Kermack, A.G. McKendrick. A Contribution to the Mathematical Theory of Epidemics. Proceedings of the Royal Society A, Mathematical, Physical and Engineering Sciences, 1927, 115(772), 700.

[7] H. Zhixing,M. Wanbiao, R. Shiguan. Analysis of the SIR Epidemic models with nonlinear incidence rate and treatment. Mathematical Biosciences, 2012, 238, 12-20.

[8] H.W. Hethcote. The Mathematics of Infectious Diseases. Siam Rev. 2000, 42(4), 599-653.

[9] Z. Lu, L. Chi, L. Chen. The effect of constant and pulse vaccination of SIR epidemic model with horizontal and vertical transmission. Mathematics and Computational Modelling, 2002, 36, 1039-1057.

[10] H. L.Smith. Subharmonic bifurcation in SIR epidemic model. Journal of Mathematical Biology, 1983, 17, 163-177.

[11] G. Adomian. A review of the decomposition method and some results for nonlinear equation. Mathematical and Computer Modelling, 1990, 13(7),17-43.

[12] G.Adomian.A Review of the Decomposition Method in AppliedMathematics. Journal of MathematicalAnalysis and Applications. 1988, 135(2), 501-509.

[13] G.Adomian. Solving Frontier Problems of Physics: The decompositionmethod. Kluwer, Academic Publishers, 1994

[14] A.M. Wazwaz. A Comparison between Adomian decomposition method and Taylor series method in the series solutions. Applied Mathematics and Computation, 1998, 97(1), 37-44.

[15] S. Momani, Z. Odibat. Analytical solution of a time-fractional Navier-Stokes equation by Adomian decomposition. Applied Mathematics and computation,2006, 177(2), 488-494.

[16] D.J. Evans, K.R. Raslan. The Adomian decomposition method for solving delay differential equations. International Journal of Computer Mathematics, 2005, 82(1), 49-54.

[17] J.H. He. A review of some recently developed nonlinear analytical techniques. International Journal of Nonlinear Sciences and Numerical Simulations, 2000, 1(15), 51-70.

[18] Y. Cherruault, K. Abbaoui. Convergence of Adomian's Method appliedto Nonlinear Equations. *Mathematical and Computer Modelling*. 1994, 20(9), 69-73.

[19] H. Jafari, V. Daftardar-Gejji. Revised Adomian decomposition method for solving a system ofnonlinear equation. Applied Mathematics and computation, 2006

[20] K. Al-khaled, F. Allan. Decomposition Method for Solving NonlinearIntegro-Differential Equations. *Mathematics and computing*. 2005, 19(1 – 2), 415- 425.

[21] A. Ebrahim, M. Farhadi, K. Sedighl, K. Ebrahimi, G. Akbar. Solution of the Falkner-Skan equations for wedge by Adomian decomposition method. Comm. Nonlinear Sci. Numer. Sim, 2009, 14, 462-472.

[22] S.A. Khuri. A Laplace decomposition algorithm applied to a class of nonlinear differential equation. Journal of Applied Mathematics,2001, 1, 141-155.

[23] S.A. Khuri. A new Approach to Bratu's problem. Applied Mathematics Computation,2004, 147, 131-136.

[24] J. Fadaei.Application of Laplace Adomian decomposition method on linear and nonlinearsystem of PDEs. Applied Mathematical Sciences, 2011, 5, 1307-1315.

[25] M. Khan, M. Hussain, H. Jafari, Y. Khan. Application of Laplace decomposition method to solve nonlinear coupled partial differential equations. World Applied Science Journal, 2010, 9, 13-19.

[26] E. Yusufoglu. Numerical solution of the Duffing equation by the Laplace decomposition algorithm. Applied Mathematics computation, 2006, 177, 572-580.

[27] M.Y. Ongun. The Laplace Adomian decomposition for solving a model for HIV infection of CD4+Tcells. Mathematics and computational modelling, 2011, 53, 597-603.

[28] P. Pue-on. Laplace Adomian decomposition method for solving Newell-Whitehead-Segel Equation. Applied Mathematical Sciences, 2013, Vol 7, No. 132, 6593-6600.

[29] N. Doğan. Solution of the System of Ordinary Differential Equation by Combined Laplace Transform–Adomian Decomposition Method. Mathematical and Computational Applications. 2012, 17(3), 203-2012.

[30] F.A. Hendi.The Combined Laplace Adomian decomposition Method Applied for Solving Linear and Nonlinear Volterra Integral Equation with Weakly kernel. Studies in Nonlinear Sciences. 2011, 2(4), 129-134.

[31] A.M. Wazwaz. The combined Laplace transform–Adomian decomposition method for handling nonlinear Volterra Integro–differential equations. Applied Mathematics and Computation. 2010, 216(4), 1304–1309.

[32] A.H. Waleed. Solving nth-order Integro-differential equation using the combined Laplace transform-Adomian decomposition method. Applied Mathematics, 2013, 4, 882-886.

[33] J. Manafianheris. Solving the Integro-differential equations using the modified Laplace Adomian decomposition method. Journal of mathematical Extension, 2012, 6, 41-55

[34] M.A. Koroma, S. Widatalla, A.F. Kamara, C. Zhang. Laplace Adomian decomposition method applied to a two-dimensional viscous fluid with shrinking sheet. 2013, 7, 525-529.

[35] S. Islam, Y. Khan, N. Faraz, F. Austin. Numerical solution to Logistic differential equation by using Laplace decomposition method. World Applied Science Journal, 2010, 8, 1100-1105.

[36] J. B. Yindoula, P. Youssouf, G. Bissanga, F. Bassino, B. Some. Application of the Adomian decomposition method and Laplace transform method to solving the convection diffusion-dissipation equation. International Journal of Applied Mathematical Research, 2014, 3, 30-35.

[37] J. Hou, C. Yang. An approximate solution of nonlinear fractional differential equation by Laplace transforms and Adomian polynomials. Journal of Information and Computational Science, 2013, 10, 213-222.

[38] L. Ebiwareme, Y.A. Da-Wariboko. Modified Adomian decomposition method and Padé approximant for the numerical approximation of the crime deterrence model in society.The International Journal of Engineering Sciences,2021, Vol 10, Issue 7, Series 1, pp 01-12.

[39] G.A. Baker, P. Graves-Morris. Essentials of Padé Approximants. Cambridge University Press, Cambridge, 1996.

[40] J, Boyd. Padé Approximant algorithm for solving nonlinear ordinary differential equation boundary value problems on an unbounded domain. Computers in Physics, 1997, 11(3), 299-303.

[41] A.M. Wazwaz. Analytical approximations and Padé approximants for Volterra's population model. Applied Mathematics and Mathematical Computation, 1999, 100, 31-35.

[42] A.M. Wazwaz. The Modified decomposition method and Pade's approximants for solving Thomas-Fermi equation. Applied Mathematics and Mathematical Computations, 1999, 105, 11-19.

[43] S, Momani, Q, Rami. Numerical approximation and Padé approximation for a fractional population growth model, 2007, 31, 1907-1914.

Study of Chemical ion Transport through the Soil using combined Variational Iteration and Homotopy Perturbation Methods.

Liberty Ebiwareme, Iyai Davies
Department of Mathematics, Rivers State University, Port Harcourt, Nigeria.

Fun-Akpo Pere Kormane
Department of Civil Engineering, Rivers State University, Port Harcourt, Nigeria.

ABSTRACT

The aim of this present article is to solve numerically the resulting governing equation in the modelling of the chemical ion transport through the soil. The governing equation was transformed to a nonlinear ordinary differential equation through similarity transformation. The hybrid semi-analytical coupling of the variational iteration and Homotopy perturbation method was proposed to solve the resulting equation. The effect of the pertinent parameters of the flow namely, the porosity parameter, Hartmann number and Reynold number on the concentration, velocity profiles and volumetric flow rate are analysed, and the result presented in tables and graphs. The result obtained revealed, this hybrid method is computationally easy, convenient, and showed promise to solve most highly nonlinear differential equation. The parameters significantly have impacts on the system.

Keywords:Chemical ion, Variational Iteration method (VIM), Homotopy Perturbation method (HPM), Variational Homotopy Perturbation Method (VHPM)

I. INTRODUCTION

Most of the real-life phenomena of physical significance in science, engineering, social sciences, biology, agriculture, and others are modelled in the form of differential or partial differential equations which are inherently nonlinear in nature. Due to this nonlinearity, solutions of equations governing these phenomena are difficult to obtain. Academics over the years have proposed several methods to finding for their solutions ranging from numerical and analytical. The nature of the complexity posed by the nonlinearityenable academics to choose numerical methods as the best method for solving them. Examples of some of the earliest numerical methods employed include: Runge-Kutta, Crank-Nicolsen, Euler's, Modified Euler, Finite difference method, Finite element method and Finite volume method [1-2].

In contemporary times, due to the advent of powerful computers with incredible capabilities and symbolic computational software'sin mathematics like Mathematica, Maple, MATLAB and COMSOLE Multiphysics, these problems can be solved at a canter regardless of the degree of nonlinearity. After numerical methods lost its appeal in tackling these problems, next comes weighted residual methods (Galerkin, Petrov-Galerkin, Moment method, Collocation method, least square method, and subdomain method) and variational method (Rayleigh-Ritz) have been used to obtain solutions to these equations. Depending on the nature of the nonlinearity, most of the methodsmentioned above are difficult to implement and not computationally convenient and time consuming Babolian et al [3].

Most recently, semi-analytical methods which give the solution in a series of convergent iterative step is fast gaining popularity among academics due to their ease of implementation and computational convenience. Solutions using these methods agree with exact solutions with high degree of accuracy. Examples of these methods include: Adomian decomposition method (ADM), Differential transformation method (DTM), Homotopy perturbation method (HPM), Variational iteration method (VIM), Differential Quadrature method (DQM), Akbari-Ganji method (AGM), Homotopy Analysis method (HAM), Exp-Function method. Others are the combination of two or more of these methods, notable among these ones includes: Laplace Variation Iteration method (LVIM), Laplace Adomian decomposition method (LADM), Optimal Homotopy Asymptotic method (OHAM), Spectral Homotopy Analysis method (SHAM), Spectral Homotopy perturbation method (SHPM), Optimal Homotopy perturbation method (OHPM), Laplace Homotopy Perturbation method (LHPM) and Variational Homotopy perturbation method (VHPM) [4-10].

The variational Homotopy perturbation method (VHPM) is a semi-analytical method which combines the variational iteration and Homotopy perturbation methods This method requires firstly by taking the variational iteration method of the given system under consideration to give an iterative system. Secondly, applying the Homotopy perturbation to the resulting system and equating corresponding powers of the perturbation parameter, give different set of equations of the unknowns. Solving this equation give the solution in approximate form. This method though nascent has been extensively applied in solving several problems in both science and engineering. Malinfar and Mahdavi [11] have examined the application of the variational Homotopy perturbation method on the generalized Fisher's equation. Allahviranloo et al [12] have investigated variational Homotopy perturbation method as an efficient iterative scheme in solving partial differential equations in fluid mechanics. The approximate solution of the foam drainage equation with time and space fractional derivative have been studied by Bouhassoun et al. [13]. Ji-Huan [28] used the coupled Variational iteration and Homotopy perturbation techniques for solving nonlinear problems. Ebiwareme and Kormane [14] have employed VHPM to solve analytically the nonlinear equations governing MHD Jeffery-Hamel flow in the presence of magnetic field. The study showed that that the velocity profile is significantly affected for both the convergent/divergent channel for different values of the Reynold number, magnetic field, and angle of inclination. Fredholm integrodifferential equations of fractional order have been analysed using combined variational iteration and Homotopy perturbation methods [15]. Linear and nonlinear heat transfer equations in engineering have been investigated using VHPM [16]. Yangqin [17] used VHPM to solve fractional initial boundary value problems. Mohyud-in and Mohammed [18-19] have studied higher order dimensional initial boundary value problems utilizing VHPM

The motivation in this present study is to propose the novelty of applying variational Homotopy perturbation method to solve the nonlinearequations governing the transport of chemical ion through the soil. Theorganization of the study is as follows: Section 2 presents the formulation of the problem with the accompanying governing equations and boundary conditions. The fundamentals of variation iteration and Homotopy perturbation methods are given in section 3 and 4. Basics of variational Homotopy perturbation method which is the coupling of VIM and HPM is presented in section 5. Section 6 give the detailed mathematical analysis of the problem using VHPM. In the final analysis, the results and discussion of the obtained solution is graphically presented in section 7 while the conclusion of the study is contained in section 8 with the major findings in the study itemized.

II. MATHEMATICAL FORMULATION

We consider a steady Newtonian fluid flow in a porous channelandsandwiched between two parallel plates under the influence of transverse external pressure applied at both ends. Then centre of the channel parallel to the channel surface is represented by the $x-a$xis, whereas the transverse direction is along the y −axis. The flow is assumed to be asymmetrical about the x −axis and the channel walls are represented by $y = h$ and $y = \delta h$, where h denotes the width of the channel.

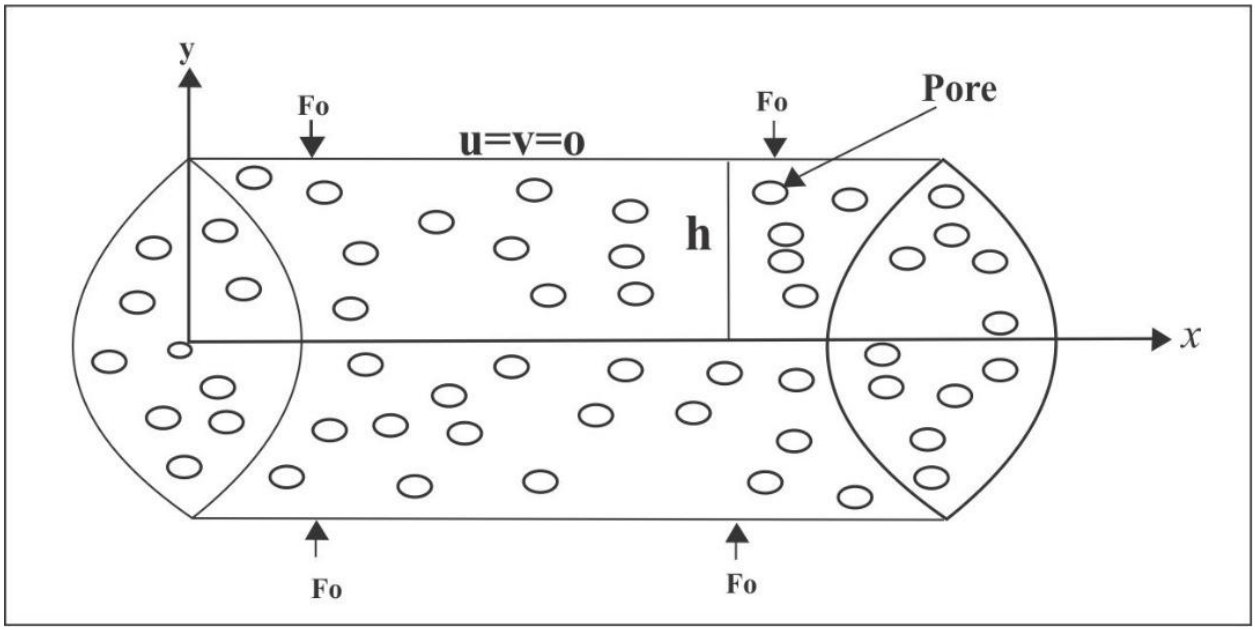

Figure 1. Schematic configuration of the problem (Adopted from Poonam et al. 2019)

Let (u, v) be the velocity component of the fluid along the x and y axes and F_0 be the external force applied to the top and bottom plates. Assuming the pressure gradient to be zero, then the governing equationsof continuityand momentum for the boundary layer of incompressible fluid is given by

Continuity Equation

$$\frac{\partial u}{\partial x} + \frac{\partial v}{\partial y} = 0 \tag{1}$$

Momentum Equation

$$u\frac{\partial u}{\partial x} + \frac{\partial u}{\partial y} = \nu\frac{\partial^2 u}{\partial y^2} - \frac{\nu}{\kappa}u - \frac{F_0^2 u}{\rho} \tag{2}$$

Where ν, ρ, κ denote the kinematic coefficient of viscosity, density of the solute and permeability of the porous medium respectively

Since the flow of the fluid is symmetric along the central line, $y = 0$ of the channel. We therefore focus our attention to the flow region, $0 \leq y \leq h$, where the suitable boundary conditions are given by

$$u = v = 0 \text{ at } y = h \tag{3}$$

$$\frac{\partial u}{\partial y} = 0, v = 0 \qquad \text{at } y = 0 \tag{4}$$

Using the Non-dimensional parameters of the form

$$\varepsilon = \frac{x}{h}, \eta = \frac{y}{h}, u = \frac{U_0 x f'(\eta)}{h}, v = -U_0 f(\eta) \tag{5}$$

Where U_0 is the characteristic velocity

Using Eq. (5) into Eqs. (1) and (2), we obtain the governing equations in non-dimensional form as

$$f''(\eta) + Re\left(f(\eta)f'(\eta) - \left(f'(\eta)\right)^2\right) - \frac{\nu}{\kappa}f'(\eta) = 0 \tag{6}$$

Where Re and κ are the Reynold and porosity permeability parameter defined by

$$Re = \frac{U_0 h}{\nu}, \mathcal{K} = \frac{\kappa}{h^2}, \psi = (F_0^2 + K^{-1}) \quad (7)$$

Subject to the boundary conditions

$$f(1) = f'(1) = 0$$
$$f(0) = f''(0) = 0 \quad (8)$$
$$f'(0) = \alpha$$

III. VARIATIONAL ITERATION METHOD (VIM)

Consider the ordinary differential equation of the form

$$Ly + N(y) = f(x), \qquad x \in I \quad (9)$$

Where L and N are linear and nonlinear operators respectively, and $f(x)$ is any given inhomogeneous terms defined for $x \in I$

We defined a correctional functional for Eq. (8) as follows

$$y_{n+1}(x) = y_n(x) + \int_0^x \lambda(\xi)\left(Ly_n(\xi) + N(\tilde{y}_n(\xi)) - f(\xi)\right) d\xi \quad (10)$$

Where $\lambda(\tau)$ is a Lagrange multiplier obtained through variational theory, $y_n(x)$ is the nth approximation of $y(x)$ and $\tilde{y}_n(x)$ is a restricted variation meaning $\delta\tilde{y}_n(x) = 0$

By imposing the variation of both sides of Eq. (9) and taking the restricted variation we obtained

$$\delta y_{n+1}(x) = \delta y_n(x) + \delta(\int_0^x \lambda(\xi) L y_n(\xi) d\xi \quad (11)$$

$$\delta y_{n+1}(x) = \delta y_n(x) + \left[\lambda(\xi)(\int_0^\tau L y_n(\xi) d\xi\right]_{\xi=0}^{\xi=x} - \int_0^x \lambda'(\xi)\left(\int_0^\tau L\delta y_n(\xi)\right) d\xi \quad (12)$$

Now by applying the stationary condition, the value of the Lagrange multiplier, $\lambda(\xi)$ can be found. Then the successive approximations, $y_n(x), n = 0,1,2,3$ .... Can be found in the form

$$y_{n+1}(x) = y_n(x) + \int_0^x \lambda(\xi)\left(Ly_n(\xi) + N(y_n(\xi)) - f(\xi)\right) d\,\xi \quad (13)$$

The exact solution is then obtained as the limit of the successive approximations from Eq. (12)

$$y(x) = \lim_{n\to\infty} y_n(x) \quad (14)$$

IV. HOMOTOPY PERTURBATION METHOD (HPM)

In this section, the fundamentals of the Homotopy perturbation method as proposed by He. J. Huan is discussed

Consider a functional differential equation of the form

$$\mathcal{A}(u) - f(r) = 0, r \in \Omega \quad (15)$$

Subject to the boundary condition

$$\mathcal{B}\left(u, \frac{\partial u}{\partial t}\right) = 0, r \in \mathcal{T} \quad (16)$$

Where $\mathcal{A}$ is a differential operator, $\mathcal{B}$ is a boundary operator, $\mathcal{B}$ is a boundary operator, $\mathcal{T}$ is the boundary of the domain Ω, $f(x,t)$ is a known analytic function and $u(x,t)$ is an unknown function

Dividing the operator, $\mathcal{A}$ into two parts comprising linear, $(\mathcal{L})$ and nonlinear $(\mathcal{N})$

$$\mathcal{A} = \mathcal{L} + \mathcal{N} \quad (17)$$

In view of Eq. (16), we rewrite Eq. (15) in the form

$$\mathcal{L}(u) + \mathcal{N}(u) - f(r) = 0 \quad (18)$$

Embedding an artificial parameter p on Eq. 18) as follows

$$\mathcal{L}(u) + p(\mathcal{N}(u) - f(r)) = 0 \quad (19)$$

where $p \in [0,1]$ is the embedding or artificial parameter.

Next, we construct a Homotopy, $\mathcal{H}(r,p)$: $\Omega \times [0,1] \longrightarrow \Re$ to Eq. (19) that satisfies

$$\mathcal{H}(r,p) = (1-p)[\mathcal{L}(v) - \mathcal{L}(u_0)] + p[\mathcal{L}(v) + \mathcal{N}(v) - f(r)] = 0 \quad (20)$$

and

$$\mathcal{H}(r,p) = \mathcal{L}(v) - \mathcal{L}(u_0) + p\mathcal{L}(u_0) + p[\mathcal{N}(v) - f(r)] = 0 \quad (21)$$

Where $u_0(x)$ is the initial approximation which satisfies the boundary condition.

Putting $p = 0$ and $p = 1$ into Eq. (20), we obtain the following equations

$$\left.\begin{aligned}\mathcal{H}(r,0) &= \mathcal{L}(v) - \mathcal{L}(u_0)\\ \mathcal{H}(r,1) &= \mathcal{A}(u) - f(r)\end{aligned}\right\} \quad (22)$$

Clearly as p changes monotonically from zero to unity, $\mathcal{H}(r,p)$ changes from $u_0(x)$ to $u(x)$. This is called deformation, whereas the terms $\mathcal{L}(v) - \mathcal{L}(u_0)$ and $\mathcal{A}(u) - f(r)$ are homotopic to each other.

Now we consider a power series solution in p as follows

$$v = \sum_{n=0}^{\infty} p^{(n)} v_n \quad (23)$$

The approximate solution of Eq. (23) can be obtained by setting $p = 1$

$$u(x) = \lim_{p\to 1} v_n = v_0 + v_1 + v_2 + \cdots \quad (24)$$

Similarly, the nonlinear term, $\mathcal{N}(u)$ can be expressed as He's polynomial

$$\mathcal{N}(u) = \sum_{n=0}^{\infty} p^{(m)} H_m(v_0 + v_1 + \cdots + v_m) \quad (25)$$

Where $H_m(v_0 + v_1 + \cdots + v_m) = \frac{1}{m!}\frac{\partial^m}{\partial p^m}[\mathcal{N}(\sum_{k=0}^{m} p^k v_k)]_{p=0}, m = 0,1,2,\ldots$ (26)

where,

$$H_0 = \mathcal{N}(u_0)$$

$$H_1 = u_1\mathcal{N}'(u_0)$$

$$H_2 = u_2\mathcal{N}'(u_0) + \frac{1}{2}\mathcal{N}_1^2\mathcal{N}''(u_0)$$

$$H_3 = u_3\mathcal{N}'(u_0) + u_1u_2\mathcal{N}''(u_0) + \frac{1}{6}\mathcal{N}_1^3\mathcal{N}'''(u_0)$$

$$H_4 = u_4\mathcal{N}'(u_0) + (\tfrac{1}{2}u_2^2 + u_1u_3)\mathcal{N}''(u_0) + \tfrac{1}{2}u_1^2u_2\mathcal{N}_1^3\mathcal{N}'''(u_0) + \tfrac{1}{24}u_4^3\mathcal{N}^{(iv)}(u_0) \quad (27)$$

V. VARIATIONAL HOMOTOPY PERTURBATION METHOD (VHPM)

To implement the VHPM, firstly we construct the correctional functional for Eq. (6) is given as

$$f_{n+1}(\eta) = f_n(\eta) + \int_0^{\eta} \lambda(\xi)\left[\frac{d^3f_n(\xi)}{d\eta^3} - \psi\frac{df_n(\xi)}{d\eta} + Re\left(f_n(\xi)\frac{df_n(\xi)}{d\eta} - \left(\frac{df_n(\xi)}{d\eta}\right)^2\right)\right]d\xi\,, n \geq 0 \quad (28)$$

where $\lambda(\xi)$ is the Lagrange multiplier which is obtained via optimal variation. Next, we apply the Homotopy perturbation to the functional, we get.

$$\sum_{n=0}^{\infty} p^{(n)}u_n = f_0(\eta) + p\int_0^{\eta}\frac{(\tau-\eta)^2}{2}\left[\frac{d^3u}{d\eta^3} - \psi\frac{du}{d\eta} + Re\left(\sum_{n=0}^{\infty} p^{(n)}A_n\right) - \left(\sum_{n=0}^{\infty} p^{(n)}B_n\right)\right] \quad (29)$$

Taking $u = \sum_{n=0}^{\infty} p^{(n)}u_n = u_0 + pu_1 + p^2u_2 + \cdots.$ (30)

Substitution into the above expression, we obtain

$$\sum_{n=0}^{\infty} p^{(n)}u_n = f_0(\eta) + p\int_0^{\eta}\frac{(\tau-\eta)^2}{2}\left[\left(\frac{d^3u_0}{d\eta^3} + p\frac{d^3u_1}{d\eta^3} + p^2\frac{d^3u_2}{d\eta^3} + \cdots\right) - \psi\frac{d}{d\eta}\left(\frac{du_0}{d\eta} + p\frac{du_1}{d\eta} + p^2\frac{du_2}{d\eta} + \cdots\right) + Re\left(\sum_{n=0}^{\infty} p^{(n)}A_n\right) - \left(\sum_{n=0}^{\infty} p^{(n)}B_n\right)\right] \quad (31)$$

VI. ANALYTICAL PROCEDURE VIA VHPM

In this section, we analyse eq. (15) subject to the boundary conditions in Eq. (16) using the variational Homotopy perturbation method. This proposed method is the fusion of two semi-analytical methods viz, variational iteration method (VIM) and Homotopy perturbation method (HPM).

The correction functional for Eq. (6) is given by

$$f_{n+1}(\eta) = f_n(\eta) + \int_0^\eta \lambda(\xi)\left[\frac{d^3 f_n(\xi)}{d\eta^3} - \psi\frac{df_n(\xi)}{d\eta} + Re\left(f_n(\xi)\frac{df_n(\xi)}{d\eta} - \left(\frac{df_n(\xi)}{d\eta}\right)^2\right)\right]d\xi \tag{32}$$

Now, we apply Homotopy Perturbation method to the correction functional in Eq. (9), we have

$$\sum_{n=0}^{\infty} p^{(n)}u_n = f_0(\eta) + p\int_0^\eta(\xi-\eta)\left[\frac{d^3}{d\eta^3}(u_0 + pu_1 + p^2u_2 + \cdots) - \psi\frac{d}{d\eta}(u_0 + pu_1 + p^2u_2 + \cdots) + Re\left(\sum_{n=0}^{\infty} p^{(n)}A_n\right) - \left(\sum_{n=0}^{\infty} p^{(n)}B_n\right)\right] \tag{33}$$

Where A_n and B_n are called the He's polynomial defined as follows

$$A_n = \frac{1}{k!}\frac{\partial^k}{\partial\lambda^k}[N(\sum_{n=0}^{\infty} f_n\lambda^n)]_{\lambda=0},\ k = 0,1,2,3\ldots \tag{34}$$

$$B_n = \frac{1}{k!}\frac{\partial^k}{\partial\lambda^k}[N(\sum_{n=0}^{\infty} f_n\lambda^n)]_{\lambda=0}, k = 0,1,2,3\ldots \tag{35}$$

The first six terms of the He's polynomials are explicitly defined as follows

$$\begin{aligned}
A_0 &= f_0f_0'\\
A_1 &= f_0f_1' + f_1f_0'\\
A_2 &= f_0f_2' + f_1f_1' + f_2f_0'\\
A_3 &= f_0f_3' + f_1f_2' + f_2f_1' + f_3f_0'\\
A_4 &= f_0f_4' + f_1f_3' + f_2f_2' + f_3f_1' + f_4f_0'\\
A_5 &= f_0f_5' + f_1f_4' + f_2f_3' + f_3f_2' + f_4f_1' + f_5f_0'\\
A_6 &= f_0f_6' + f_1f_5' + f_2f_4' + f_3f_3' + f_4f_2' + f_5f_1' + f_6f_0'
\end{aligned} \tag{36}$$

$$\begin{aligned}
B_0 &= (f_0')^2\\
B_1 &= 2f_0'f_1'\\
B_2 &= 2f_0'f_2' + (f_1')^2\\
B_3 &= 2f_0'f_3' + 2f_1'f_2'\\
B_4 &= (f_2')^2 + 2f_1'f_3' + 2f_0'f_4'\\
B_5 &= 2f_0'f_5' + 2f_1'f_4' + 2f_2'f_3'\\
B_6 &= (f_3')^2 + 2f_0'f_6' + 2f_1'f_5' + 2f_2'f_4'
\end{aligned} \tag{37}$$

Equating the coefficients of the like powers of p, we obtain the resulting equations as follows

$$p^{(0)}:\ f_0(\eta) = f(0) + \eta f'(0) + \frac{\eta^2}{2}f''(0) \tag{38}$$

$$p^{(1)}:\ f_1(\eta) = \int_0^\eta \frac{(\tau-\eta)^2}{2}\left[Re(A_0 - B_0) - \psi f_0'\right]d\tau \tag{39}$$

$$p^{(2)}:\ f_2(\eta) = \int_0^\eta \frac{(\tau-\eta)^2}{2}\left[Re(A_1 - B_1) - \psi f_1'\right]d\tau \tag{40}$$

Plugging Eqs. (35)– (36) into Eq. (37)–(39), we obtain the first three iterative solutions as

$$f_0(\eta) = \alpha\eta \tag{41}$$

$$f_1(\eta) = \frac{1}{6}Re\alpha^2\eta^4 - \frac{\alpha}{6}(Re + \psi)\eta^3 \quad (42)$$

$$f_2(\eta) = -\frac{\alpha}{6}[2Re^2\alpha(1+\phi) + (Re+\phi)]\eta^5 + \frac{2}{9}Re\alpha^2[Re(\alpha-1)+1]\eta^6 + \frac{5}{36}Re^2\alpha^3\eta^7 \quad (43)$$

Using the limiting relation, we compute the three-term approximation for the solution as

$$f(\eta) = \lim_{n\to\infty} f_n(\eta) = f_0(\eta) + f_1(\eta) + f_2(\eta) + \cdots \quad (44)$$

$$f(\eta) = \alpha\eta - \frac{\alpha}{6}(Re+\psi)\eta^3 + \frac{1}{6}Re\alpha^2\eta^4 - \frac{\alpha}{6}[2Re^2\alpha(1+\phi) + (Re+\phi)]\eta^5 + \frac{2}{9}Re\alpha^2[Re(\alpha-1)+1]\eta^6 + \frac{5}{36}Re^2\alpha^3\eta^7 \quad (45)$$

Setting $Re = 50, \psi = 5$ and using the condition, $f(1) = 0$, we obtain the value of the constant, $\alpha = 0.9905$

Substituting the value of $\alpha = 0.9905$ back into Eq. (44) yields the approximate solution given by

$$f(\eta) = 0.9905\eta - 0.165083(Re+\psi)\eta^3 + 0.163515Re\eta^4 + \cdots \quad (46)$$

DifferentiatingEq. (45) for the velocity profile and using the condition, $f'(1) = 0$, we obtain the constant as $\alpha = 0.995$

The volumetric flow rate, V_m is given by

$$V_m = 2\int_0^1 f'(\eta)d\eta$$

$$V_m = 2\int_0^1 (0.995 - 0.4975(Re+\psi)\eta^2 + 0.660017Re\eta^3)d\eta \quad (47)$$

VII. RESULTS AND DISCUSSION

In this section, we present the result of the problem for the temperature as well the velocity profile graphically for variations in porosity and Reynold numbers. The result show both porosity and Reynold numbers significantly impacted the flow. Similarly for the volumetric flow rate, an increase or decrease leads to a corresponding increase or decrease.

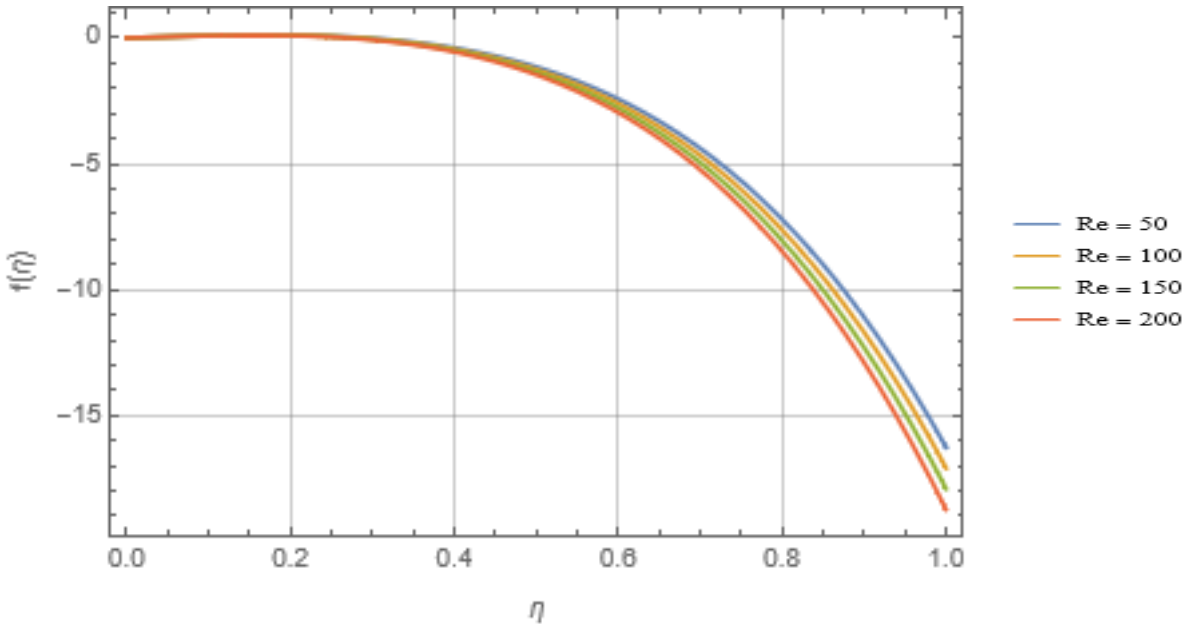

Figure 1. Variation of $f(\eta)$ with η for different values of Reynold number

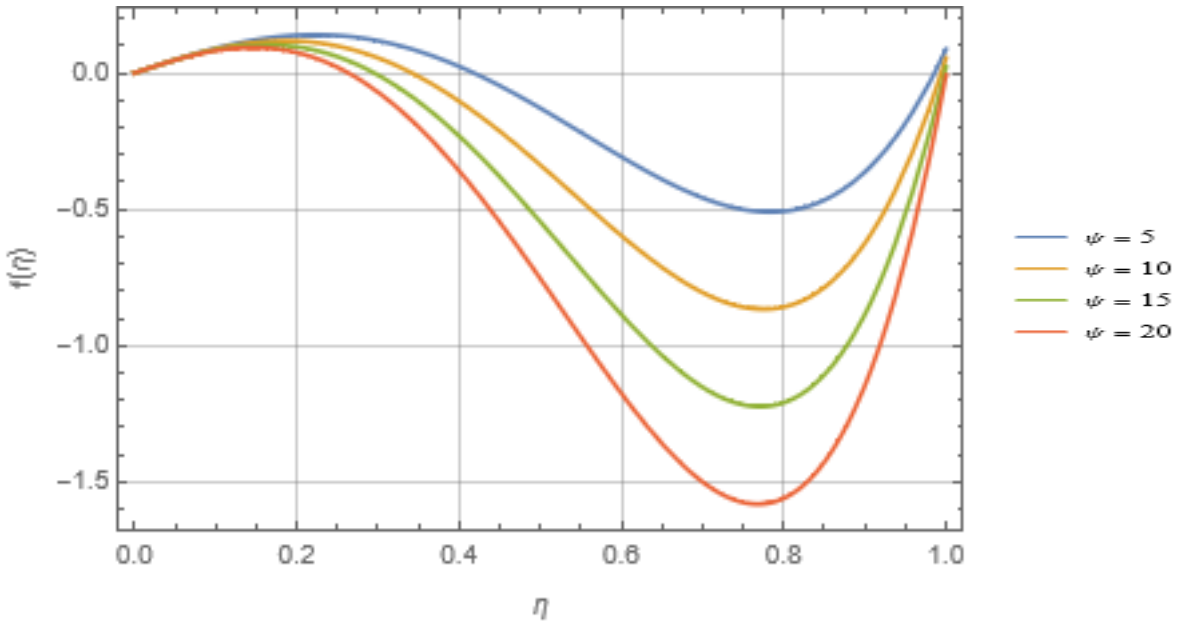

Figure 2. Variation of $f(\eta)$ with η for different values of porosity parameter

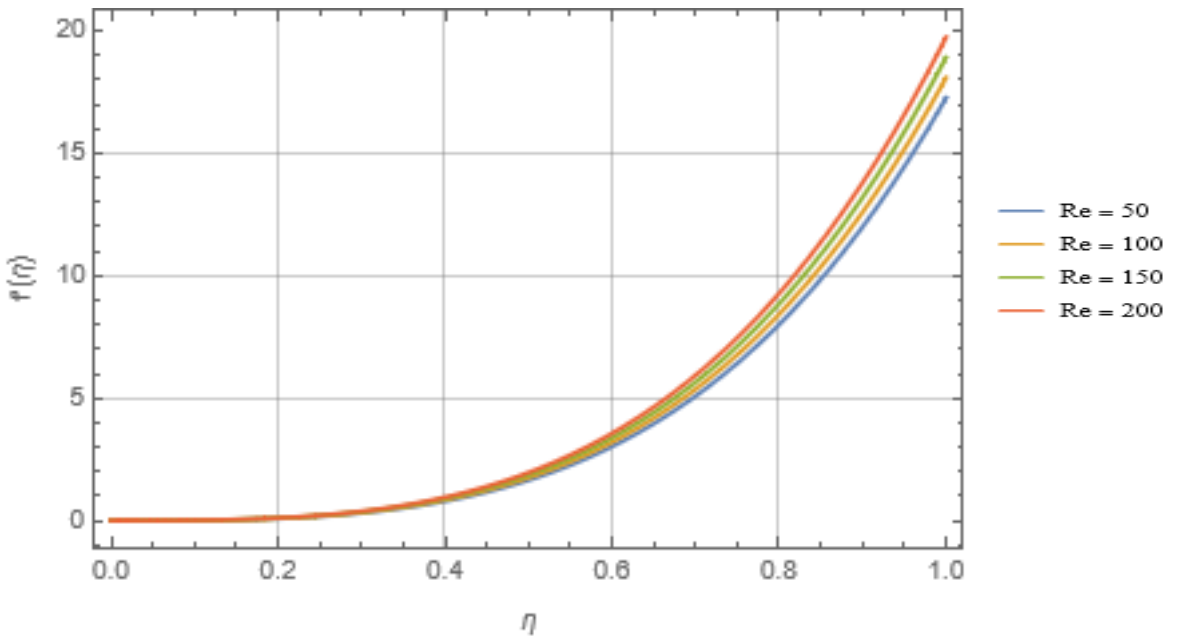

Figure 3. Variation of $f'(\eta)$ with η for different values of Reynold number

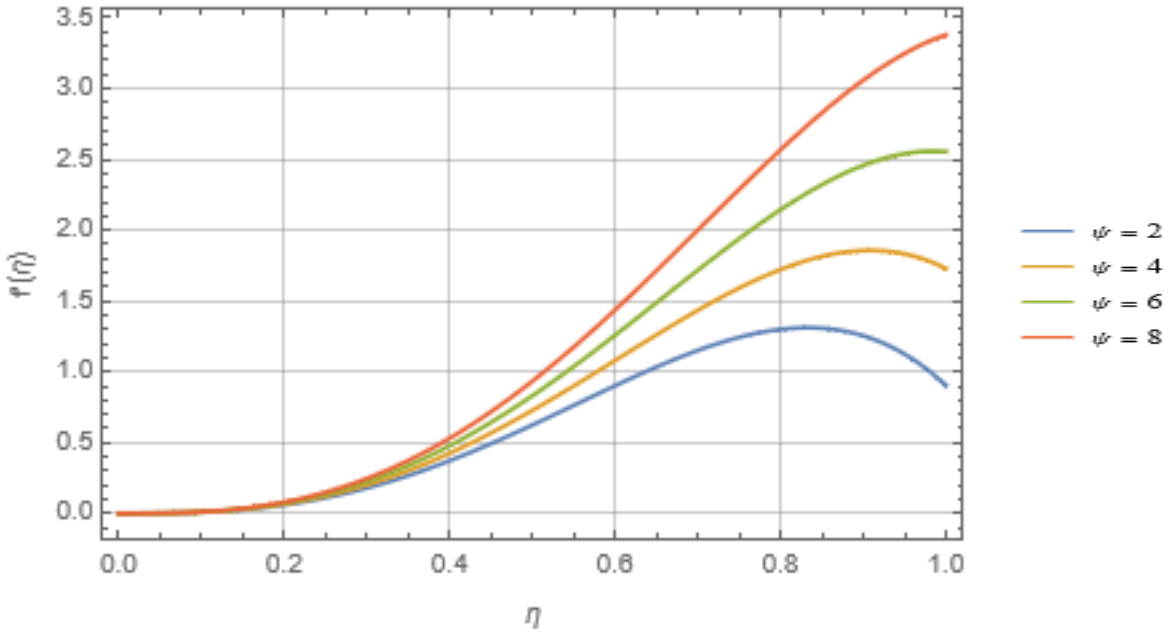

Figure 4. Variation of $f^{'}(\eta)$ with $\eta$for different values of porosity parameter

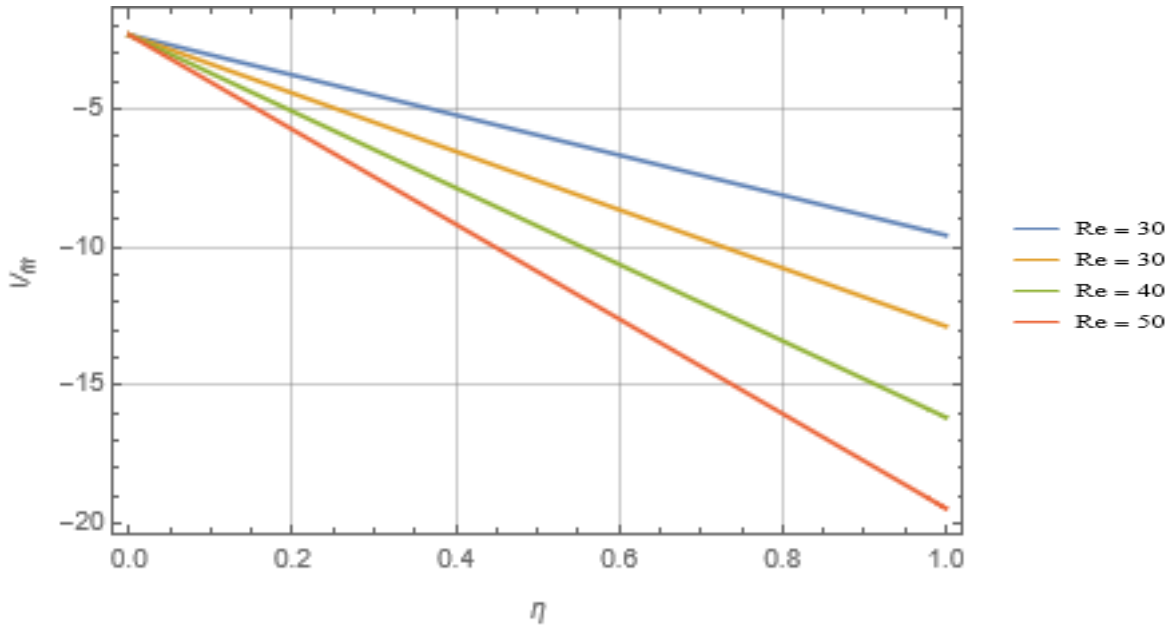

Figure 5. Variation ofV_m with η for different values of Reynold number

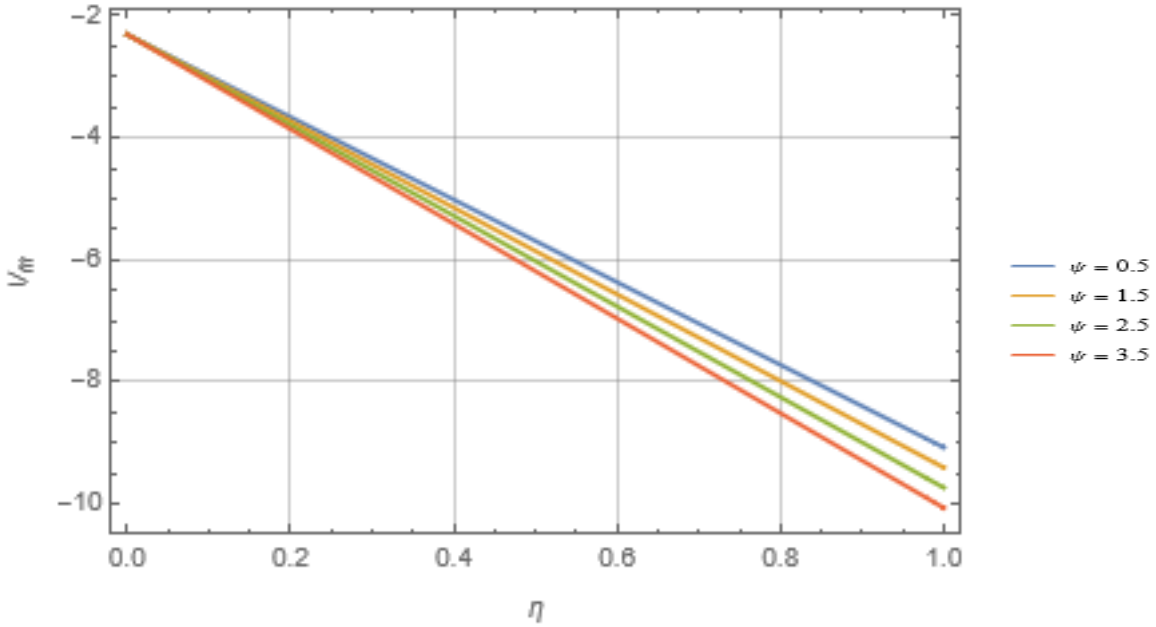

Figure 6. Variation of V_m with $\eta$for different values of the parameter, ψ

VIII. CONCLUSION.

In this research article, we analytically investigate the transport of chemical ion through the soil. The governing equations were transformed to a nonlinear ordinary differential equation, where they were solved using Variational Homotopy perturbation method. The findings of thearticle are summarized as follows.

(i) Increase in Reynold number, Re leads to decrease in the temperature profile, whereas the reverse is also true.
(ii) Decrease or increase in porosity parameter leads to a decrease and increase in the temperature profile of the velocity profile.
(iii) The velocity profile increases with an increase in the Reynold and porosity parameter
(iv) The volumetric flow rate for both temperature and velocity profiles decrease for increase in both porosity and Reynold numbers.

REFERENCES

[1] A. Agadjanov,E.Yusufoglu. Numerical solution of Duffing equation by the Laplace decomposition algorithm, Appl. Math. Comput., 2006, Vol. 177, pp. 572-580.

[2] E. Babolian, J. Biazar. A.R. Vahidi. A New Computational Method for Laplace Transforms by Decomposition Method, J. Appl. Maths. Comput.2004, Vol.150, pp. 841-846.

[3] J. Biazar, E. Babolian, R.Islam. Solution of the system of ordinary differential equations by Adomiandecomposition method, J. Appl. Maths. Comput., 2004, Vol. 147, pp.713-719.

[4] S. Poonam, A. Kumar, A. Rani. Laplace Adomian Decomposition Method to study Chemical ion transport through Soil. Applications and Applied Mathematics, 2019, Vol. 14, Issue 1, pp. 475-485

[5] N. Dogan. Solution of the System of Ordinary Differential Equations by Combined Laplace Transform-Adomian Decomposition Method, Math. Comput. Appl., 2012, Vol.17, No.3, pp. 203- 211.

[6] S.A. Khuri. A Laplace Decomposition Algorithm Applied to a Class of Nonlinear Differential Equations, Journal of Applied Mathematics, 2001, Vol. 1, No.4, pp. 141-155.

[7] A. Raptis. C. Perdikis. Flow of a viscous fluid through a porous medium bounded by a vertical surface, Int J Eng. Sci., 1983, Vol. 21, No.11, pp. 1327-1330.

[8] N.C. Sacheti. Application of Brinkman model in viscous incompressible flow through a porous channel, 1983, J Math Phys Sci., Vol.17, pp. 567-577.

[9] B. Sharma. Mathematical Modelling of Chemical ion transport through soil its Mechanism and Field Application., 2016, Ph.D. thesis http://hdl.handle.net/10603/206153.

[10] M. Turkyilmazoglu. Exact multiple solutions for the slip flow and heat transfer in a converging channel. Journal of Heat Transfer, 2015, Vol. 137, No.10, p. 101301.

[11] M. Malinfar, M. Mahdavi. The Application of the Variational Homotopy Perturbation method on the generalized Fisher's Equation. Mathematical Modelling & Computation, 2011, Vol-01, No. 2, 101-107.

[12] T. Allhviranloo, A. Armand, S. Pirmuhammadi. Variational Homotopy Perturbation method: An Efficient scheme for solving partial differential equations in fluid mechanics. Journal of Mathematics and Computer Science, 2014, 9, 362-369.

[13] A. Bouhassoun, M.C. Handi, M. Zellal. Variational Homotopy Perturbation Method for the approximate solution of the foam drainage equation with time and space fractional derivatives. Malaysian Journal of Mathematik, 2003, 4(1), 163-170.

[14] L. Ebiwareme, F.P. Kormane. A Variational Homotopy Perturbation Method Approach to the Nonlinear Equations Governing MHD Jeffery-Hamel Flow in the presence of magnetic field. American Journal of Engineering Research, 2022, Volume-11, Issue-02, pp-81-89.

[15] A. A. Elbelez, A. Kilicman, M.T. Bachok. Application of Homotopy perturbation and Variational Iteration method for the Fredholm Integro-differential equation of fractional order. Abstract and Applied Analysis, 2012, Volume 2012, Article ID. 763739.

[16] L. Yanqin. Variational Homotopy Perturbation Method for solving Fractional Initial boundary value problems. Abstract and Applied Analysis, 2012, Vol. 12, Article ID: 727031, 10pages, doi:10.1155/2012/727031.

[17] A.N. Muhammad, S.T. Mohyud-Din. Variational Homotopy Perturbation Method for solving higher dimensional Initial boundary value problems. Mathematical problems in Engineering, 2008, Volume 2008, Article ID: 696734, 11 pages, doi:10.1155/2008/696734.

[18] D. D. Ganji, A. R. Rezania, A.R. Ghorbali. On Homotopy Perturbation and Variational Iteration methods for linear and Nonlinear heat transfer Equation. Journal of Algorithm & Computational Technology, 2007, Vol. 2, 8003-8013.

[19] H. Ji-Huan. A Coupling method of a Homotopy Technique and Perturbation Technique for Nonlinear problems. International Journal of Nonlinear Mechanics, 2000, 35(2000), 37-43.

NOMENCLATURE

(x, y)	Cartesian coordinates of a point
(u, v)	Velocity component along $x - and\ y$ −directions

U_0	Characteristic velocity
F_0	Applied external force
k	Permeability of the porous medium
h	Half-width of the channel
η	Non-dimensional distance
μ	Coefficient of viscosity
ν	Kinematic viscosity of solute
ρ	Density of solute
Re	Reynold number
K	Permeability parameter

International Journal of Innovation Engineering and Science Research
(ISSN: 2581-4591)
www.ijiesr.com

Quad-Element MIMO Antenna with Enhanced Isolation for UWB Applications

Giday Gebrehiwot Bsrat
Andhra University College of Engineering(A)
Visakhapatnam,India

S.Aruna
Andhra University College of Engineering(A)
Visakhapatnam,India

K. Srinivasa Naik
Vignan's Institute of Information Technology,
Visakhapatnam,India

ABSTRACT

This study proposes a quad-element MIMO antenna for ultra-wide band applications. Design evolutions have been carried out in order to achieve large impedance bandwidth and good positive gain across the operating frequency range. In MIMO antenna construction, the best-performing antenna design is used as a basic radiator element. S-parameters, radiation patterns, and diversity performance findings are thus used to investigate MIMO antenna designs with various layouts.As a result, a quad-element MIMO antenna with orthogonal radiators orientation that operates in the frequency range of 3.5-11.2 GHz with >-20dB isolation in the majority of the operating band is proposed. The ECC and DG values are less than 0.006 and greater than 9.9, respectively, while the MEG and CCL are within acceptable ranges. The simulated findings agree well with the measured results.

Keywords—*Mutual couling,Envelope correlation coefficient (ECC), Diversity gain (DG), Mean effective gain (MEG), Channel capacity loss (CLL).*

I. INTRODUCTION

In modern wireless devices, because of their many advantages, microstrip antennas are the most popular antenna type. Microstrip antennas are low-profile, light-weight, simple to manufacture, and adaptable to mounting hosts, with a portable conducting patch printed on a grounded substrate. However, they naturally have a narrow bandwidth, and bandwidth improvement is usually required for many purposes. Besides, the requirements of ultra-wideband patch antennas in recent days are alarmingly increasing because of their wide frequency impedance bandwidth and solve the limitations of narrowband antennas. Ultra-wideband antennas are promising candidates for applications in UWB communications, like biomedical, military and commercial applications in general. According to the U.S FCC regulations, the spectrum of UWB covers a 3.1 to 10.6 GHz frequency bandwidth, which is intended for high-speed short-range communication [1].

Conventional microstrip patch antennas have some limitations, like narrow bandwidth, low gain and large size. Several methods of enhancing the performance of microstrip antennas have been reported in many literatures. Patch antennas with partial ground plane [1], [2], patch antenna with defected ground structure (DGS) that can be used for UWB application was proposed in [3]. The DGS significantly controls the impedance bandwidth and improves the radiation characteristics of monopole antennas by suppressing the higher modes of harmonics and reduce mutual coupling between adjacent elements[4], [5]. In, creating different-shaped slots in the ground plane can modify surface

current distribution, resulting in a change in the impedance bandwidth of a monopole, and this structure is called a defected ground structure (DGS). Using such structures, circular polarization can be achieved, multiband effect and improved radiation properties [6], [7]. On the other hand, due to the nature of forming periodic structures to possess band gap for surface wave propagation, Electromagnetic band gap structures (EBG) are also used[8], met-materials or photonic band gaps are also crucial for the impedance bandwidth and gain enhancements [9]. In a single physical package, two or more antennas can be designed for both transmission and reception applications in wireless technology. This kind of technology is known as Multiple-Input Multiple-Output (MIMO) antennas. By exploiting multiple antennas, the amount of data and range are improved compared to a single antenna using the same radio transmit power. Moreover, MIMO antennas boost link reliability and experience less fading than a single antenna system. In general, using MIMO technology, wireless capacity grows and numerous consumers can access various services at the same time too. Integration of UWB technology with MIMO techniques has become a solution to the short-range communications constraint [10], [11] which necessitates devices transmitting very small power.

Up to now, several research papers on MIMO antennas for UWB applications have been reported. Different techniques are proposed for good isolation for the reduction of mutual coupling and, as a result, to enhance the performance characteristics. In [12], a two-element UWB-MIMO antenna with >20 dB isolation over the band of 3 to 10.9GHz with a total size of 30×50×167mm^3 is proposed, to increase impedance bandwidth and improve isolation at the lower band, L-shaped open-slots are introduced in the common ground, along with a decoupling network comprised of a narrow slot and a fork-shaped slot. Additionally, a dual polarized slot antenna for ultra wideband applications with a size of 66.2 ×66.2 ×1.6 mm^3 is proposed in [13]. Better isolation > 20dB and good impedance matching are achieved by shaping the slot arms and feed section suitably and inserting narrow metallic stubs. In [14], The use of two element MIMO for UWB with reduced mutual coupling is proposed, and the middle portion of the ground structure is expanded outward to provide better isolation of > 20dB over the entire UWB with a size of 40×80×1.6mm^3. An UWB semi-ring MIMO antenna with a size of 50×90×1.52mm^3 and isolation > 10dB on the entire band is indicated in [10]. In [15], A compact two-element UWB-MIMO is reported. Without decoupling structure, high isolation is obtained between two antenna elements <−18 dB from 3.1–3.4 GHz and the overall size is 25×35×1.6mm^3. In [16], a triple notched UWB MIMO antenna with a size of 58×45×1.6mm^{3}is proposed. The structure uses a defected ground plane for the compactness and decoupling strips and a slotted ground plane for enhancing isolation which is > 15dB. Four-element MIMO antenna with a size of 80×80×1.52mm^3 is proposed in[17]. To improve the impedance bandwidth, it uses U-stab loaded on the radiator and defected ground plane, and by placing the elements orthogonally, isolation is improved to >15dB at the majority of the UWB. In [18], four-element MIMO consists of two alike slot dipoles and two alike planar monopoles with a total size of 70×41×0.8mm^3 which covers the whole UWB (3.1-10.6GHz) was developed with an isolation of >17dB . [11]reveals a 60×41×1mm^3 size compact MIMO antenna for UWB applications that achieves high isolation >20dB at the majority of the operating band due to the monopoles' complementary and asymmetrical structures, except > 10dB for 2.86–3.28 GHz . UWB MIMO antenna with double band rejection that has a size of 56×56×0.8mm^3 is depicted in [19]. The structure used rectangular and staircase-shaped stubs to obtain good isolation which is > 20dB at the majority of the band. On the other hand, in [20], The proposed compact four-element UWB-MIMO array was made up of four QSCA elements that are arranged anticlockwise to produce good impedance matching and 15 dB port-to-port isolation. Without employing any other decoupling techniques, the isolation is achieved. The total size is 40×40×1.6mm^3 .Recent MIMO antenna researches have mostly focused on the mutual coupling effect and studying several efficient strategies for reducing it. Surface current distribution is one of the critical factors in deciding the amount of mutual coupling between the antennas. In this work, a simple low-cost DGS based monopole patch antenna with triangular slot inside for UWB application is designed first, and then MIMO structures, which are two and four-element MIMO structures with different placements, are designed to come up with the desired MIMO antenna structure that has improved mutual coupling, better ECC and diversity gain. In the design, it is observed that mutual

coupling is reduced by the adjustment of the radiator element's orientation (placement). The development of the monopole antenna and simulation results are discussed in section 2, while MIMO antenna structures design, result analysis and evaluation are discussed in sections 3 and 4. All the simulations are done using CST software. Finally, in section 4.3, the suggested Quad-element MIMO antenna's simulated and measured results are discussed.

II. BASIC ANTENNA CONFIGURATION AND RESULT ANALYSIS

The UWB single-element antenna is derived from the design evolution of a full-ground-based rectangular monopole antenna fed by a 50 Ω microstrip line. Fig.1 (A-C) illustrates three different antenna designs in progress, from a simple patch to a DGS based patch with a triangular slot inside. The scaling or dimensions of an UWB antenna element for step-3 is indicated in Fig.2, and the parameters of the proposed UWB antenna are given in Table1.In the design ,FR-4 material with a dielectric constant (ε_o) of 4.3 and 1.6mm thickness is used as a substrate. In step-1, a simple rectangular microstrip element with a microstrip-line feeding technique is designed, while in step-2, a partial ground plane with two slots at $\lambda/2$ distance is designed, and in step-3, a triangular slot is introduced in the rectangular patch to achieve miniaturization and to cover the required ultra-wideband frequency. Since the key objective of the work is to propose a Quad-element UWB MIMO antenna with improved isolation, the design evolution of the three single-element antennas is evaluated according to their results.Fig.3 (a-d) presents the simulation results of the three antenna geometries to identify and select the desired antenna element.

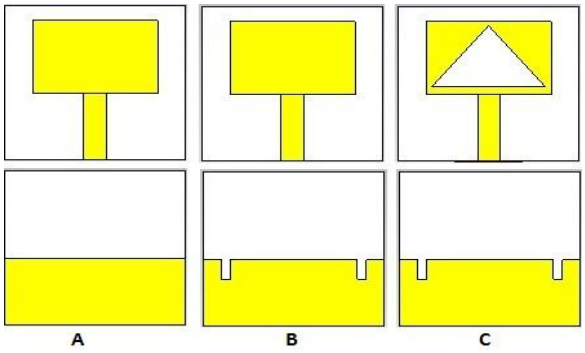

Figure 1.Monopole antenna designs: (A) Rectangular patch with full ground plane, (B) DGS based rectangular patch,(C) DGS based rectangular patch with triangular slot inside.

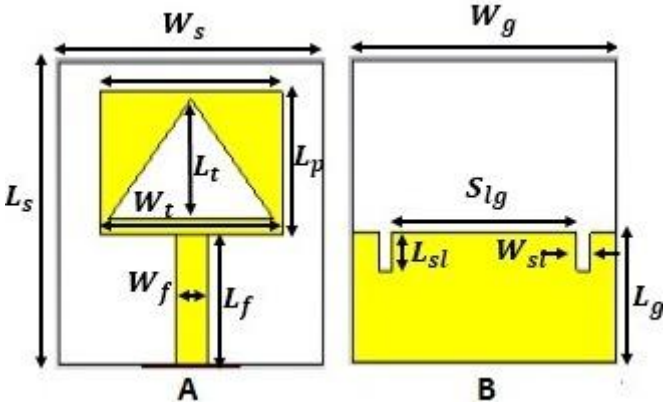

Figure 2.Scaling of UWB antenna :(A) Patch side, (B) Ground side.

TABLE 1. UWB MONOPOLE ANTENNA DIMENSIONS

Design specifications type	Dimensions	Design specifications type	Dimensions
substrate size($W_s \times L_s \times H_s$)	24×24×1.6mm3	Patch Slot width(W_t)	15.2mm
Full Ground size ($W_g \times L_{fg}$)	24×24mm2	Ground slot length(L_{sl})	3mm
Ground height (HG)	0.035mm	Ground slot width (W_{sl})	1.2mm
Partial ground plane size($W_g \times L_g$)	24×10.33mm2	Feed length (L_f)	10.33mm
Rectangular patch size($W_p \times L_p$)	16.6×11.33mm2	Feed width (W_f)	2.9mm
Patch Slot length(L_t)	9.5mm	Gap between ground slot(S_{lg})	15.2mm

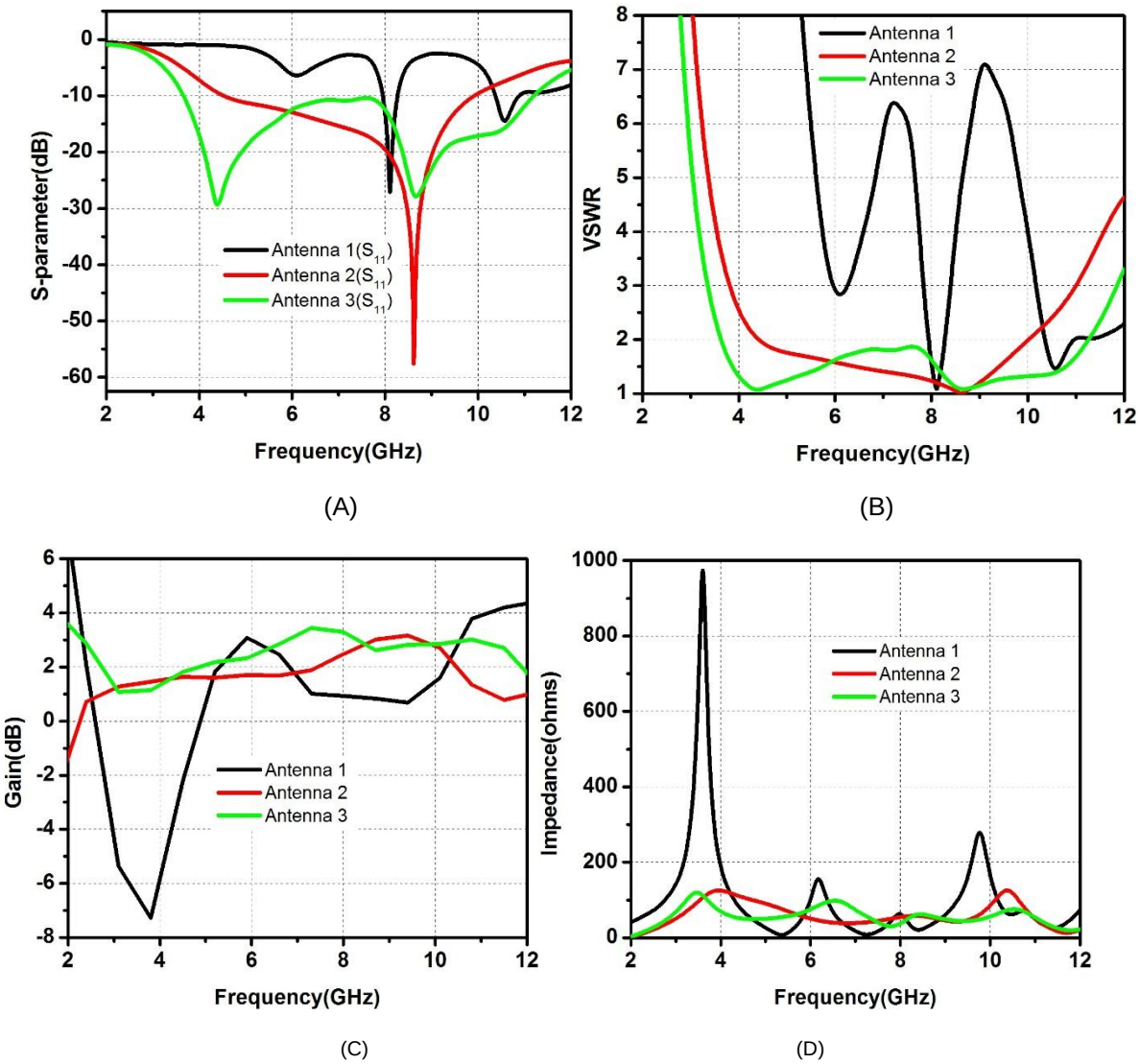

Figure.3. Simulation plots :(A) Reflection coefficient plot,(B) VSWR plot, (C) Gain plot,(D)Impedance plot.

As indicated in the plots, Step one antenna has an impedance bandwidth of 7.94-8.28GHz (4.1%) at ($|S_{11}|$< -10dB) with VSWR = 1.17 at a resonant frequency of 8.07 GHz, which is a narrow band. The second antenna has an impedance bandwidth of 4.55-9.29 GHz (68.49%) at ($|S_{11}|$ <-10dB), VSWR=1.04 at resonant frequency of 8.616 GHz, which indicates a broadband antenna. The broadband condition is happening because of the introduction of a defected ground plane, which completely altered the current distribution. The step-3 design provides an impedance bandwidth of 3.644-11.237GHz (101%) at ($|S_{11}|$<-10dB) with VSWR =1.1 at the resonant frequency. From the Gain Vs frequency plot, the peak gain in the operating band is 3.4dB. This is obtained from the third

antenna, while 3.03dB for the second antenna and 3dB for the first antenna. Fig. 3 (D) shows the impedance Vs. frequency plot, where the third antenna's curve nearly falls around the standard impedance value, which is 50 ohm (proper impedance matching effect). Therefore, from step by step geometric studies, step-3 monopole antenna design is preferable for the construction of MIMO antennas because of its ultra-wideband effect. Further, the proposed single element antenna was fabricated and tested using vector network analyzer. Fig.4.illustrates the simulation VS measurement result. Where it's$|S_{11}|$ measured values are almost similar to its simulation values.

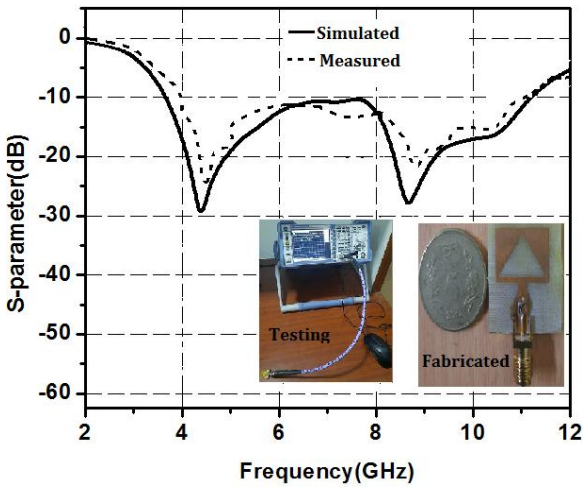

Figure 4. Measurement VS simulated result

III. MIMO ANTENNA DESIGN AND CONFIGURATION

For the two and four-element MIMO antenna structures, different antenna radiator orientations (placement) are presented in Fig. 5 (A-D). The proposed adjustments are according to the individual antenna elements' placement or layout. Fig. 5 (A) shows a two-element MIMO antenna-1.The radiators are placed on the same plane side by side with a gap of ~0.2 λ(7.4mm) and Fig. 5 (B) shows a two-element antenna-2. Here elements are oriented 180 degrees to each other with an inter-element gap of ~0.2λ (7.4 mm). Besides, the four-element MIMO antenna-1 and MIMO antenna-2 structures are presented in Fig. 5 (C) and (D), where, in the first MIMO, two antenna elements are placed in the same orientation with an inter-element gap of ~0.2λ (7.4 mm) to each other, and the remaining two elements are placed on the opposite side, oriented 180 degrees from the first two elements with an inter-element gap of ~0.12λ (4.67 mm). On the other hand, the second MIMO structure organizes two adjacent radiators orthogonal to each other where a single element has an inter-element gap of ~0.16λ (6.03mm) and ~0.13λ (5.03mm) to the two neighboring elements as indicated in the figure. The total sizes of the two-element MIMO antenna structures are 24mm×48mm×1.6mm each, while the four-element MIMO structures have a size of 48mm×48mm×1.6mm each.

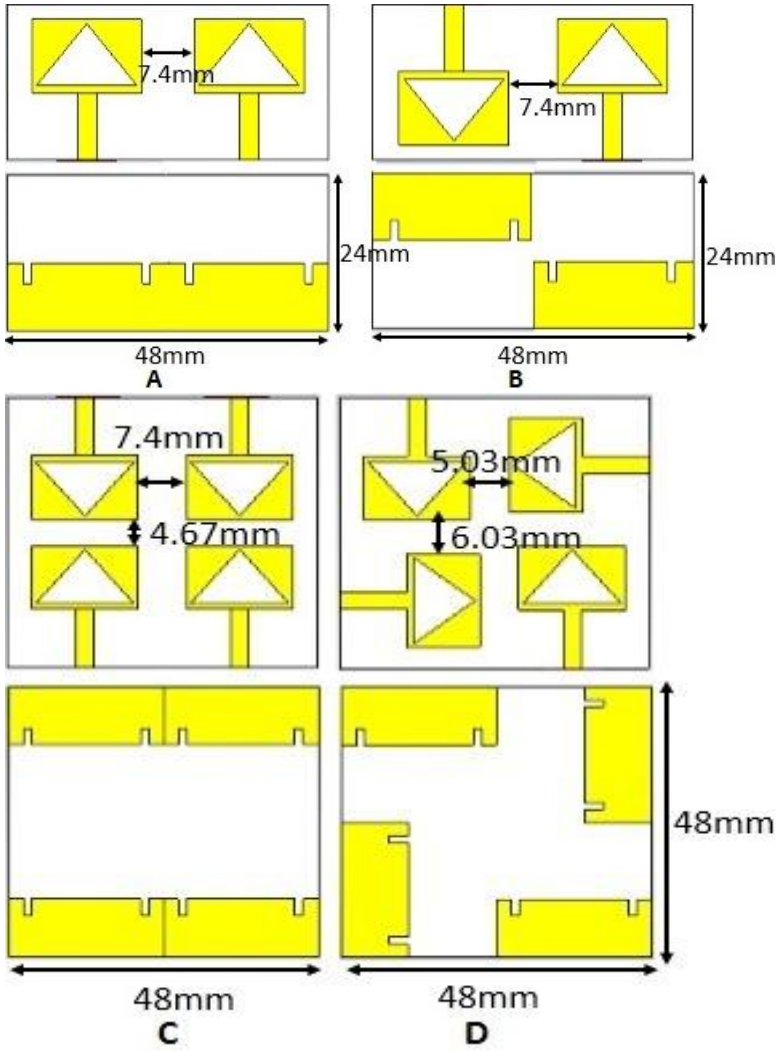

Figure 5. MIMO antennas top and bottom view: (A), (B) Two-element MIMO antenna orientaion-1& orientation-2, (C),(D) Four-element MIMO antenna orientaion-1& orientation-2.

IV. RESULT DISCUSSION

In this section, the simulation findings of the designed MIMO antennas, as well as the measurement results of the suggested four-element MIMO UWB antenna are discussed. The outcomes discussed include return loss, mutual coupling effect and diversity performance.

A. S-parameter

In this section, the return loss plot and isolation values are presented. The design geometries of both layouts are indicated in the previous section. Here, the comparative studies for both configurations based on their S-parameter results are discussed. Fig. 6 (A), shows the S-parameter simulation plot of the two-element MIMO antenna-1. Thus, the impedance bandwidth of this two-element MIMO antenna in this configuration is 3.47-11.00 GHz, and the majority of the band has < -12 dB mutual coupling effect. For the two-element MIMO antenna-2, when elements are oriented 1800 to each other, the S-parameter plot is revealed in Fig.6 (B) and the impedance bandwidth is 3.41 -11.09 GHz with the majority of its operating band has < -15 dB mutual coupling effect. In this way, the second MIMO configuration has slightly better bandwidth with enhanced isolation. Likewise, the four-element MIMO antenna simulation results are illustrated in Fig. 7 (A) and (B). The four-element MIMO antenna-1 return loss values are identical for all ports, which are 3.45-11.00 GHz with majority of its operating band's mutual coupling is < -15dB, while the four-element MIMO antenna-2 has a 3.60-11.42 GHz

impedance bandwidth and more than -20dB isolation for the majority of the operating band respectively.

B. Diversity performance

This study took into account the diversity performance of the designed configurations in order to properly evaluate the MIMO antenna. Thus, the envelope correlation coefficient (ECC) and diversity gain (DG) of all structures are compared, and the suggested quad-element antenna is also assessed against acceptable MEG and CCL criteria.

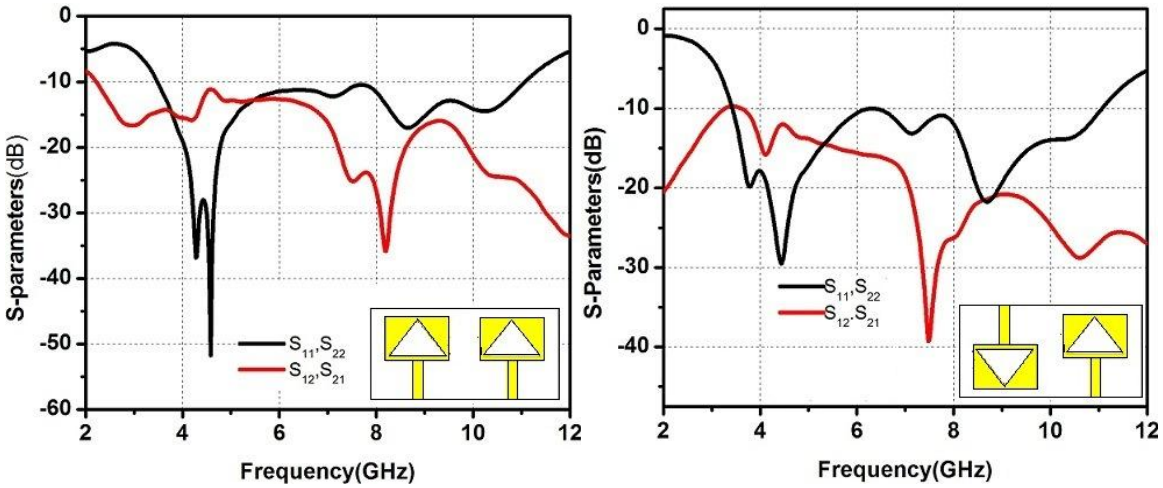

(A) (B)

Figure 6. Two element MIMO antenna S-parameter plots.(A)orientation-1,(B) orientation-2.

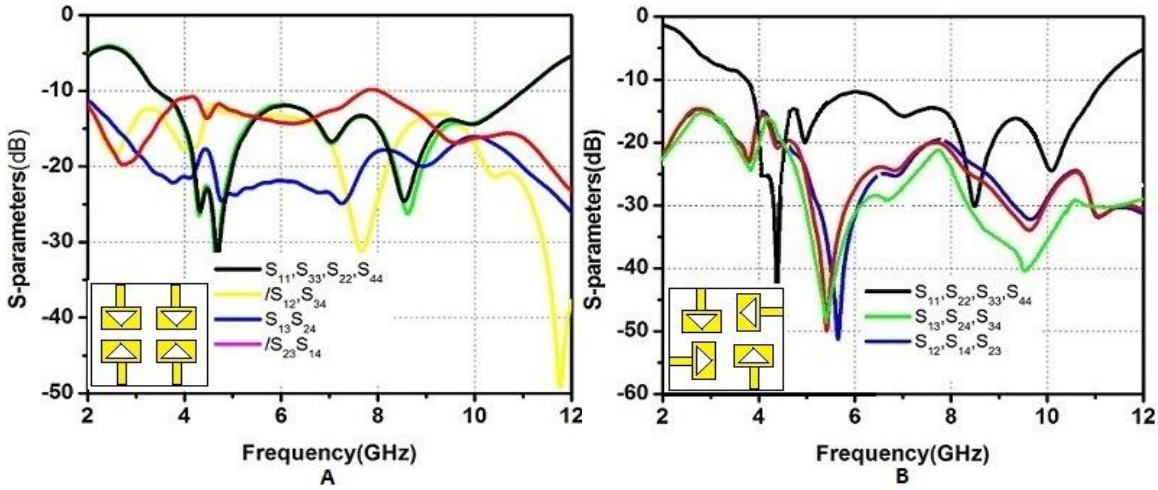

Figure 7. Four-element MIMO antenna S-parameter plots.(A) orientation-1,(B) orientation-2.

ECC is a measure of isolation between antenna elements that describes how two antenna elements' radiation patterns are independent. The signal to noise ratio of a MIMO antenna system, on the other hand, is assessed by diversity gain. In theory, it should be ten times that of the envelope correlation coefficient, but more than 9.5 is acceptable in practice. In general, maximum diversity gain is only attained when the envelope correlation coefficient is zero. The ECC is calculated using the S-parameter and the radiation pattern in Equations (1,2 and 3).[21]–[23].

$$\rho_{xy} = \frac{\left|S_{xx}^{*}S_{xy} + S_{yx}^{*}S_{yy}\right|^2}{\left(1-\left|S_{xx}\right|^2-\left|S_{yx}\right|^2\right)\left(1-\left|S_{yy}\right|^2-\left|S_{xy}\right|^2\right)} \quad [1]$$

Where S_{xy}, S_{yx} ,S_{yy} and S_{xx} are the scattered parameters and ρ_{xy} is ECC values.

$$\rho_e = \frac{\left|\iint_{4\pi} |F_1(\theta,\phi)* F_2(\theta,\phi)d\Omega\right|}{\iint_{4\pi}|F_1(\theta,\phi)|^2 d\Omega \iint_{4\pi}|F_2(\theta,\phi)|^2 d\Omega} \quad [2]$$

Where, $F_x(\theta,\emptyset)$ is the field radiation pattern when port x is excited.

Any MIMO antenna system's spectral efficiency is degraded by a larger value of the envelope correlation coefficient (ρ). As a result, achieving the lowest possible correlation coefficient is preferable. When the value of "ρ" approaches zero, a MIMO antenna system achieves near-perfect performance.

$$DG = 10\sqrt{1-(ECC)^2} \quad [3]$$

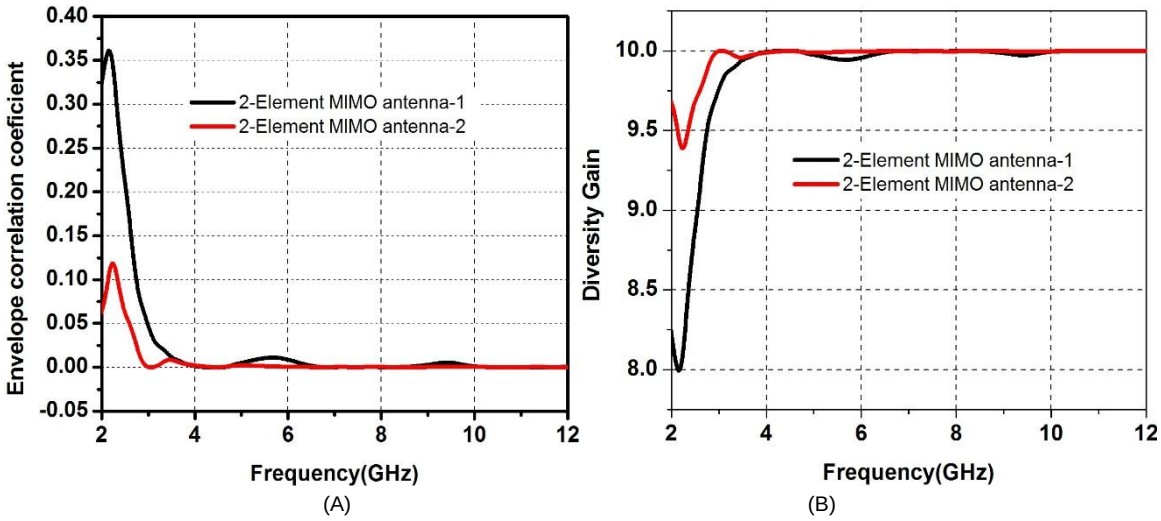

Figure 8. (A) ECC of two-element MIMO antenna orientation-1& -2, (B) DG of two-element MIMO antenna orientation-1& -2.

According to the results obtained in Fig 8 (A) & (B), the ECC and DG of orientation-1 are < 0.015 and > 9.91, while the ECC and DG of orientation-2 are < 0.006 and > 9.97 respectively. Fig. 9(a) and (b) show the ECC values of four-element MIMO antennas for both configurations, where, orientaion-1 has < 0.029 ECC value and orientation-2's ECC value is <0.006. Moreover, the DG value of the first structure is shown in Fig. 10 (A) and has a value of > 9.98 while the second structure has diversity gain > 9.99 as depicted in Fig. 10 (B). From the result indicators, the four-element MIMO antenna-2 has better diversity performance and isolation. That has to be taken to the fabrication of a prototype structure for result validation.

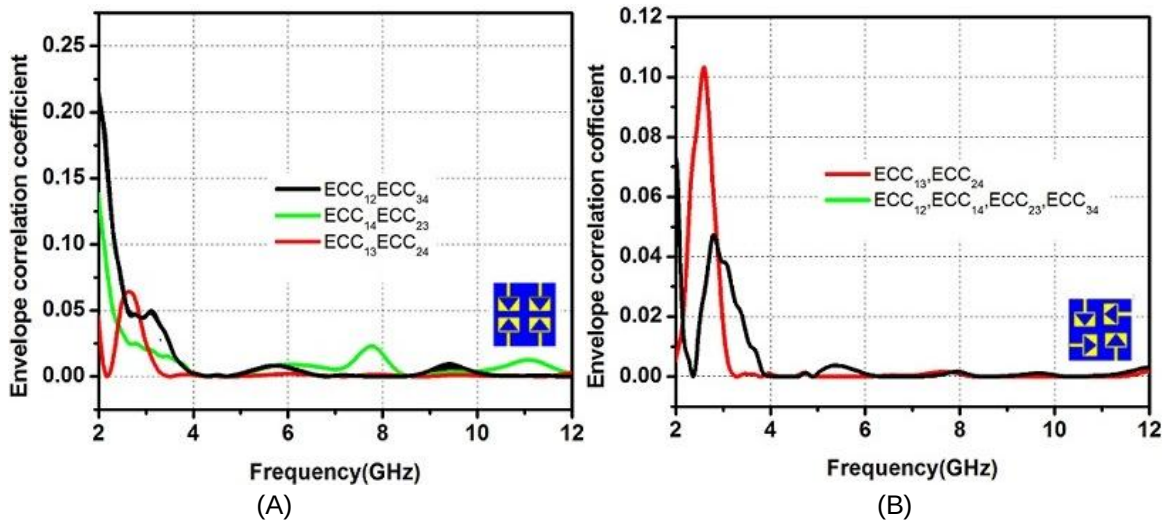

Figure 9.ECC simulation curves of four-element MIMO antenna:(A)orientation-1,(B)orientation-2.

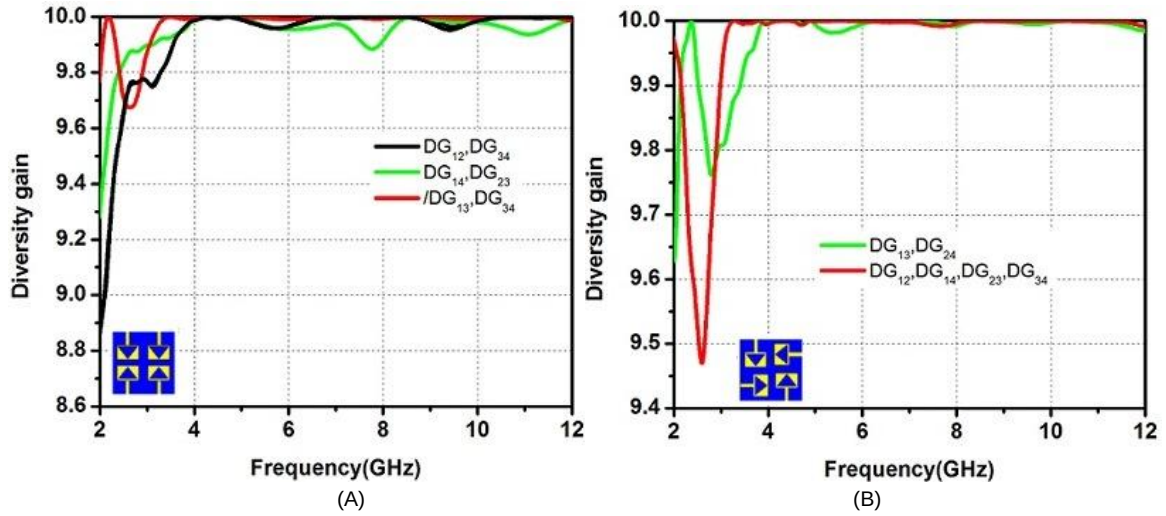

Figure 10.DG simulation curves of four-element MIMO antenna:(A)orientation-1,(B)orientation-2

The four-element MIMO antenna-2 is further investigated using the mean effective gain (MEG) and it is calculated using equation (4). For good diversity performance, the practical standard followed is that MEG should be −3 ≤ MEG (dB) <-12 [24]. Thus, as we can observe from MEG plots in Fig.11 (A), all are between -3dB and -12dB

$$MEG_i = 0.5\left(1-\sum_{j=1}^{k}\left|S_{ij}\right|\right)[4]$$

Farthermore,CLL is another significant diversity performance measure for MIMO antenna analysis. It refers to the highest possible information transmission rate at which the signal can be easily conveyed without considerable loss. The following equations are used to compute the CCL[22].

$$CCL = -\log_2 \det(\partial)[5]$$

$$\partial = \begin{vmatrix} \partial_{11} & \partial_{12} & \partial_{13} & \partial_{14} \\ \partial_{21} & \partial_{22} & \partial_{23} & \partial_{24} \\ \partial_{31} & \partial_{32} & \partial_{33} & \partial_{34} \\ \partial_{41} & \partial_{42} & \partial_{43} & \partial_{44} \end{vmatrix}$$

$$\partial_{xx} = 1 - \left(\sum_{y=1}^{M} \left| S_{xy} \right|^2 \right) \text{where, } \partial_{xy} = -\left| S_{xx}^{*} S_{xy} + S_{yy}^{*} S_{yx} \right|$$

CCL computed for the four-element MIMO antenna orientation-2 is depected in Fig.11(B). It is observed that the CCL is below 0.1 bits/sec/Hz, which is agreed with the standard value of CCL to be <0.4 bits/sec/Hz. The capacity of a MIMO antenna increases as the number of antennas grows.

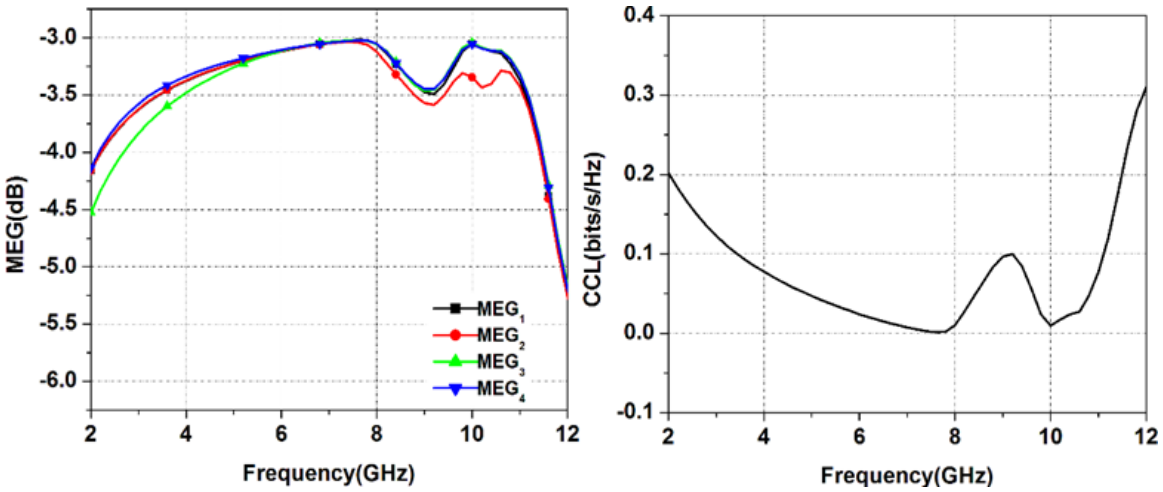

(A) (B)

Figure 11.Simulated results :(a) MEG, (b) CLL

The surface current distribution of the suggested MIMO antenna is revealed in Fig.12. Surface current analysis is carried out at 4.38GHz, which is one of the resonant frequencies. Antenna radiator-1 is excited at this resonance frequency, and the other radiators are regarded to be suited to the 50 ohm impedance. This method is used to look into the antenna parts that affect the MIMO structure's radiation characteristics and reveal the amount of coupling between radiator elements. It is clear that the surface current density is highest on the triangular slot's edges, around the feed line, and a significant amount also appears on the defected ground structure.

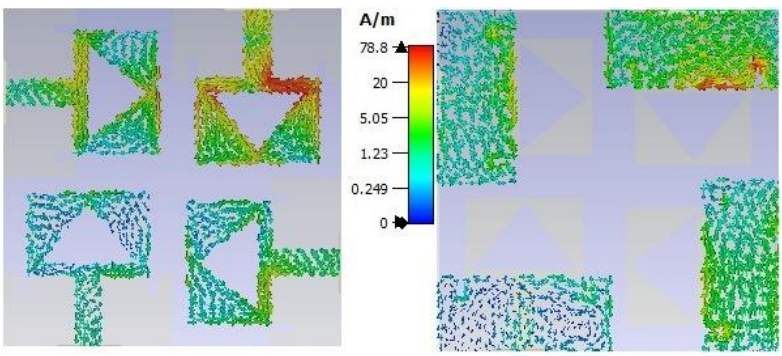

(A) (B)

Fig.12. Surface current distribution :(a) patch side, (b) ground side.

The comparison table of the designed MIMO antennas is stated in Table 2. From this table, two-element MIMO antenna-2's element isolation is better than two-element MIMO antenna-1 by 3 dB. But for the four-element MIMO antenna, MIMO antenna-2 isolation is better than MIMO antenna-1by 5 db. Therefore, MIMO Antenna-2 is more efficient compared to the MIMO Antenna-1 in both cases.

TABLE 2.SIMULATION RESULT COMPARISONS ON THE DESIGNED MIMO ANTENNA STRUCTURES

MIMO structure type		MC (on majority Of the band)	Impedance Bandwidth	ECC	DG
Number of elements	Orientation				
2-element	MIMO-1	<-12dB	3.47GHz-11.00GHz	<0.015	>9.91
	MIMO-2	<-15dB	3.41GHz-11.09GHz	<0.006	>9.97
4-element	MIMO-1	<-15dB	3.45GHz-11.00GHz	<0.029	>9.80
	MIMO 2	<-20dB	3.60GHz-11.42GHz	<0.006	>9.90

C.Measurement and simulation results discussion

The fabricated prototype of the MIMO antenna-2 is depicted in Fig. 13. The experimental results [25], [26]are tested using a vector network analyzer and compared with the simulated results as illustrated in the graphs of Fig .15 (A-C). It operates from 3.5 to 11.2GHz and has good element isolation with some un-smoothness in the curves and a little deviation from the simulation results. Besides, the elements have a less mutual coupling effect, as can be noticed from the curves, with the majority of the band falling below <-20dB. Farther more, the measured ECC and DG values almost agree with the simulated results. The slight mismatching effect in all curves is due to fabrication imperfection, soldering of connectors that produces losses.

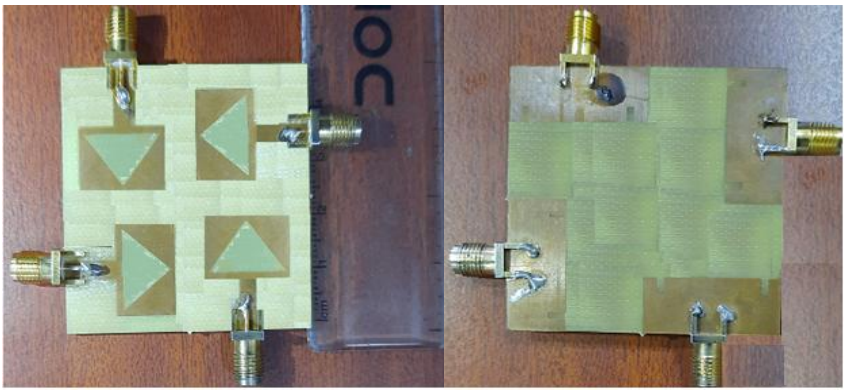

(A) (B)

Figure 13.Prototype. (A) Top view, (B) Bottom view.

Comparisons table i.e. Table 3 summarizes results comparisons among recently proposed MIMO antenna systems, and our design has comparatively high isolation, as can be shown, low ECC value and nearly 10 diversity gain and is small in size. But, the peak gain is moderate compared to the indicated references. Therefore, the proposed structure will be important for UWB MIMO application.

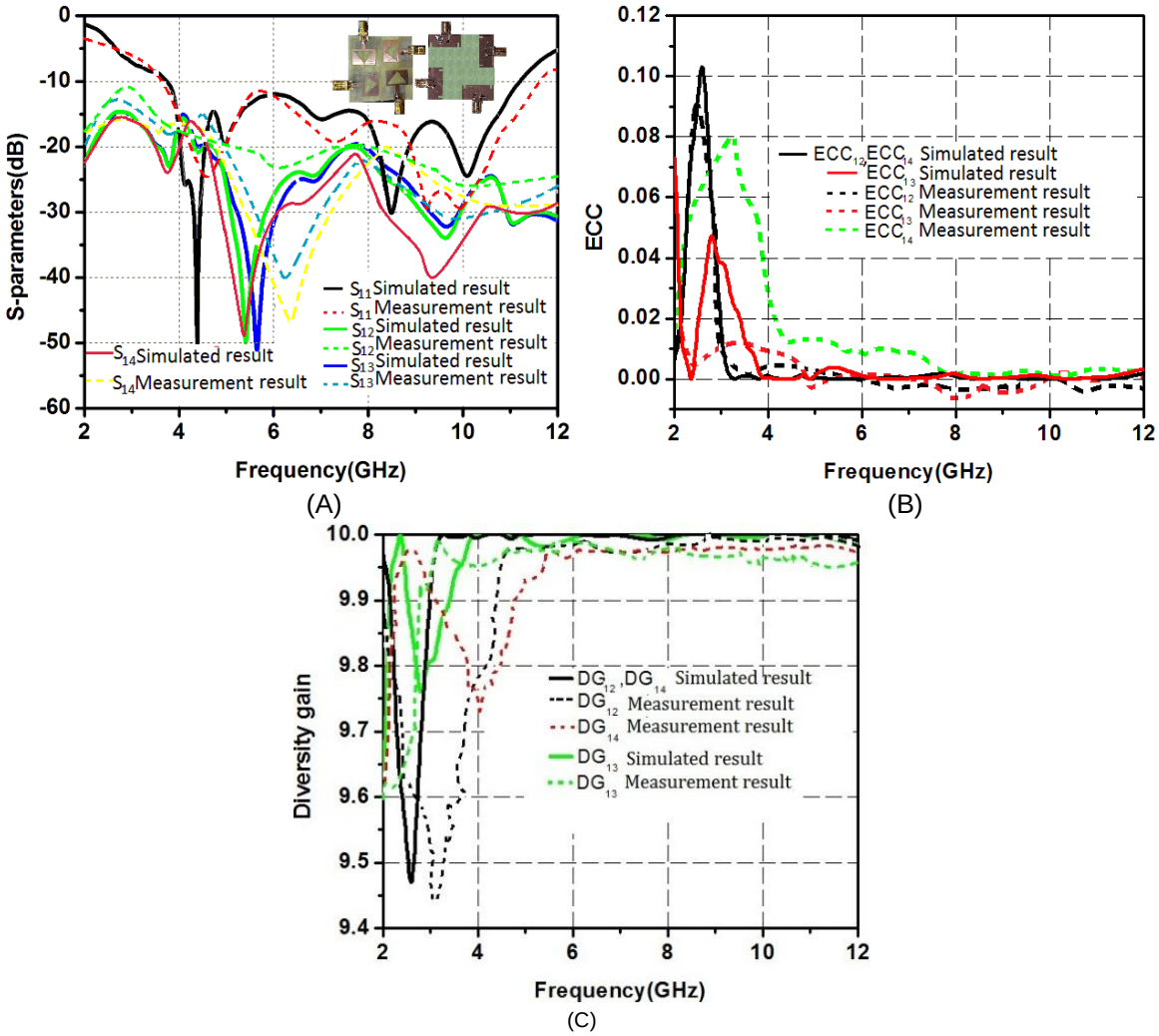

Figure14. Simulated Vs measured values :(A) S-parameter plot, (B) ECC plot,(C)diversity gain Plot.

The radiation pattern depicts the angular distribution of radiated power density in the far field. According to IEEE standards, the E-plane of an antenna is the plane containing the electric field vector and the maximum radiation direction or it is kept aligned along the desired orientation[27], while the H-plane is the plane containing the magnetic field vector and the maximum radiation direction .The simulated and measured E- and H-plane radiation patterns at 4.38, 8.5, and 10.5 GHz are shown in Fig.15 (A-C).The measured results are suited with the simulated result except for slight deviation as revealed in the radiation plot.

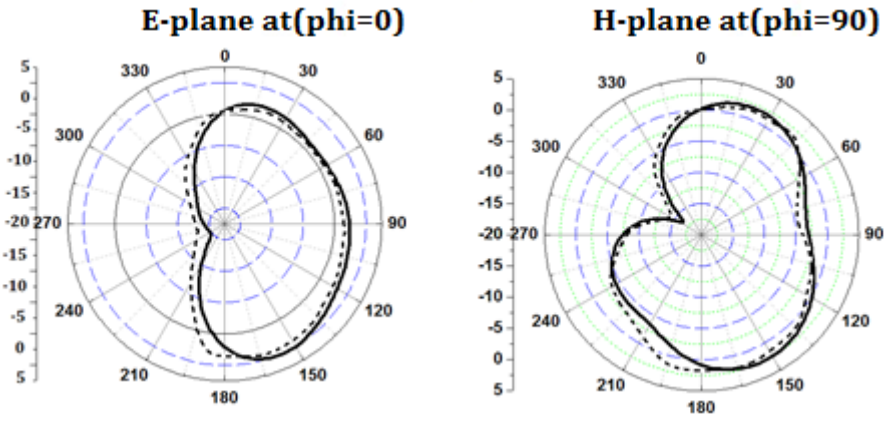

(A)

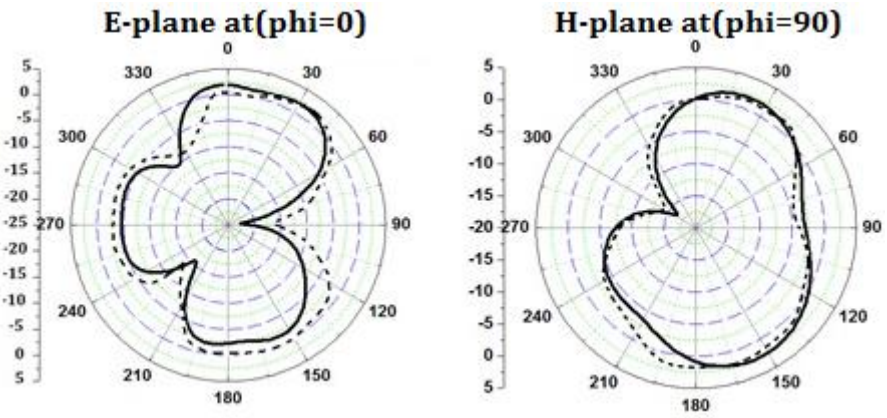

(B)

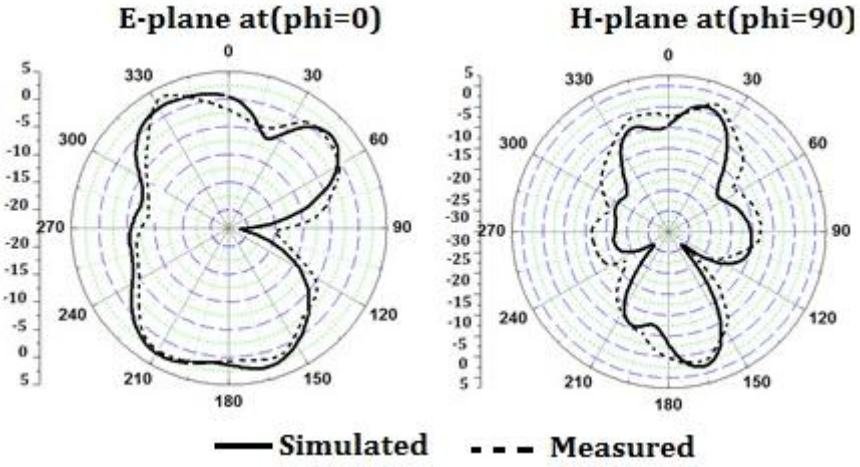

(C)

Figure 15. Measured Vs simulated radiation patterns: (A) 4.38 GHz; (B) 8.5 GHz,(C) 10.5 GHz

TABLE 3.COMPARISON OF THE PROPOSED STRUCTURE WITH OTHER ANTENNA

Reference	Number radiating elements	Impedance BW(<10dB) in GHz	MC(on majority Of the band)	Size (mm3)	ECC	D.G.
[12]	2	3.00-10.90	<-20	30×50×1.6	<0.06	>9.6
[13]	2	3.00-12.00	<-20dB	66.2×66.2×1.6	<0.005	_
[14]	2	3.00-11.00	<-20dB	40×80×1.6	_	_
[10]	2	1.85-10.60	<-10dB	50×90×1.52	<0.16	>9.5
[15]	2	3.10-3.40	<-18dB	25×35×1.6	<0.005	-
[16]	2	3.10-11.00	<-15dB	58×45×1.6	<0.5	_
[17]	2/4	3.18-11.50	<-15dB	80×80×1.52	<0.015	>9.98
[18]	4	3.10-10.60	<17dB	70×41×0.8	<0.012	>9.95
[11]	4	3.10-10.60	<-20dB	60×41×1.0	<0.250	-
[19]	4	3.20-10.70	<-20dB	56×56×1.6	-	-
[20]	4	2.95-12.10	<-15dB	40×40×0.8	<0.04	-
Proposed work	4	3.20-11.20	<-20dB	48×48×1.6	<0.006	>9.99

V. CONCLUSION

In this paper, a quad-element MIMO antenna is proposed for UWB communication. The miniaturization and high performance of the basic monopole antenna is achieved by introducing defected ground structure and slots on the patch. Different placements (orientations) both for two–element and four-element MIMOs are analyzed and compared using the results obtained from the simulation. The MIMO structures are investigated for best performance in return loss, mutual coupling effect, and diversity performance. It has been discovered that the Quad-element MIMO antenna with orthogonal placement operates in the UWB range with better element isolation and better diversity performance. Except for slight deviations and un-smoothness of the curves, the suggested Quad-element MIMO antenna's measured and simulated results are in good accord. Consequently, the overall dimension of the proposed Quad-element MIMO antenna is $48\times48\times1.6mm^3$ and it could be a good fit for UWB-MIMO wireless communication applications

REFERENCES

[1] Z. Khan, A. Razzaq, J. Iqbal, A. Qamar, and M. Zubair, "Double circular ring compact antenna for ultra-wideband applications," IET Microw. Antennas Propag., vol. 12, no. 13, pp. 2094–2097, Oct. 2018, doi: 10.1049/iet-map.2018.5245.

[2] K. Kamakshi, J. A. Ansari, A. Singh, M. Aneesh, and A. K. Jaiswal, "A novel ultrawideband toppled trapezium-shaped patch antenna with partial ground plane," Microw. Opt. Technol. Lett., vol. 57, no. 8, pp. 1983–1986, Aug. 2015, doi: 10.1002/mop.29231.

[3] D. Venkatachalam and M. Govindasamy, "A miniaturized planar antenna with defective ground structure for UWB applications," IEICE Electron. Express, vol. 16, no. 14, pp. 20190242–20190242, 2019, doi: 10.1587/elex.16.20190242.

[4] M. K. Khandelwal, B. K. Kanaujia, and S. Kumar, "Defected Ground Structure: Fundamentals, Analysis, and Applications in Modern Wireless Trends," Int. J. Antennas Propag., vol. 2017, pp. 1–22, 2017, doi: 10.1155/2017/2018527.

[5] S. Pramono and B. B. Subagio, "Mutual Coupling Reduction & Bandwidth Enhancement Using a Simple Folded Slot-PartialGround Plane in Dualband MIMO Antenna," in 2018 International Seminar on Intelligent Technology and Its Applications (ISITIA), Bali, Indonesia, Aug. 2018, pp. 19–22. doi: 10.1109/ISITIA.2018.8711213.

[6] K. Wei, J. Y. Li, L. Wang, R. Xu, and Z. J. Xing, "A New Technique to Design Circularly Polarized Microstrip Antenna by Fractal Defected Ground Structure," IEEE Trans. Antennas Propag., vol. 65, no. 7, pp. 3721–3725, Jul. 2017, doi: 10.1109/TAP.2017.2700226.

[7] N. Kishore, A. Prakash, and V. S. Tripathi, "A multiband microstrip patch antenna with defected ground structure for its applications," Microw. Opt. Technol. Lett., vol. 58, no. 12, pp. 2814–2818, Dec. 2016, doi: 10.1002/mop.30151.

[8] A. Ahmed, "Electromagnetic Band Gap Coupled Microstrip Antenna for UWB Applications," IOSR J. Electron. Commun. Eng., vol. 2, no. 6, pp. 01–03, 2012, doi: 10.9790/2834-0260103.

[9] B. P. Smyth, S. Barth, and A. K. Iyer, "Dual-Band Microstrip Patch Antenna Using Integrated Uniplanar Metamaterial-Based EBGs," IEEE Trans. Antennas Propag., vol. 64, no. 12, pp. 5046–5053, Dec. 2016, doi: 10.1109/TAP.2016.2618854.

[10] S. K. Dhar and M. S. Sharawi, "A UWB semi-ring MIMO antenna with isolation enhancement," Microw. Opt. Technol. Lett., vol. 57, no. 8, pp. 1941–1946, Aug. 2015, doi: 10.1002/mop.29245.

[11] X.-L. Liu, Z.-D. Wang, Y.-Z. Yin, J. Ren, and J.-J. Wu, "A Compact Ultrawideband MIMO Antenna Using QSCA for High Isolation," IEEE Antennas Wirel. Propag. Lett., vol. 13, pp. 1497–1500, 2014, doi: 10.1109/LAWP.2014.2340395.

[12] E. Wang, W. Wang, X. Tan, Y. Wu, J. Gao, and Y. Liu, "A UWB MIMO slot antenna using defected ground structures for high isolation," Int. J. RF Microw. Comput.-Aided Eng., vol. 30, no. 5, May 2020, doi: 10.1002/mmce.22155.

[13] R. V. S. R. Krishna and R. Kumar, "A Dual-Polarized Square-Ring Slot Antenna for UWB, Imaging, and Radar Applications," IEEE Antennas Wirel. Propag. Lett., vol. 15, pp. 195–198, 2016, doi: 10.1109/LAWP.2015.2438013.

[14] M. Li, Y. Yu, and T. Hong, "A Compact UWB MIMO Antenna with Extended Ground to Reduce Coupling," in 2019 IEEE International Symposium on Broadband Multimedia Systems and Broadcasting (BMSB), Jeju, Korea (South), Jun. 2019, pp. 1–3. doi: 10.1109/BMSB47279.2019.8971882.

[15] Y. Wu, K. Ding, B. Zhang, J. Li, D. Wu, and K. Wang, "Design of a Compact UWB MIMO Antenna without Decoupling Structure," Int. J. Antennas Propag., vol. 2018, pp. 1–7, 2018, doi: 10.1155/2018/9685029.

[16] N. Jaglan, S. D. Gupta, B. K. Kanaujia, S. Srivastava, and E. Thakur, "TRIPLE BAND NOTCHED DG-CEBG STRUCTURE BASED UWB MIMO/DIVERSITY ANTENNA," Prog. Electromagn. Res. C, vol. 80, pp. 21–37, 2018, doi: 10.2528/PIERC17090702.

[17] M. N. Hasan, S. Chu, and S. Bashir, "A DGS monopole antenna loaded with U-shape stub for UWB MIMO applications," Microw. Opt. Technol. Lett., vol. 61, no. 9, pp. 2141–2149, Sep. 2019, doi: 10.1002/mop.31877.

[18] L. S. Yang, M. Xu, and C. Li, "Four-Element MIMO Antenna System for UWB Applications," Radioengineering, vol. 27, no. 1, pp. 60–67, Apr. 2019, doi: 10.13164/re.2019.0060.

[19] Mengyuan Lin and Zengrui Li, "A compact 4 × 4 dual band-notched UWB MIMO antenna with high isolation," in 2015 IEEE 6th International Symposium on Microwave, Antenna, Propagation, and EMC Technologies (MAPE), Shanghai, China, Oct. 2015, pp. 126–128. doi: 10.1109/MAPE.2015.7510281.

[20] J.-F. Yu, X. L. Liu, X.-W. Shi, and Z. Wang, "A COMPACT FOUR-ELEMENT UWB MIMO ANTENNA WITH QSCA IMPLEMENTATION," Prog. Electromagn. Res. Lett., vol. 50, pp. 103–109, 2014, doi: 10.2528/PIERL14110804.

[21] K. S. Sultan and H. H. Abdullah, "PLANAR UWB MIMO-DIVERSITY ANTENNA WITH DUAL NOTCH CHARACTERISTICS," Prog. Electromagn. Res. C, vol. 93, pp. 119–129, 2019, doi: 10.2528/PIERC19031202.

[22] W. M. Abdulkawi, W. A. Malik, S. U. Rehman, A. Aziz, A. F. A. Sheta, and M. A. Alkanhal, "Design of a Compact Dual-Band MIMO Antenna System with High-Diversity Gain Performance in Both Frequency Bands," Micromachines, vol. 12, no. 4, p. 383, Apr. 2021, doi: 10.3390/mi12040383.

[23] A. A. Ibrahim, M. A. Abdalla, and Z. Hu, "Compact ACS-fed CRLH MIMO antenna for wireless applications," IET Microw. Antennas Propag., vol. 12, no. 6, pp. 1021–1025, May 2018, doi: 10.1049/iet-map.2017.0975.

[24] M. Khalid et al., "4-Port MIMO Antenna with Defected Ground Structure for 5G Millimeter Wave Applications," Electronics, vol. 9, no. 1, p. 71, Jan. 2020, doi: 10.3390/electronics9010071.

[25] S. K. Oruganti, A. Khosla, and T. G. Thundat, "Wireless Power-Data Transmission for Industrial Internet of Things: Simulations and Experiments," IEEE Access, vol. 8, pp. 187965–187974, 2020, doi: 10.1109/ACCESS.2020.3030658.

[26] S. K. Oruganti et al., "Experimental Realization of Zenneck Type Wave-based Non-Radiative, Non-Coupled Wireless Power Transmission," Sci. Rep., vol. 10, no. 1, p. 925, Dec. 2020, doi: 10.1038/s41598-020-57554-1.

[27] J. Malik, S. K. Oruganti, S. Song, N. Y. Ko, and F. Bien, "Electromagnetically induced transparency in sinusoidal modulated ring resonator," Appl. Phys. Lett., vol. 112, no. 23, p. 234102, Jun. 2018, doi: 10.1063/1.5029307.

International Journal of Innovation Engineering and Science Research
(ISSN: 2581-4591)
www.ijiesr.com

Qualitative characteristics of small ruminant skins from Niger: comparative study of Maradi goats (Red and Black) *vs* Sahel goat and sheep (Oudah and Balami)

Adam Kadé Malam Gadjimi
Département Productions Animales, Faculté d'Agronomie
Université Abdou Moumouni Dioffo
BP: 10 662 Niamey, Niger

Mamman Mani
Département Productions Animales
Institut National de la Recherche Agronomique du Niger, INRAN
BP: 429 Niamey, Niger

Akourki Adamou
Département Productions Animales, Faculté d'Agronomie et Sciences de l'Environnement
Université Dan Dicko Dankoulodo
BP: 465Maradi, Niger

Charles-Dayo Guiguigbaza-Kossigan
Unité de Recherche Maladies à vecteurs et Biodiversité,
Centre International de Recherche-Développement en zone Subhumide, CIRDES
01 BP : 454Bobo-Dioulasso 01, Burkina Faso

Balkissa Maman Dabo
Département Productions Animales, Faculté d'Agronomie et Sciences de l'Environnement
Université Dan Dicko Dankoulodo
BP: 465Maradi, Niger

Marichatou Hamani
Département Productions Animales, Faculté d'Agronomie
Université Abdou Moumouni Dioffo
BP: 10 662 Niamey, Niger

ABSTRACT

The objectiveof this study was to compare qualitative and quantitative post-mortem characteristics of Maradi Red and Black goats' skins to those of Sahel goats, Oudah and Balami sheep, all of which were subjected to traditional tanning in Niger, in order to determine the relationship between animal live weight and skin weight parameters, as well as to assess texture, resistance, solidity, suppleness, and smoothness under independent qualitative rating by 8 locals. Sheep skin has much more texture than goat skin ($p = 0.000$), according to statistical analyses. The texture of Red and Black goat skins does not change significantly ($p = 0.856$).

The skin resistance of Red and Black goats was higher than that of Sahelian goats and sheep. A significant difference between breeds was discovered using analysis of variances ($p = 0.001$). According to the Scheffe post hoc test, the difference between the Black goat and the Oudah sheep was not significant, but it was significant between the Red goat and the Balami sheep ($p = 0.013$) and the Sahelian goat ($p = 0.016$).

Except for Black goat (p = 0.272), the skin of Red goats was significantly stronger than that of the other breeds (Red vs Sahel, p = 0.001; vs Oudah, p = 0.027, and vs Balami, p = 0.001).
The difference in skin suppleness between Black and Red goats (p = 0.390) was not significant, however it was significant between these two goat groups and Sahel goat (p = 0.000) and Black goat and Oudah sheep (p = 0.001).
The following classification was noticed in decreasing order based on skin fineness: Black, Sahelian, Red, Balami, and Oudah. According to ANOVA and the Scheffe post hoc test, the difference between the Black goat and the Oudah sheep was significant (p = 0.000).
For all breeds and species studied together, principal component analysis of skin's quantitative parameters (weight after skinning, trimming, drying, and tanning) revealed a substantial positive connection between these and animal live weight (R^2 = 0.851; 0.838; 0.788; and 0.854).
Despite phenotypic differences, Red and Black Maradi goats performed similarly in all qualitative and quantitative skin metrics evaluated, and had benefits over Balami and Oudah sheep and Sahelian goats. (*Abstract*).

Keywords*—qualitative parameters, quantitative parameters, Maradi Red goat, Maradi Black goat, Sahelian goat, Oudah sheep, Balami sheep, Niger (key words)*

RESUME

L'objectif de ce travailétait de comparer les caractérisques qualitatives et quantitatives *post-mortem* des peaux de chèvres Rousse et Noire de Maradi entre elles puis avec celles du Sahel et des moutons Oudah et Balami, toutes soumises au tannage traditionnel au Nigerpour mettre en évidence la relation entre le poids vif et les paramètres pondéraux de la peau et apprécier la texture, la résistance, la solidité, la souplesse et la finesse grâce à une notation qualitative indépendante par 8 cordonniers traditionnels expérimentés locaux.
L'analyse statistique a ressorti que la peau des ovins a significativement plus de texture que celle des caprins (p=0,000). Il n'y avait pas de différence significative de texture entre les peaux de chèvres Rousse et Noire (p=0,856).
La résistance de la peau a été plus importante chez les caprins Roux et Noirs que la chèvre du Sahel et les ovins. L'analyse de variances a montré une différence significative entre races (p = 0,001). Suivant le test post hoc de Scheffe, cette différence n'a pas été significative entre la Noire et le Oudah avec toutes les autres races; elle l'est seulement qu'entre la Rousse avec le Balami (p = 0,013) et la chèvre du Sahel (p = 0,016).
L'analyse des variances à un facteur et le test post hoc de Scheffe ont montré que la peau de la chèvre Rousse est statistiquement plus solide que celles de toutes les autres races (Rousse vs Sahel, p = 0,001; vs Oudah p = 0,027 et vs Balami p = 0,001) à l'exception de la chèvre Noire (p = 0,272).
Il est ressorti que la différence de souplesse de la peau n'a pas été significative entre la Noire et la Rousse (p=0,390) mais plutôt entre ces 2 groupes caprins et celle du Sahel (p=0,000) et entre la chèvre Noire et le mouton Oudah (p=0,001).
En matière de finesse de peau, il a été noté le classement par ordre décroissant suivant: Noire, Sahel, Rousse, Balami etOudah. Cette différence selon l'ANOVA suivi du test post hoc de Scheffe a été significative entre la chèvre Noire et le mouton Oudah (p=0,000).
L'Analyse en Composantes Principales des paramètres quantitatifs de la peau (poids après dépouille, rognage, séchage et tannage), toutes races et espèces étudiées confondues a établi une corrélation positive significative entre ceux-ci et le poids vif (respectivement R^2= 0,851; 0,838; 0,788 et 0,854).
En dépit de différence de phénotypes, les chèvres Rousse et Noire de Maradi ont occupé une position très similaire pour l'ensemble des paramètres qualitatifs et quantitatifs étudiés de la peau et ont présenté des avantages comparatifs devant celles des moutons Balami, Oudah et chèvre du Sahel.(*Abstract*)

Mots-clés*: caractéristiques, peaux, chèvre Rousse de Maradi, chèvre Noire de Maradi, chèvre du Sahel, mouton Oudah, mouton Balami, Niger. (key words)*

I. INTRODUCTION

Because of the quantity of its livestock and the amount of butchering that occurs each year, Niger is a major supplier of hides and skins. According to [1], goats are the top producers of hides and skins. The evident features of red goat skin make it a popular choice. According to [2], Maradi Red goat skin is supple, fine, and has a wonderful solidity, which is highly valued in leather goods and luxury gloves. In a similar vein, [3] reported that leather and skin experts in Paris, London, Hamburg, and New York

ranked Red goat skin from Niger first among all competitors for its remarkable attributes in gloves, luxury footwear, and women's clothes.
Red goats share the same biotope with their black counterparts, whose skin quality is unknown.
Comparative data on the quality of hides and skins of different types or breeds of goats in Niger is essentially non-existent, according to [4]. The goal of this study was to compare post-mortem qualitative characteristics of skins from Maradi Red and Black goats with those from Sahel goats and Oudah and Balami sheep, all of which were exposed to traditional tanning in Niger.

II. MATERIALSAND METHODS

A. Study location

The study took place in the Urban Community of Maradi, capital of region of the same name (Fig. 1).

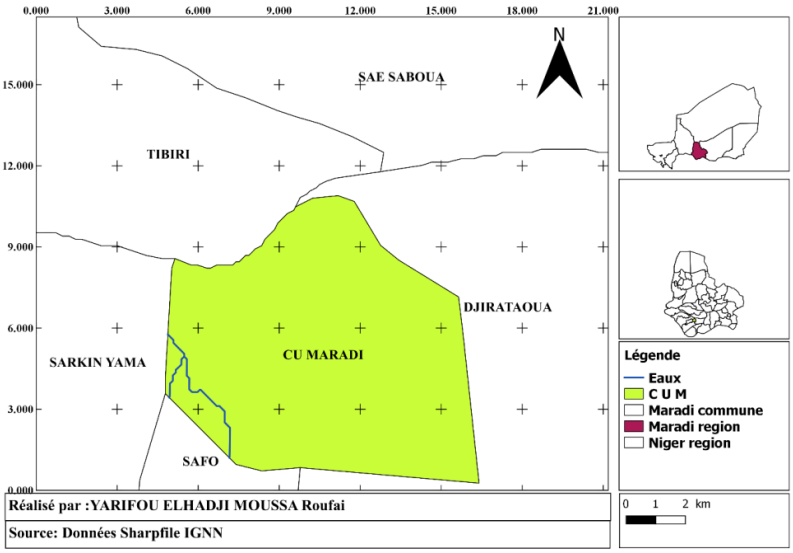

Fig. 1: Location of Urban Community of Maradi.*(figure caption)*

Maradi is essentially an agro-pastoral region. The livestock industry plays a vital role in the socioeconomic life of the inhabitants. It is the second most important activity in the region, after agriculture, and it affects more than 89 percent of the people. The region is experiencing changes in agro-sylvo-pastoral production practices as a result of intensification of agricultural production, which is experiencing significant growth, use of harnessed and mechanical cultivation, development of cattle and sheep fattening, popularization of the Azawak cattle breed and Red goat, and securing of land for breeders (TABLEI). It contributes a large amount to state and local budgets, which is why some extremely positive features for its development have been recognized, including, among others:

- presence of livestock management structures, in particular regional directorate with its annexes (1 refrigerated slaughterhouse, 2 livestock multiplication centers, 1 training center for livestock volunteers);
- presence of various development partners (projects, programs, NGOs and associations) working for development of livestock farming;
- existence of a vast pastoral zone (2,455,693 hectares), and 182 pastoral enclaves (157,162 hectares) in the agro-pastoral and agricultural zones which deserve to be preserved, developed and well managed;
- emergence of private initiatives in poultry and livestock farming.

TABLE I:EVOLUTION OF LIVESTOCK IN THE MARADI REGION FROM 2009 TO 2019.*(Table head)*

Year	Cattle	Sheep	Goats	Camels	Horses	Donkeys	Total
2009	1,430,255	1,745,090	2,327,891	264,184	17,031	197,553	5,982,003
2010	1,495,780	1,735,242	2,374,730	264,966	16,577	198,136	6,085,431
2011	1,585,527	1,795,975	2,469,719	268,411	16,743	202,099	6,338,474
2012	1,680,658	1,858,835	2,568,508	271,900	16,910	206,141	6,602,952
2013	1,781,498	1,923,894	2,671,248	275,435	17,079	210,264	6,879,417
2014	1,888,388	1,991,230	2,778,098	279,015	17,250	214,469	7,168,450
2015	2,001,691	2,060,923	2,889,222	282,642	17,423	218,758	7,470,659
2016	2,121,793	2,133,055	3,004,791	286,317	17,597	223,134	7,786,686
2017	2,249,100	2,207,712	3,124,982	290,039	17,773	227,596	8,117,203
2018	2,384,046	2,284,982	3,249,982	293,809	17,950	232,148	8,462,918
2019	2,527,089	2,364,957	3,379,981	297,629	18,130	236,791	8,824,576

Source: DS/MAG/EL, 2020. *(Table footnote)*

Economically, the proximity to Nigeria encourages favorable commercial links, especially in livestock, hides, and skins.

Pasteurellosis, sheep pox, and smuts are the most common animal diseases in the region during the wet season. Various public and private services vaccinate cattle on a regular basis each year.

Maradi City (the site of our research) is located at latitude 13°28'29.9N, longitude 7°8'38.1E, and elevation 384 m. The relief of the region is flat, with a non-functional hydrographic network, with the exception of the GoulbiN'Kaba and some of its tributaries, which present an ephemeral water flow during the rainy season, between July and September,[4].

With a long dry season and a short rainy season, the climate is tropical dry, semi-arid, or sahelian. Annual rainfall reaches 650 mm with substantial interannual fluctuation. The average monthly temperature is particularly high (with a maximum of 32.7°C in May and a minimum of 23.5°C in January). From May to September, the prevailing winds are from the south-west, with a direction of 240 to 210 degrees. They determine the rainy season since they come from the Atlantic Ocean and are humidified. From November to March, the prevailing wind comes from the north-east, with a fairly consistent 60-degree direction. Harmattan is a highly dry wind that originates in the Sahara (Tibesti - Bilma). It is occasionally coupled with sandstorms.

Maradi is the economic capital of Niger. Its economy is centered on trade (import-export), agriculture, particularly peanuts, for which it was a center of excellence, cowpeas, millet, and the breeding of cows, camels, and small ruminants, notably the famed Maradi Red goat [5].

In 2018, the population of Maradi's Urban Community was estimated to be 326,804 people[6]. Maradi Refrigerated Slaughterhouse slaughters agricultural animals every day to feed its rising population (TABLE II).

TABLE II:EVOLUTION OF CONTROLLED MEAT PRODUCTION AT MARADI REFRIGERATED SLAUGHTERHOUSE FROM 2010 TO 2019.*(Table head)*

Year	Meat production (tons)
2010	1,767.614
2011	2,314.372
2012	1,847.194
2013	1,856.148
2014	2,103.164
2015	2,176.596
2016	2,103.444
2017	1,981.260
2018	1,883.360
2019	1,511.570

Source:DREIA Maradi, 2020.*(Table footnote)*

B. Experimental materials

Used materials consist of:

- skins of small ruminants (Red and Black goats, Sahel goats, Balami and Oudah sheep);
- a 100 kg scale for weighing selected animals before slaughter;

- a load cell of 25 kg for weighing skins;
- markers for identification of weighed animals;
- a knife for fleshing and trimming hides.

C. Study sample

The sample was made up of 50 skins from small ruminants slaughtered at the Maradi Urban Community's Refrigerated Slaughterhouse. There were 40 goat skins, with 15 Black goats (7 females and 8 males), 15 Red goats (7 females and 8 males), and 10 Sahel goats (5 females and 5 males), as well as 10 sheep skins, with 6 Oudah (4 males and 2 females) and 4 Balami (3 females and 1 male). Animals belonged to people who decided to collaborate after their subjects were choosing. The skins of identified animals were purchased at prices negotiated with their owners in preparation for the next steps of the operation.

D. Data collection

Data of two types of parameters (quantitative and qualitative) were collected in different stages, starting with a live animal and ending with the utilization of skin. Each hide was identified (numbered) and tracked throughout the research process.

E. Animal identification

It was conducted on animals destined for slaughter at Maradi Refrigerated Slaughterhouse's stable yard after *ante-mortem* inspection. Animals that met typical phenotypic characteristics of different breeds were selected. Age of animals was determined using [7] scale. TABLEIII shows the characteristics that were used to make animal selections.

TABLEIII:CHARACTERISTIC TRAITS OF ANIMAL BREEDS SELECTED BEFORE SLAUGHTER.*(Table head)*

N°	Animalbreed	Head profile	Dresscolor	Bearing of goatee	Bearing of horns	Wearingears	Wearing pendants	Tail port
1	Red goat*	Fixed, domed forehead often covered with longer and darker hair in males than in females; rectilinear chamfer sometimes subconcave	Redorbrown	Constantly carried by males and often by older females	In ibex (lying backwards), rarely markhar type (vertically erect)	Short and erect	Absence	Short and upright
2	Black goat*	Fixed, domed forehead often covered with longer and darker hair in males than in females; rectilinear chamfer sometimes subconcave	Black	Constantly carried by males and often by older females	Mainly markhar and rarely ibex	Short and erect	Absence	Short and upright
3	Sahel goat**	Thin, flat-fronted triangular. In the adult male, the forehead bears a tuft of hair	Extremely variable: plain (black, chocolate, brown, white) and compound (grey, roan, pie-black, pie-red, black-pie or red-pie)	Can be carried by individuals of both sexes but always by the adult billy goat	Mostly ibex (lying backwards), sometimes markhar type (upright and diverging); fine in females, coarse and often twisted in males	Three types: Long and drooping; Medium and stalked; Short and erect	Worn by individuals of both sexes and most often by females	Short and upright
4	Oudahsheep***	Convexiline	Bicolor with constant white posteriorly and variability anteriorly: black-white, brown-white, fawn-white	Absence	Very developed and spiral horns in males, long and thin in females	Drooping	-	Goes down below the hocks
5	Balamisheep****	Big	White	Absence	Spiral horns	Long et wide	Presence	Big and long reaching below the hocks

Sources:*[8], ** [9],[10].*(Table footnote)*

- *Slaughtering, processing, preservation and tanning of hides*

Slaughtering, processing and preservation of hide were carried out at Maradi Regional Refrigerated Slaughterhouse. Tanning was done in traditional way by artisanal tanners of Maradi.

- *Collected data*

Quantitative data were: animal live weight, skin weights after skinning, trimming, drying and tanning. Load cells with capacities of 100 kg and 25 kg were used for weighing animals and skins respectively.
Qualitative data were: texture, resistance, solidity, flexibility and smoothness. Eight experienced local traditional shoemakers (at least ten years of activity) were identified in order to assess independently and qualitatively according to [11] (with 1=very bad, 2=poor, 3=average, 4 =good, 5=very good) on a sample of skins from each category of small ruminants (Red, Black and Sahel goats, Oudah and Balami sheep).

F. Data processing

All data collected was entered on an EXCEL 2010 spreadsheet model.
Statistical analysis were performed using SPSS 17.0, XLSTAT 2014 and MINITAB 14 software. Quantitative data were expressed as means, standard deviations and extrema, and qualitative data as their numbers and frequencies.
For quantitative parameters, Ryan Joiner's test made it possible to check normality of distribution, that of Levens was used to check equivalence of variances according to genetic types studied and Analysis of Variances was used for averages comparison (at 5% statistical threshold). Quantitative data were also subject of multivariate analysis using XLSTAT software, in particular Discriminant Factor Analysis and Simple Linear Regression in order to establish relationships between various weight parameters measured.
Regarding to qualitative parameters, Factorial Analysis of weightings by shoemakers on different studied genetic types was carried out using XLSTAT software and results presented in form of factorial maps. Analysis of Variances of average weightings assigned by shoemakers was also carried out to distinguish skin's qualities of studied different species and breeds.

III. RESULTS

A.Factorial analysis of hides weightings qualitative parameters

- *Texture*

It is the physical quality of skin that is perceptible by touch or sight.Fig. 2 shows factor map of shoemakers weightings on texture.

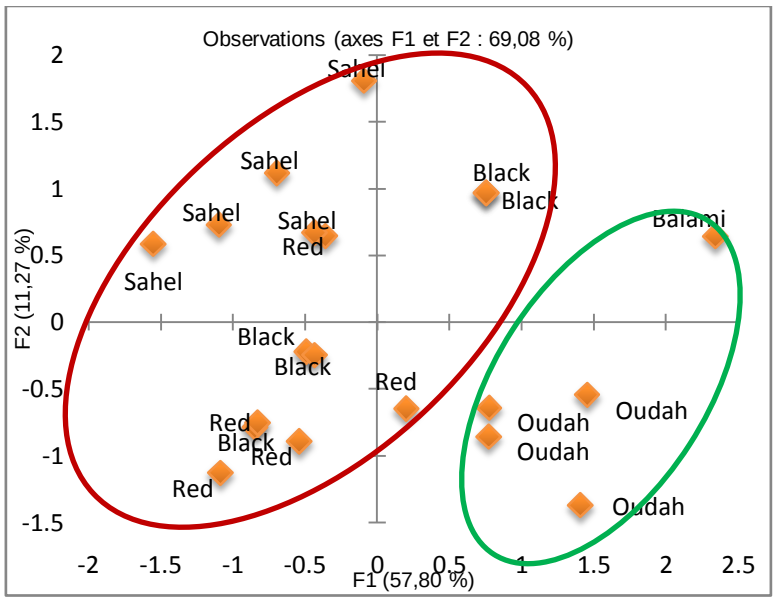

Fig.2: Factorial map of skin texture of studied differentgenetic types, all sexes combined.*(figure caption)*

It emerged globally that the skin texture of animals of the same species is similar. It is higher in sheep than goats, regardless of the gender of the animal. The Sahelian goat's texture is less prominent than that of the Red and Black goats (Fig. 2). Using one-way analysis of variance and Scheffe's post hoc test, the following results were obtained:

- Balami skin texture is statistically superior to that of 3 goat breeds (p values are 0.005; 0.000 and 0.000 respectively with Black, Red and Sahel);
- Oudah skin, statistically better than that of Red and Sahel (p = 0.003 and p = 0.000 respectively);
- there is no significant difference between skin of Black and Redhead (p = 0.856) and
- Sahelian goat skin texture is statistically weaker than that of Black, as well as 2 sheep breeds.

- *Resistance*

It refers to the skin's ability to withstand being injured or transformed by an external force. Fig. 3 shows a factorial map of goat and sheep skin resistance, split down by breed and sexes.

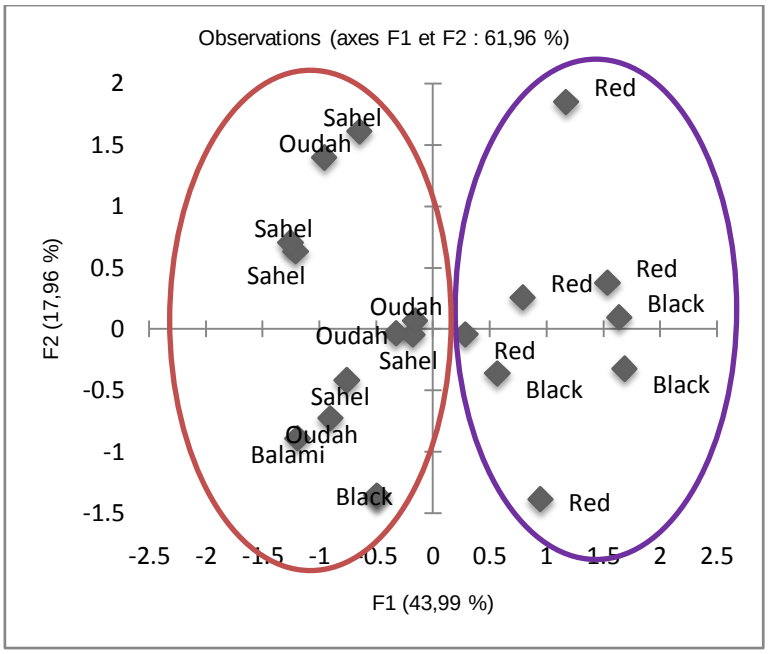

Fig. 3: Factorial map of skin resistance of different genetic types studied for all sexes combined.*(figure caption)*

Fig. 3 illustrates that depending on breed and species, skin resistance is higher in Red and Black goats than in Sahelian goats and sheep.Significant differences across breeds were observed using analysis of variances (p = 0.001). With all other breeds, Scheffe's post hoc test revealed that the difference between Black goat and Oudah sheep is not significant. While that of the Red goat with Balami sheep (p = 0.013) and the Sahel goat (p = 0.016) are significant.

- *Solidity*

Solidity, toughness, and durability are terms used to describe the ability of skin to survive time's wear and strain. Figure 4 summarizes shoemakers' perspectives on the solidity of the hides of the various breeds and species tested.

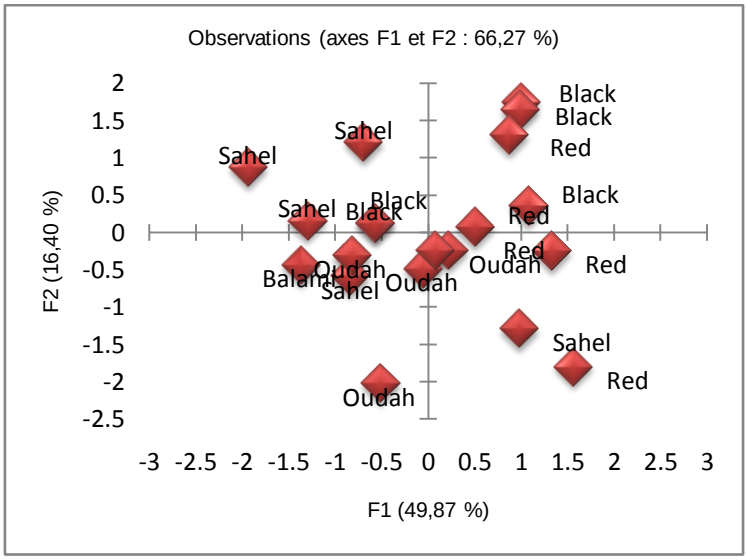

Fig.4: Factorial map of skin solidity of different studied genetic types for all sexes combined.*(figure caption)*

One-way analysis of variances and Scheffe's post hoc test show that Red goat skin is statistically stronger than that of all other breeds (Red vs Sahel, p = 0.001; vs Oudah, p = 0.027 and vs Balami, p = 0.001) except for Black goat (p = 0.272).

- *Suppleness or flexibility*

When skin is elastic or easily flexible, it is said to be supple or flexible. Fig. 5 presentsassessmentsanalysis of skin flexibility by shoemakers.

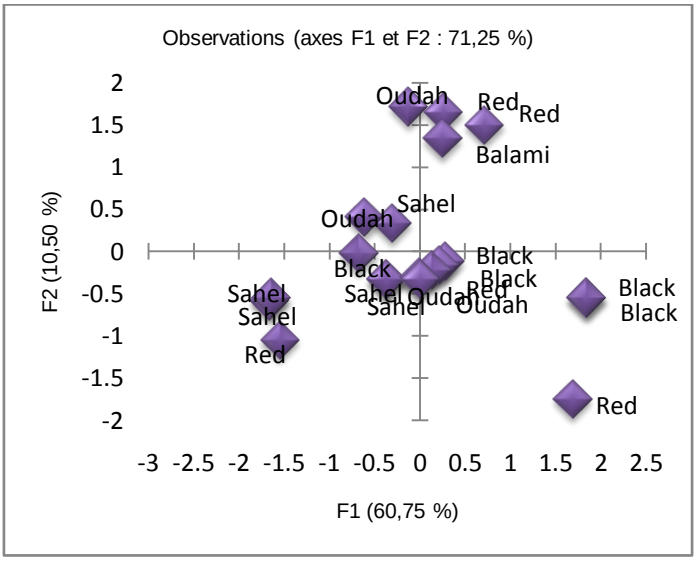

Fig.5: Factorial map of skin flexibility of different studiedgenetic types all sexes combined.*(figure caption)*

Fig. 5 shows that Black and Redgoats'skinis more supple than that of Sahelian goats and Oudah and Balami sheep. However, one-way analysis of variances shows that difference in flexibility between different genetic types is very significant (p=0.000). Scheffe's post hoc test made it possible to understand that difference in skin flexibility is not significant between Black and Red goats (p=0.390) but rather between these 2 goat groups and Sahel goat (p =0.000) and between Black goat and Oudah sheep (p=0.001).

- *Smoothness*

The term "smoothness" (thinness) refers to the skin's thinness, delicacy, or refinement in form and material. Fig. 6 shows a factorial analysis of scoring for this metric by breed and species.

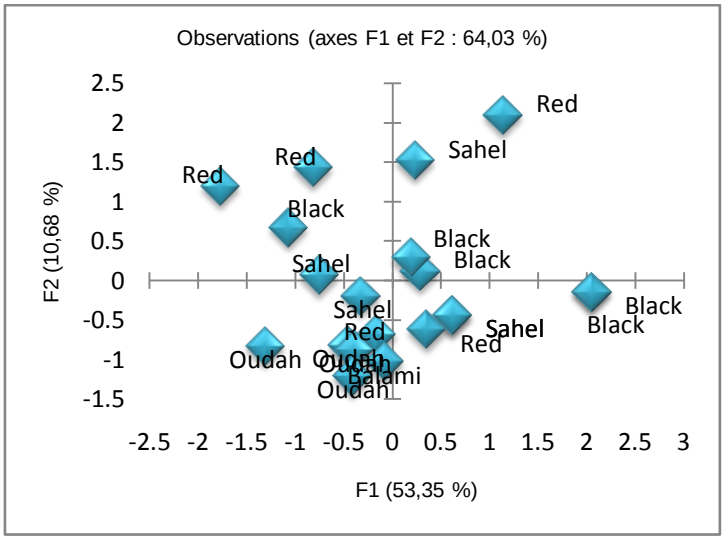

Fig.6: Factorial map of skin smoothness (thinness) of different studied genetic types all sexes combined.*(figure caption)*

The following breeds are classified in decreasing order of skin smoothness in Fig. 6: Black, Sahel, Red, Balami, and Oudah. According to the ANOVA and the Scheffe post hoc test, the difference between the Black goat and the Oudah sheep was significant (p=0.000).

B. Analysis of variation in hide weight from slaughter to tanning

Discriminant Factor Analysis (DFA) of skins weights of studied different genetic types from slaughter to tanning is presented in Fig. 7.

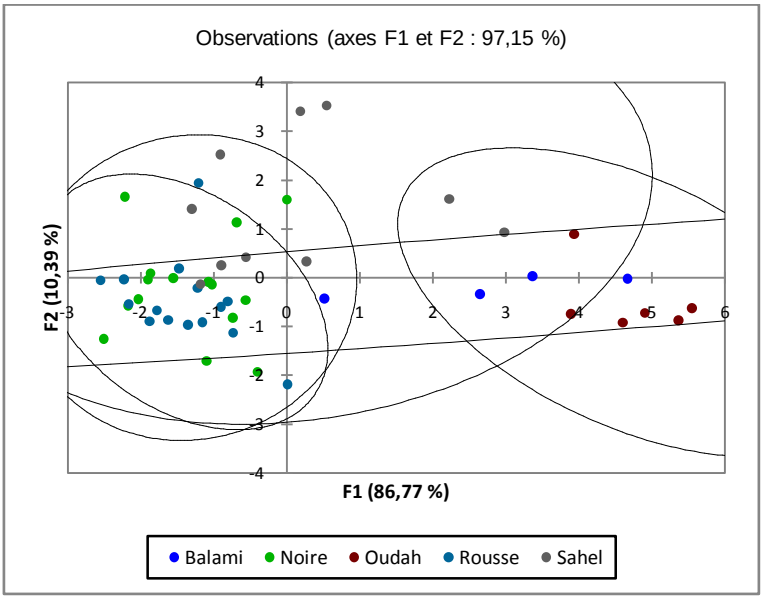

Fig.7: Discriminant Factor Analysis (DFA) of skins weights of studied different genetic types (Balami=Balami sheep, Noire=Black goat, Oudah=Oudah sheep, Rousse=Red goat, Sahel=Sahel goat).*(figure caption)*

At all levels of weighing, DFA highlights a similarity between the skins of Red and Black goats on one side and Oudah and Balami sheep on the other (live weight, weight after skinning, weight after trimming, dry weight and weight after tanning). The skin of the Sahelian goat, on the other hand, exhibits a mixture of traits.

Depending on sex in same breed, it appeared that at all weighing stages,skins weights of females are higher than those of males in all studied breeds with exception of Balami sheep (Fig. 8).

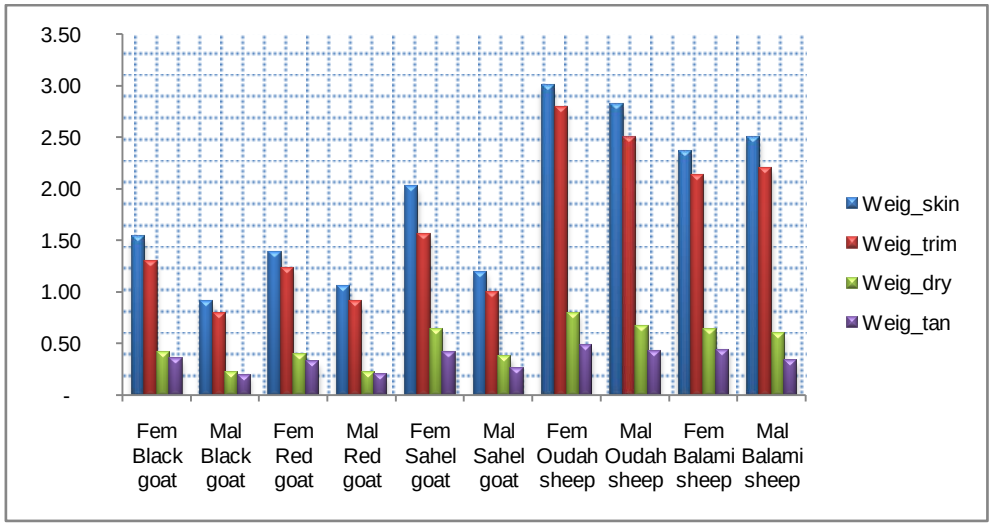

Fig.8: Variation in hide weight after skinning, trimming, dryingand tanning according to sex, breed and species of the animal.*(figure caption)*

All analyzed species and breeds combined demonstrated a substantial positive connection (TABLEIV) between weights at different stages of skin and animal living weight using Principal Component Analysis (PCA). The animal's age, live weight, and weights after skinning, cutting, drying, and tanning all had a strong positive connection (p=0.01).

TABLEIV: PEARSON CORRELATION MATRIX.*(Table head)*

	Age	**Live weight**	**Weightafterskinning**	**Weightaftertrimming**	**Weightafter drying**	**Weightaftertanning**
Age	**1**					
Live weight	0.590**	**1**				
Weightafterskinning	0.398**	0.922**	**1**			
Weightaftertrimming	0.391**	0.916**	0.983**	**1**		
Weightafter drying	0.465**	0.888**	0.893**	0.864**	**1**	
Weightaftertanning	0.617**	0.924**	0.851**	0.833**	0.930**	**1**

**. Correlation is significant at the 0.01 level (two-sided).*(Table footnote)*

TABLEV presents summary of results (R^2, Fisher's F probabilities and model equations) of simple regression of weights at different stages of skin as a function of animal live weight.

TABLE V:REGRESSION OF WEIGHT PARAMETERS OF SKIN ACCORDING TO THE ANIMAL LIVE WEIGHT. *(Table head)*

Types of régression	**R^2 Value**	**Fisher'sProbability F**	**Model equation**
Weights after skinning - Live weight	0.851	< 0.0001	WS = 0.01124+0.07757*LW
Weights after trimming - Live weight	0.838	< 0.0001	WTr = 0.08010+0.07141*LW
Weights after drying - Live weight	0.788	< 0.0001	WD = 0.00426+0.02126*LW
Weights after tanning - Live weight	0.854	< 0.0001	WTa = 0.04849+0.01334*LW

It emerges from TABLEV that R^2 values are all close to 1 and Fisher F are very significant.Fig. 9 (a, b, c and d) gives graphical representation of different regression models. It shows a good distribution of points around the regression line.

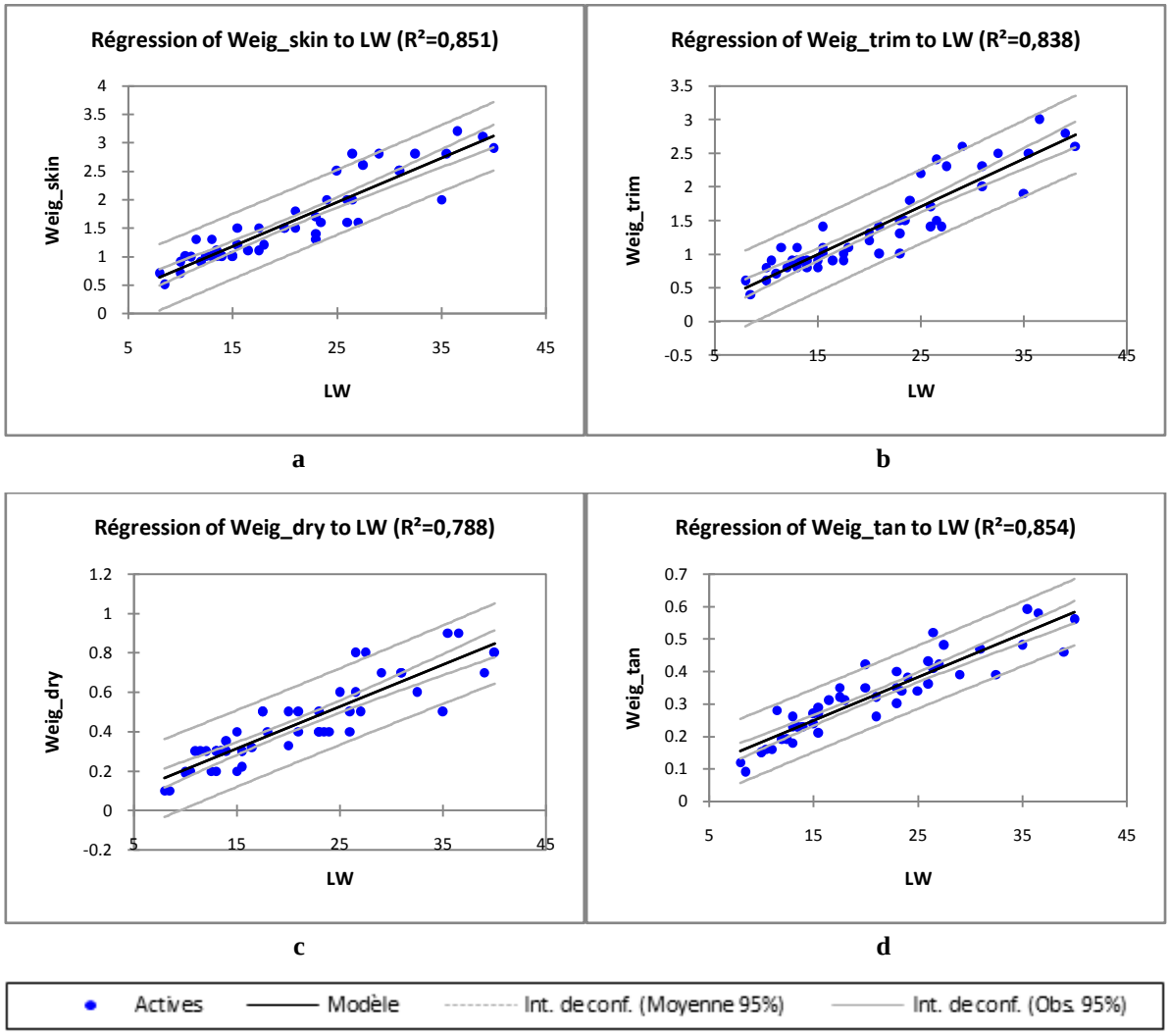

Fig. 9: Regression models of weights at different skin stages as a function of live weights for all studied genetic types.*(figure caption)*

Fig. 10 shows the normalized residuals distribution for several models (a, b, c and d). This figure shows that 88 percent, 94 percent, 94 percent, and 92 percent of observations of the model's weight after skinning, trimming, drying, and tanning were in the confidence interval] – 1.96; 1.96].

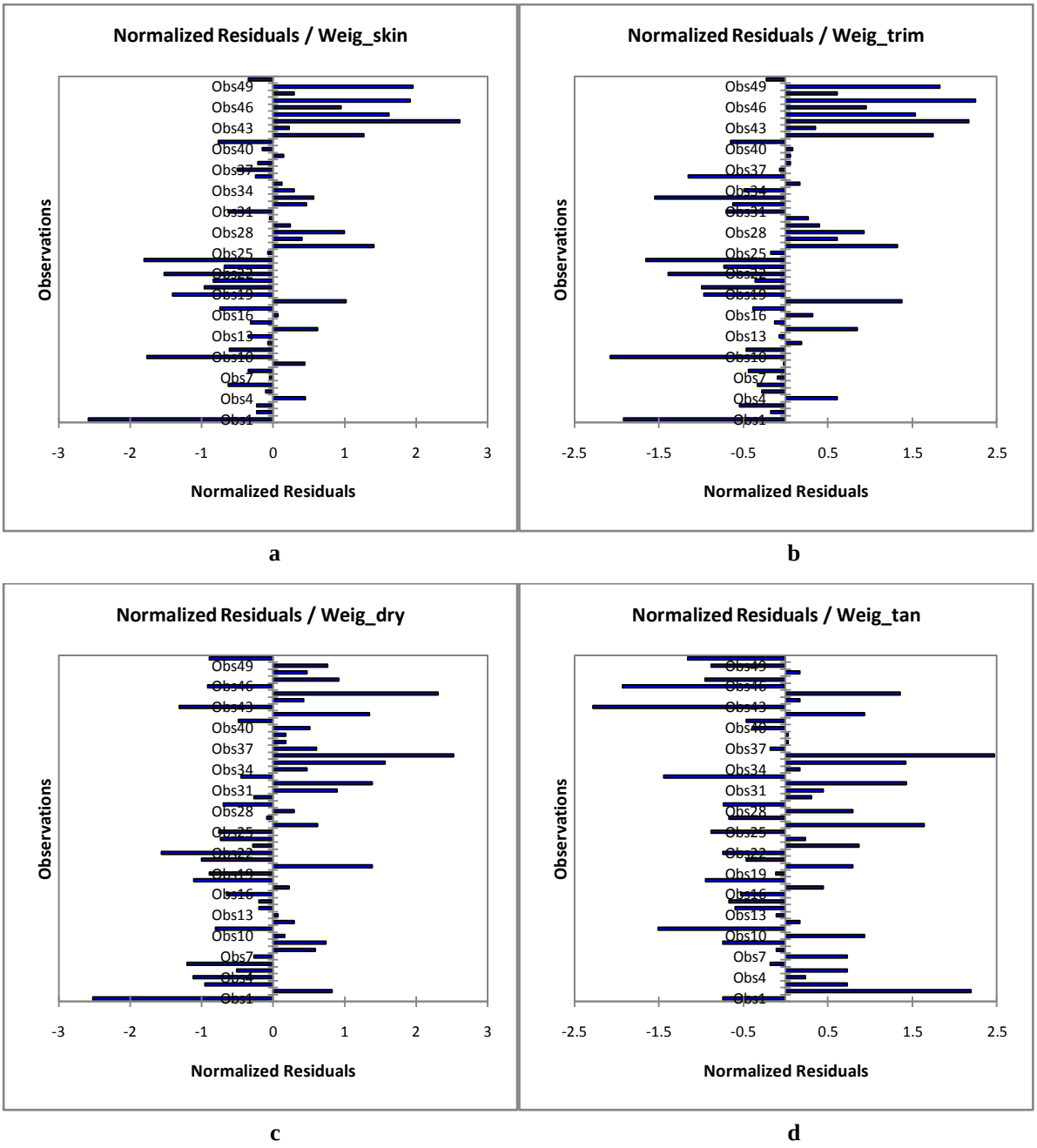

Fig.10:Observations of normalized residuals of regression models of skin weights at different stages as a function of live weights for all studied genetic types.*(figure caption)*

IV. Discussion

A. Qualitative parameters

Sheep (Oudah and Balami) have a much higher texture than goats (Rousse, Noire, and Sahel goats, in decreasing order) (p=0.000). In comparison to goatskin, sheepskin has a spongy structure and loose texture, according to [12]and [13]. The findings of this study agree with [14], who stated that "the intrinsic features of sheepskin (surface, thickness, loose yet resistant texture, low elasticity) are highly valued by the Nigerian customer for which it corresponds to various jobs."To the point where tanners compete directly with buyers of raw hides."

The skin resistance of Red and Black goats is higher than that of Sahelian goats and sheep. According to [15], goatskin has a structure that is comparable to that of calfskin in certain ways and similar to that of sheepskin in others, but its overall structure has unique properties. The blossom is resistant and the fibers are tighter than sheep's. However, this difference is not significant between the

Black and the Oudah with all other breeds; only the Redhead with the Balami (p = 0.013) and the Sahel goat (p = 0.016) are significant.

Analysis of shoemakers' opinions on skin solidity of different breeds and species shows that, with the exception of the Black goat (p = 0.272), the skin of Red goats is statistically stronger than that of all other breeds (Red vs Sahel, p = 0.001; vs Oudah, p = 0.027, and vs Balami, p = 0.001). This not only proves that the skins of Maradi's Red and Black goats are similar in terms of strength and that goat skin can be used raw as a lace or tie, but it also indicates that, due to its high plastic characteristics and strength, it should be tanned with caution[16].

Reference [17] observed that the difference in skin elasticity between Black and Red goats (p=0.390) is not significant, but rather between these two goat groups and Sahel goat (p=0.000) and Black goat and Oudah sheep (p=0.001). According to [14], goat skin has a deep and noticeable grain, and its dense and compact elastic fibers, which are not too oily, accept food and work effectively, resulting in a supple, nervous skin that is suitable for leather goods, gloves, bookbinding, and high-quality shoes.

Ranking the fineness of the skins of Black, Sahel, and Red goats, as well as Balami and Oudah sheep, in decreasing order, confirms the comparative study by unpublished [18], which concludes that Red and Black goats have a finer flower than particolored goats, even if the difference is only significant between Black goat and Oudah sheep (p=0.000). In comparison to sheep skin, goat skin has a finer and more flexible structure, according to [13], since the first has more elastic fibers, which are desirable in gloves and shoe uppers.

Reference [12] who adds age, sex, coat, climate, nutrition, and health state to our observations on variance in qualitative parameters of skin according to species and breeds, confirmed our findings. This was also [19]'s point of view, who related these components to breeding conditions. The comparative study by unpublished [18], which concludes that Red and Black goats have finer flowers than particolored goats, even if the difference is only significant between Black goat and Oudah sheep (p=0.000), confirms the fineness of the skins of Black, Sahel, and Red goats, as well as Balami and Oudah sheep, in decreasing order. According to [13], goat skin has a finer and more flexible structure than sheep skin, which has more elastic fibers, which are ideal in gloves and shoe uppers.

B. Quantitative parameters

Analysis of quantitative measures of small ruminant skin, such as weights at various stages from slaughter through tanning, revealed that those of sheep were higher than those of goats, owing to the texture of the former being more developed. According to [20], based on average weight, sheep fall into the "light" category (450-680 g) and goats fall into the "medium" category (300-680 g). According to [12],[18]and [19], the average of each quantitative parameter in females was higher than in males in both species of small ruminants, with the exception of Balami sheep, possibly due to the size of the test sample.

Within the same species, Oudah sheep had a heavier dry skin weight than Balami sheep, while in goats, the dried skin of Sahel weighed more than its sisters, Black and Red, which are fairly similar in this regard.

Principal Component Analysis of weights of all breeds and species aggregated at different phases of skin (weight after skinning, cutting, drying, and tanning) demonstrated a positive association with animal live weight. R^2 was close to 1 in a simple linear regression of these distinct weights as a function of animal live weight (R^2 between 0.788 and 0.854).

Given Fisher's F test is less than 0.0001, there is a risk of error of less than 0.01 % in concluding that animal live weight can provide considerable information about weights at various stages of hide from slaughter to tanning. Furthermore, the distribution of residuals according to animal live weight in confidence intervals of 88 %, 94 %, 94 %, and 92 % of Linear Regression Models of weight after skinning, weight after trimming, weight after drying, and weight after tanning in confidence intervals of 1.96; 1.96] strengthens this hypothesis.

V. CONCLUSIONS

For all skin qualitative parameters (texture, resistance, solidity, suppleness, and fineness) are quite comparable in Red and Black Maradi goats, more so than in Sahel goats, and they are different from sheep (Oudah and Balami), who have a higher texture.
Quantitative parameters, such as skin weights after each stage of the skinning, cutting, drying, and tanning process, all had a significant positive correlation (p=0.01) with animal live weight.
The skins of Maradi's Red and Black goats are extremely similar qualitatively and quantitatively, and they have some benefits over sheep and Sahel goat skins for use in traditional indigenous crafts in Niger.

AKNOWLEDGMENTS(*Heading 6*)

Authors express their gratitude to General Director of Livestock Multiplication Centers, Mr Moussa Keita, to Director of Goat Center of Maradi, MrNouhou Moussa, to Regional and Deputy Livestock Directors of Maradi respectively, Dr MahamaneAmadou Soumaïla and Dr ChitouSoulé, as well as to Dr Nouri Brah and Mr Ali Koura Abdoulaye, Researchers at National Instituteof Agronomic Researchof Niger, for their assistance in this work. May all traditional tanners and shoemakers involved, all staff and trainees of Regional Directorate of Livestock of Maradi be thanked for their contribution to this work.

REFERENCES

[1] B.Karimou, Caractérisation phénotypique et zootechnique de la chèvre rousse de Maradi. Thèse de Doc., Université Abdou Moumouni de Niamey. p. 142, 2015.
[2] A.H.Robinet, La chèvre rousse de Maradi, Son exploitation et sa place dans l'économie et l'élevage de la République du Niger, Revue d'Elevage et de Médecine Vétérinaire des Pays tropicaux, Paris, 1967.
[3] P. Jean, Interview dans la rubrique ''*Voix d'Afrique*''. Courrier de l'Association., N°11: 10 -14, 1972.
[4] H.Marichatou, L. Mamane, M. Banoin, G. Baril, Performances zootechniques des caprins du Niger : étude comparative de la Chèvre Rousse de Maradi et de la chèvre à robe noire dans la zone de Maradi, Revue d'Elevage et de Médecine Vétérinaire des Pays tropicaux, Paris, 2002.
[5] https://fr.wikipedia.org/wiki/Maradi consulté le 3 août 2019 à 17h40.
[6] Niger, Le Niger en chiffres, INS, p.88, Novembre 2018.
[7] Y Alemu. and R. C. Merkel, Sheep and Goat Production Handbook in Ethiopia. ESGPIP-USAID-MoARD. p. 349, 2008.
[8] M. G. Adam Kadé, M. Mani, G. K.Dayo, H. Marichatou, Etude comparative des caractéristiques morphobiométriques des chèvres Rousse et Noire de Maradi au Niger: analyse des paramètres quantitatifs et qualitatifs. Int. J. Biol. Chem. Sci. 13 (3): 1431 – 1443, ISSN 1997-342X (Online), ISSN 1991-8631 (Print),2019.
[9] M.Mani, H. Marichatou, I. Moumouni, A. Saw, I. Chaibou, M. Chaibou, G.J. Sawadogo, Les pratiques d'élevage caprin au Niger. Revue Africaine de Santé et de Productions Animales, Dakar, 2014.
[10] Niger, Répertoire des races bovines, ovines et caprines du Niger. Rapport provisoire. Enabel.be. p.47, 2019.
[11] J.Fracheboud, Utilisation des échelles dans l'évaluation. Mémoire de diplôme ESTE. Centre de Didactique Universitaire, Université de Fribourg, Suisse,p. 54,2016.
[12] D. T. O.Salaou, Contribution à l'étude des cuirs et peaux au Niger. Thèse de doct. Vét. EISMV, Dakar, 127 p,1989.
[13] N.J.S. Kouadio, Contribution à l'amélioration de la qualité des cuirs salés verts de bovins au Sénégal et destinés à l'exportation: cas de la Société de Gestion des Abattoirs du Sénégal (SOGAS).Thèse Doct. Vet. N°16, EISMV Dakar. 143p, 2007.
[14] A.H. Robinet, Etudes techniques et économiques; cuirs et peaux du Niger: production-perspective. Revue d'Elevage et de Médecine Vétérinaire des Pays tropicaux, 17, N°1. (103-149), 1964.
[15] A. Senoussi, Caractérisation microbiologique de la peau de chèvre utilisée dans la fabrication de fromage traditionnel algérien «*Bouhezza*». Mémoire MSA, INATAA, Univ. Constantine I, 109 p, 2013.
[16] https://journals.openedition.org/encyclopedieberbere/2346 consulté le 9 mars 2019 à 17h48.
[17] I. M. S.Zangui, L'élevage des bovins, ovins, caprins au Niger: étude ethnologique. Thèse de doct. Vét. EISMV, Dakar. 131 p,1986.
[18] B.Djariri, Etude sur la monographie de la chèvre rousse de Maradi. Consultation pour le MRA, 2006.
[19] A. I. Adamou, Etat des connaissances des races caprines locales du Niger. Mémoire Lic. es Sc. Agro. 27 p, 2017.
[20] A. L Ibrahim, Production, conservation, tannage et commercialisation des cuirs et peaux: cas de la Tannerie Malan Yaro de Zinder. Rap. Maîtrise es Sc. Agro. FA/CRESA/UAM. 56 p,2005.

Common Prompters and Deterrents to Adoption of Insurance Policies as a Measure of Construction Risk Mitigation in South East Nigeria

WOKOCHA CHUKWULEKWURU CHRISTOPHER
Department of Architecture
Federal University of Technology Owerri Imo state

NKELEME IFEANYICHUKWU EMMANUEL
Department of Building
Federal University of Technology Owerri- Imo State

EZEH CHRISTIAN CHINEDU
Department of Building
Imo State University

ACHIGBU ONYEMA IKENNA
Department of Building
Federal University of Technology Owerri- Imo State

OZOH CHUKWUDI STANLEY
Department of Architecture
Federal University of Technology Owerri Imo state

ABSTRACT

Risk in construction is a major problem in many construction organization, the risk is inherent considering that it requires a lot of input from varied participants and that it take place in open. No amount of planning can completely overcome the occurrence of risk, thus the need to identify common promoter and deterrent to the adoption of Insurance policies as risk mitigation strategy. The field survey entailed the distribution of questionnaires to construction professional in 60construction firms with 50 returned well filled. Data collected was analyzed using SPPS version 16.0. The result revealed among others that; the major deterrent to the adoption of insurance arrange in their order of severity are 'high premium cost experience by the firms', ' lack of awareness of the insurance', and 'lack of enforcement of the Act' arranged in the order of severity. Consequently,it can be deduced that absolute awareness of the insurance has not yet been achieved among contractors, the study shows that out of various risk mitigating mechanism in construction great importance was place on insurance cover but not all category of project are covered. Hence there is need for increase in the level of awareness of insurance, insurance company should try as much as possible to minimize the premium cost

Keywords: *Deterrent, Insurance and Risk mitigation*

I. Background of the Study

It's understood that risks are inherent in construction projects, that no amount of planning can absolutely overcome the occurrence of risk on the inability to control chance events. . Construction projects involve numerous unpredictable and complex processes which are plague with risk. Size can be one of the major causes of risk, so can change in political or commercial planning, other factors carrying risk with them include complexity of construction project, location, speed of construction and familiarity with the type of work. The level of risk in construction projects is due to the uniqueness of every project, the uncertainties introduce by the project stake holders, regulatory protocol, and many other factors at the start of any project. In the context of project Larson (2008) define risk an uncertain event or condition that if occurs, has positive or negative impact on a project objectives. Risk condition could include organization or project environment than enhance the risk. A risk has a one or more causes and if occurs has will have one or more impact. For example, accident may bring down a team member, or there could be change in scope requirement, market fluctuation if any of these uncertain event occurs, it will have impact to the cost, schedules, and quality of the project. Risk in construction has been the object of attention because of time and cost overrun associated with construction project. Too often these risk are not dealt with satisfactorily and the industry has suffered poor performance as a result (Tah and Carr, 2000)

According to Bailey (2017) insurance is defined as a contract where by an insurer agrees, in consideration of the premium paid by the insured to indemnify the insured against loss on the happening of certain events. The main objective of indemnity is to place the insurer, after the loss in position as before the event. Hence Construction insurance is a practice of exchanging a contingent claim for a fixed payment to protect the interests of parties involved in a construction project. Construction insurance is a major method of managing risks in the construction industry. Its primary function is to transfer certain risks from clients, contractors, subcontractors and other parties involved in the construction project to insurers, to provide contingent funding in time of difficulty. Construction insurance plays an increasingly important role in guaranteeing the success of projects, with insurers sharing losses resulting from natural disasters and other contingencies.

Liyadu (1995) postulate that by taking up insurance, a contractor eliminate the risk of suffering financially crippling losses by substituting a small definite cost (the premium) for the variability of construction losses, under a mechanism, where the unfortunate who suffer the misfortune are compensated by the fortunate many who escape loss. Queen &Satheesh, (2018) observed that construction by its very nature is a hazardous industry where collapses of buildings is becoming prevalent, accidents, fire incident, vandalism, and theft are almost common on all construction site. These generate abilities and acquire specific actions which ought to be taken care of by the insurance company.

The loss may be small or large so the impact, but one thing is sure, that if a building under construction collapse, or is damage by fire or vandalism, loss of project as a result of delay in production, compensation to infused employees and other responsibilities which the client would be ill-equipped to meet at the very time any of them might occur.

Risk in construction is a major problem in many construction organizations particularly in under-developed countries such as Nigeria, and to some extent even among the develop countries around the world such as Britain. Risk has a lot of negative impact on the client and stack holders interest into construction due to its influence of set back to their financial sources.

That is why the need to study the risk effects on construction arises, there by addressing method to counter there impact as well as educating the construction organization toward understanding the issue of insurance in general, there by highlighting the main problems associated with the insurance in construction and Providing possible solutions respectively (Emmanuel, 2020).

This research work intend to outline the challenges faced by professionals in construction industry specifically contractors in insuring construction projects with the view to suggesting possible ways through which its use could be improved.

II. Literature Review

Insurance in construction

From the legal viewpoint, insurance allocates the risks to which the project is exposed, between the parties. From an insurance aspect, risk forms the basis of insurability and premium calculation (Bunni, 2003) highlighted insurance as a risk transfer mechanism that the insured transfer from a state of uncertainty to a state of certainty at the certain cost of the insurance premium. It is a cost-smoothing mechanism, in which contractors exchange a regular known annual premium for an unknown potential loss.

In insurance, the insurance policy is a contract (generally a standard form contract) between the insurer and the insured, known as the policyholder, which determines the claims which the insurer is legally required to pay. In exchange for payment, known as the premium, the insurer pays for damages to the insured which are caused by covered perils under the policy language. Insurance contracts are designed to meet specific needs and thus have many features not found in many other types of contracts. Since insurance policies are standard forms, they feature boilerplate language which is similar across a wide variety of different types of insurance policies

The insurance policy is generally an integrated contract, meaning that it includes all forms associated with the agreement between the insured and insurer. In some cases, however, supplementary writings such as letters sent after the final agreement can make the insurance policy a non-integrated contract. One insurance textbook states that "courts consider all prior negotiations or agreements ... every contractual term in the policy at the time of delivery, as well as those written afterwards as policy riders and endorsements ... with both parties' consent, are part of written policy". The textbook also states that the policy must refer to all papers which are part of the policy. Oral agreements are subject to the parole evidence rule, and may not be considered part of the policy. Advertising materials and circulars are typically not part of a policy. Oral contracts pending the issuance of a written policy can occur (Hamzah, Wang, &Mohamad ,2015).

i. Insurance contracts are generally considered contracts of adhesion because the insurer draws up the contract and the insured has little or no ability to make material changes to it. This is interpreted to mean that the insurer bears the burden if there is any ambiguity in any terms of the contract. Insurance policies are sold without the policyholder even seeing a copy of the contract. In (Robert Keeton) suggested that many courts were actually applying 'reasonable expectations' rather than interpreting ambiguities, which he called the 'reasonable expectations doctrine'. This doctrine has been controversial, with some courts adopting it and others explicitly rejecting it.
ii. Insurance contracts are aleatory in that the amounts exchanged by the insured and insurer are unequal and depend upon uncertain future events. In contrast, ordinary non-insurance contracts are commutative in that the amounts (or values) exchanged is usually intended by the parties to be roughly equal. This distinction is particularly important in the context of exotic products like finite risk insurance which contain "commutation" provisions.
iii. Insurance contracts are unilateral, meaning that only the insurer makes legally enforceable promises in the contract. The insured is not required to pay the premiums, but the insurer is required to pay the benefits under the contract if the insured has paid the premiums and met certain other basic provisions.
iv. Insurance contracts are governed by the principle of utmost good faith which requires both parties of the insurance contact to deal in good faith and in particular it imparts on the insured a duty to disclose all material facts which relate to the risk to be covered

Early insurance contracts tended to be written on the basis of every single type of risk (where risks were defined extremely narrowly), and a separate premium was calculated and charged for each.

III. RESEARCH METHOD

Study Population and Sample Size

The target population in this work were professional involve in the construction industry practicing within Imo state and Abia State, the respondents are all experienced and practicing professionals who worked with small, medium and large scale construction firms and Also have an awareness on insurance

Sample Size

Sample size of 60 questionnaires was administered out of which only 50 were fully completed and returned. Question regarding the problem of this research work were drawn up and computed in a questionnaire soliciting information from respondents

Method of Data Collection

The methods employed for data collection in the research work are: Questionnaire survey and Literature review, with the aim of acquiring both primary and secondary date.

Questionnaire

Structured questionnaire was administered to professionals in construction firms who have reasonable knowledge related to construction matters.

Question regarding the purpose of this research work were drawn up based on selection and ranking using Likert scale principle, toward this research question.

RESEARCH TOOL

Questionnaires will be the basic tool for this study. The questionnaire will comprise of close-ended questions asking multi choice questions. The questionnaire consists of three sections, they are:

1. Section A; this section will request personal data of the respondents
2. Section B; this section contains questions risk and risk management in construction.

METHOD OF DATA ANALYSIS

The data acquired from the field survey will be analyse using; Descriptive statistic frequency, Frequency distribution tables and mean weight. The data was arranged in a table and percentage out of each question determined. For those have to do with ranking, the mean weight will be determined as: Mean weight (M_w) $=\frac{\sum fx}{\sum f}$

Where f= frequency of the respondent and x= is the ranking scale of respondent.

IV. DATA, PRESENTATION, ANALYSIS AND DISCUSSION

Data Presentation and Analysis

Table 1 presents the percentage response gotten from the distribution of the questionnaires. From the Table it can be deduced that out of a total of 60 questionnaires distributed 50 were returned satisfactorily filled which represent a response rate of 83.33 percent.

Table 1: Percentage Response

Questionnaire	number	percentage (%)
Distributed	60	100
Returned	50	83.33%

Source: Field Survey, 2018

Respondent Level of awareness

Table 2, presents the analysis of the level of awareness of insurance policies among the professionals, the type of projects indemnified with insurance in the firms and the percentage of the total project as premium. The table reveals that largest proportion of the respondents were aware of insurance policies 34.0% of the total, the next indicate that they were averagely aware of the policies 32% of the total. The lease percentage of respondentswere those whom claim to be totally aware of the policies (15) making 30.0% of the total respondents, and the least proportion of the respondent out of the total respondents indicate that they were not aware of the policies (2) making 4% of the total

The table highlight that highest proportion of the respondents covers large scale projects with insurance making 70% of the total, followed by the respondents that covers medium scale projects making 20% of the total. The least proportion of the respondents cover small scale projects with insurance making 10% of the total respondents

The table reveals that largest proportion of the respondents indicates that they pay 5%-10% of the total budget as a premium cost making 40% of the total, the next group falls under 1%-5% making 28% of the total, and 10%-20% making 18% of the total, However the least proportion of the respondents falls above 20% making 6% of the total.

Table 2: Respondent Level of awareness

S/N	Profile	Option	Frequency (No)	Percentage (%)
1	level of Awareness of insurance policies	a) Totally aware	15	30.0
		b) Aware	17	34.0
		c) Averagely aware	16	32.0
		d) Not aware	2	4.0
		Total	**50**	**100**
2	Type of project indemnified with insurance in the firm	a) Small scale projects	05	10.0
		b) Medium scale projects	10	20.0
		c) Large scale projects	35	70.0
		Total	**60**	**100**
3	percentage of total project budget paid as premium	a) 1% - 5%	14	28.0
		b) 5% - 10%	20	40.0
		c) 10% - 20%	9	18.0
		d) Above 20%	7	14.0
		Total	**60**	**100**

Source: Field Survey, (2018)

Percentage of Project Averagely Covered With Insurance Annually

Table 3 shows the percentage of project covered with insurance by construction firms on annual bases. The table reveals that largest proportion of the respondents falls within 5%-10% group making

48% of the total, the next groups are 1%-5% making 28% of the total followed by 10%-20% making 20% of the total and the least fall within above 20% making just 2% of the total respondents.

Table 3:Percentage of Project Averagely Covered With Insurance Annually

Types of project	frequency	percentage (%)
1% - 5%	14	28.0
5% -10%	24	48.0
10% - 20%	10	20.0
Above 20%	2	4.0
Total	50	100.0

Source: Field Survey, 2018

Some Major Problems Associated With Insurance When Use As A Tool for Mitigating Risk

Table 4:*Some Major Problems Associated With Insurance When Use As A Tool for Mitigating Risk In Construction,*

S/N	Problems	∑F	∑FX	MEAN	RII	RANK
1	Lack of implementation	50	138	2.76	0.55	4th
2	Lack of enforcement	50	178	3.52	0.71	2nd
3	Unconcern attitude	50	155	3.1	062	3rd
4	Delay of payment of claims	50	200	4.0	0.80	1st

Source: field Survey, 2018

Where 1=least problem, 2=less problem, 3=moderately problem, 4=problem, 5=main problem

Table 4: shows ranking of some major problems associated with insurance when use as a tool for mitigating risk in construction, it could be seen from the table that, delay of payment insurance claim (RII= 0.80) was identified as the most reoccurring problem. This was closely followed by 'lack of enforcement of the insurance Act' (RII=0.71), 'unconcern attitude toward insurance' (RII= 0.62) and 'lack of implementation of the Act' (RII= 0.55), which ranked second, third and fourth respectively. Details of the ranking is as presented in the Table.

Factors mitigating the use of insurance cover for projects by construction industry

Table 5 The table show the degree of importance of some factors that militate the use of insurance cover for construction projects by construction firms, from the table it could be deduce that the 'high premium cost experience by the firms is the most important factor weighing 4.56, the next factors are lack of awareness of the insurance and lack of enforcement of the Act weighing 4.08 and 3.9 respectively which are important factors, while the moderate problems is lack of implementation of the insurance Act, however the less problems is bid to reduce contract sum weighing 1.86.

Table 5: Factors mitigating the use of insurance cover for projects by construction industry

S/N	Factors	∑F	∑FX	MEAN	RII	RANK
1	High premium cost	50	228	4.56	0.91	1st
2	Lack of awareness	50	204	4.08	0.82	2nd
3	Lack of implementation	50	155	3.1	0.62	4th
4	Lack of enforcement	50	195	3.9	0.78	3rd
5	Bid to reduce contract cost	50	93	1.86	0.37	5th

Source: field Survey, 2018

Where 1=least important, 2=less problem, 3=moderately important, 4=important, 5=most important

Factors in encouraging the use of insurance in construction

Table 6 shows the degree of importance of some approaches through which the use of insurance in construction can be encourage, the table reveals that the most important approach that will be employed to increase the utilization of insurance by construction firms is reduction of premium cost weighing 4.68, the next are the enforcement of the act, minimizing bureaucracy claim payment and increasing insurance coverage which are important weighing 4.28, 4.24 and 3.86 respectively, while the moderately important are the implementation of the Act, changed in concern attitude of the firms and increasing the awareness of the Act weighing 3.3, 3.02 and 2.8 respectively

Table 6Factors in encouraging the use of insurance in construction

S/N	Approaches	∑F	∑FX	MEAN	RII	RANK
1	Reduction of premium cost	50	234	4.68	0.94	1st
2	Enforcement of the Act	50	214	4.28	0.86	2nd
3	Increasing insurance coverage	50	193	3.86	0.77	4th
4	Implementation of the Act	50	165	3.30	0.66	5th
5	Making the Act to be known	50	140	2.80	0.56	7th
6	Min. bureaucracy claim payment	50	212	4.24	0.85	3rd
	Construction firms	50	151	3.02	0.60	6th

Source: field Survey, 2016
Where 1=least important, 2=less important, 3=moderately important, 4=important, 5=most important

Insurance coverage policies employed by construction industry

Table 7: shows the degree of usage of some of the insurance policies employed by construction company, the table reveals that the most frequent policy use by construction company is construction all risk insurance weighing 4.68, the moderately frequent are plant all risk insurance, commercial general liability, workmen compensation, erection all risk insurance, and builders all risk insurance weighing 3.46, 3.24, 3.0, 2.86 and 2.76 respectively, while the less frequent policy are theft and burglary, professional liability and controlled insurance plan (wrap up) weighing 2.24, 2.4 and 1.76 respectively

Table 7: Insurance coverage policies employed by construction industry (degree of usage)

S/N	Policies	∑F	∑FX	MEAN	RII	RANK
1	Construction all-risk	50	234	4.68	0.94	1st
2	Plant all-risk	50	173	3.46	0.69	2nd
3	Workmen compensation	50	150	3.0	0.60	4th
4	Theft and burglary	50	112	2.24	0.45	8th
5	Professional liability	50	140	2.40	0.48	7th
6	Controlled insurance plan (wrap up)	50	212	1.76	0.35	9th
7	Commercial general liability	50	162	3.24	0.65	3rd
8	Erection all risk insurance	50	143	2.86	0.57	5th
9	Builders all risk insurance	50	138	2.76	0.55	6th

Source: field Survey, 2016

Where 1=least frequent, 2=less frequent, 3=moderately frequent, 4=frequent, 5=most frequent

V. SUMMARY, CONCLUSION AND RECOMMENDATION

5.1 SUMMARY

i. Various stake holders face severe problems in carrying out complex construction work due to the unsatisfactory attitude of insurance.
ii. Responses from the survey were analyzed using frequencies and mean values.
iii. The reliable risk mitigating tool was found to be insurance, though it associated with certain number of various problem such as lack of enforcement, high premium cost, delay of payment of claim, however the utilization of insurance cover can be encourage by reasonable reduction of predetermined premium.

5.2 Conclusions

The construction industry is proved to several risks in which the contractor or client cannot shoulder alone when it happens. There is therefore a need for the contractor to take up insurance to cover these risks. But from the survey carried out, the absolute awareness has not yet sink into contractors. The study shows that, out of various risks mitigating mechanism in construction, great importance was place on the use of insurance cover, but not all category of projects are covered with insurance. The paper highlight major problems associated with insurance to be lack of implementation of the Act, lack of enforcement of the Act, delay of payment of claims, high premium but great importance was placed on delay of payment of claim and high premium. Which are the main factors mitigating the use of insurance cover by construction firm, the study highlights some of the approaches through which the use of insurance can be encourage; great importance was placed on reduction of high premium as well as enforcement of the Act. The study also shows the various policies adopted by construction firm, where construction all risk insurance policy is the most frequently used.

5.3 Recommendations

i. Insurance companies should endeavor to carry out proper documentation and make their policies well known and understood by operators of the construction companies.
ii. Insurance companies should try as much as possible to honor settlement of claim as at when due. In general, government should monitor, control and enforce insurance Act.
iii. Insurance company should minimize the premium to reasonable amount which will increase the desire of construction firm toward employing insurance cover.
iv. Level of awareness of insurance of insurance should be increase to create understanding of the administration of insurance services in the industry.
v. The government should implement and make it mandatory for construction companies to undertake at least one of the established insurance policies as it applies to the construction industry
vi. Provisions for the inclusion of insurance cover should be also be made compulsory for all categories of project and its administrative framework be strengthened.

REFERENCES

[1.] Bailey, J. (2017). Health insurance and the supply of entrepreneurs: New evidence from the Affordable Care Act. *Small Business Economics*, *49*(3), 627-646.

[2.] Bunni, N. G. (2003). *Risk and insurance in construction*. Routledge.
[3.] Dada, J.O. and Jagboro, G.O. (2007) an evaluation of the impact of risk on project cost overrun in Nigerian construction industry, journal of financial management of property and construction

[4.] Emmanuel, N. I., Effiong, O. B., Ozoh, C. S., Chidi, U., &Ayodeji, O. O.(2020) AN ASSESSMENT OF PROJECT MONITORING PRACTICES ON CONSTRUCTION SITES IN ABUJA NIGERIA.

[5.] Hamzah AR, Wang C, Mohamad FS (2015) Implementation of risk management in Malaysian construction industry: case studies. J ConstrEng

[6.] Larson G.I (2008) project management: the managerial process MC Graw Hill international edition united states of publication

[7.] Queen M, Satheesh Kumar S (2018) A study on insurance in construction industry. Int Res J EngTechnol (IRJET) 5(4):3991–3393

[8.] Sola, A. J., Arowojolu-Alagwe, T., Taiwo, E. M., &Abiodun, B. T. (2013). Adequacy of builders risk insurance policy in Nigeria building industry. *PM World Journal*, *2*(XI), 1-12.

[9.] Tah, J. H., &Carr, V. (2000). A proposal for construction project risk assessment using fuzzy logic. *Construction Management & Economics*, *18*(4), 491-500.